FORMULATION AND IMPLEMENTATION OF CONFORMING FINITE ELEMENT APPROXIMATIONS TO STATIC AND EIGENVALUE PROBLEMS FOR THIN ELASTIC SHELLS

by

R. A. EVE

A thesis submitted in partial fulfilment of the requirements
for the degree of Master of Science in the Faculty of Engineering

University of Cape Town
Department of Civil Engineering
March 1987

DECLARATION

I, Robin Andrew Eve, do declare that this thesis is my own work and that no part of it has been submitted for a degree at any other university.

Signed by candidate

R A EVE
March 1987

DEDICATION

To my parents

ACKNOWLEDGEMENTS

I would like to extend my appreciation to Professor B D Reddy*, under whose supervision this work was conducted, for his patient assistance and constructive guidance. I also thank Professor J B Martin** for checking of the final draft.

My colleagues in the Applied Mechanics Research Unit for their help with computer and programming related matters.

The Council for Scientific and Industrial Research for their financial assistance.

Mrs Shirley Breed for her help with the typing of this document.

Mr Harold Cable for the printing of the thesis.

* Departments of Applied Mathematics and Civil Engineering,

** Dean of the Faculty of Engineering,

University of Cape Town.

ABSTRACT

In deriving asymptotic error estimates for a conforming finite element analyses of static thin elastic shell problems the French mathematician Ciarlet (1976) proposed an approach to the formulation of such problems. The formulation he uses is based on classical shell theory making use of Kirchhoff-Koiter assumptions. The shell problem is posed in two dimensional space to which the real problem, in three dimensional space, is related by a mapping of the domain of the problem to the shell mid-surface. The finite element approximation is formulated in terms of the covariant components of the shell mid-surface displacement field.

In this study Ciarlet's formulation is extended to include the eigenvalue problem for the shell. In addition to this the aim of the study is to obtain some indication of how well this approach might be expected to work in practice. The conforming finite element approximation of both the static and eigenvalue problems are implemented. Particular attention is paid to allowing generality of the shell surface geometry through the use of an approximate mapping.

The use of different integration rules, in-plane displacement component interpolation schemes and approximate geometry schemes are investigated. Results are presented for shells of different geometries for both static and eigenvalue analyses, these are compared with independently obtained results.

TABLE OF CONTENTS

CHAPTER 1

INTRODUCTION

A shell is a special case of a three-dimensional continuum. It is a solid medium contained in a narrow space between two parallel or almost parallel curved surfaces (Flugge 1969). The thickness of the shell is the distance between these two bounding surfaces. The shell thickness is small compared to other dimensions of the shell, in particular, the span of the shell surface or its radius of curvature. Shells with radius of curvature to thickness ratio larger than 100:1 are described as "thin". The shell mid-surface is defined to be the surface which lies midway between the upper and lower boundary surfaces ; it is used to describe the geometry of the shell (figure 1.1).

Shell problems are generically complex; they constitute an area of structural mechanics which has received considerable attention over many years. The finite element method in particular is now a well-established tool in the analysis of shell problems. Procedures exist for solving three-dimensional continuum problems with the finite element method (see Dhatt and Touzot 1984 and Zienkiewicz 1977). In order to describe the flexural modes of a shell with three-dimensional elements several nodes would be required through the thickness of the shell. Since a shell is relatively thin in comparison to its span, either very large

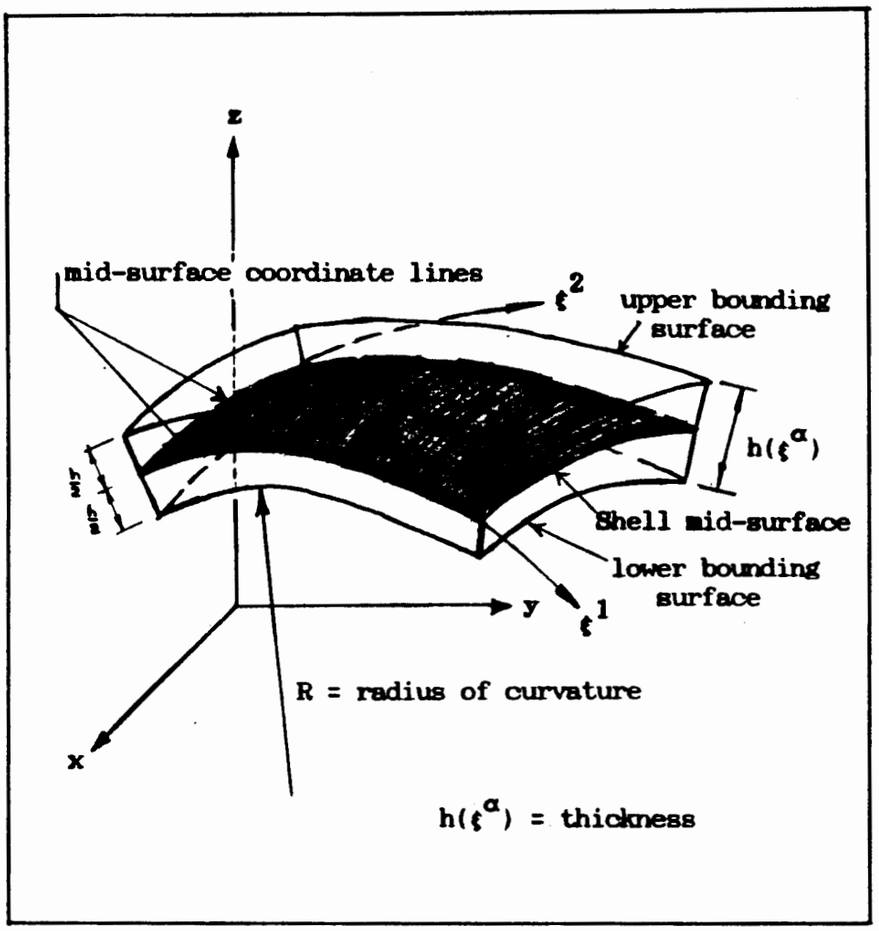

Figure 1.1.: A section of a shell.

numbers of elements, or elements with very large aspect ratios would be required to model it. Large aspect ratios for three-dimensional elements would in turn result in ill-conditioning of the matrices which arise in the finite element calculations. Attempts have been made to improve three-dimensional elements so that they can be used for shell analysis. Reduced integration and incompatible displacement mode techniques have been tried but these methods exhibit convergence problems (Dovey 1974).

In general the use of three-dimensional elements for the analysis of shells either fails or becomes prohibitively expensive (Kanok-Nakulchai 1979), so that a special class of shell elements is required. Two major approaches to the formulation of shell elements have evolved : the first makes use of classical shell theory and the second is based on a degeneration of three-dimensional elements. These two approaches are outlined later in this chapter, and are compared and summarised in figure 1.2 (Kanok-Nakulchai, Taylor and Hughes 1981).

Many of the shell element formulations proposed are restricted to linear elastic analyses. Application of these formulations to static analyses are usually tested but their application to free vibration analyses is rarely investigated. The determination of natural frequencies and mode shapes requires the modelling of the inertia of the shell, i.e. formulation of a mass matrix. The free vibration eigenvalue problem is solved by standard procedures which are independent of the structural nature of the problem. Determination of the mass matrix is thus the only extra formulation required.

Simple standard procedures for obtaining consistent mass matrices are in many cases directly applicable to proposed formulations. Alternatively, lumped mass methods in many cases prove more accurate and economical, especially where displacement incompatibilities are used (Clough and Wilson 1971). Reasonably simple closed form solutions or "bench mark" examples for free vibration modal frequencies and mode shapes of curved and doubly curved shells appear scarce.

Classical Shell Element Formulations A classical shell theory results when the three-dimensional field equations of a shell are simplified by making assumptions based on the special geometric characteristics of the shell continuum. The shell theories most commonly used are based on the Kirchhoff-Love hypothesis : normals to the mid-surface are assumed to remain straight, normal and unchanged in lengh through a deformation of a shell. The assumption that the normals do not change length implies a state of plane strain in the shell. Koiter (1970) replaced this assumption with one of plane stress. The assumption that normals remain normal and straight implies that transverse shear strain energy in the shell is zero; the shell theory is thus only valid for thin shells where the transverse shear strain energy is negligible. Application of these assumptions allows all the quantities of interest through the thickness of the shell to be described in terms of mid-surface values. The mid-surface displacement components are used; these are functions only of the two mid-surface coordinates ξ^1 and ξ^2 shown in figure 1.1.

The equations of the Kirchhoff-Koiter shell theory are a coupled set of second order differential equations in the in-plane components of mid-surface displacement and a fourth order differential equation in the transverse component. Variational formulations of shell problems based on classical shell theory, which are used in the finite element method, thus yield the requirement that the finite element approximation of the transverse displacement component function be a continuously

differentiable function. To achieve this inclusion with the application of the finite element method requires the use of large numbers of element degrees of freedom, including derivative degrees of freedom. Such elements are termed conforming finite elements. Much work has been done in an effort to circumvent this C^1 continuity requirement and many non-conforming elements have proved successful (for examples see Zienkiewicz 1977). Most of the work done on both conforming and non-conforming elements has been carried out in the context of flat plates where only the transverse displacement is of interest (Bell 1969, Hsieh, Clough and Toucher 1965).

Degeneration Concept Shell formulations are obtained by modifying three-dimensional elements to comply with shell assumptions. The shell continuum is first discretised, a single layer of continuum elements being used. Nodal displacements are then replaced by mid-surface nodal displacements and rotations. It is assumed that normals to the shell's mid-surface remain straight but not necessarily normal through deformation (Mindlin 1951). The three-dimensional field equations are thus reduced or "degenerated" to be dependent only on mid-surface displacements and rotations. These are independent variables, hence the resulting set of equations describing the behaviour of the shell are a set of second order differential equations, requiring only C^0 continuity of the finite element basis functions. Transverse shear is taken into account since no Kirchhoff-Love hypothesis is used. These elements are thus applicable to thick shells, but when applied in thin shell situations excessive stiffness characteristics are observed. This

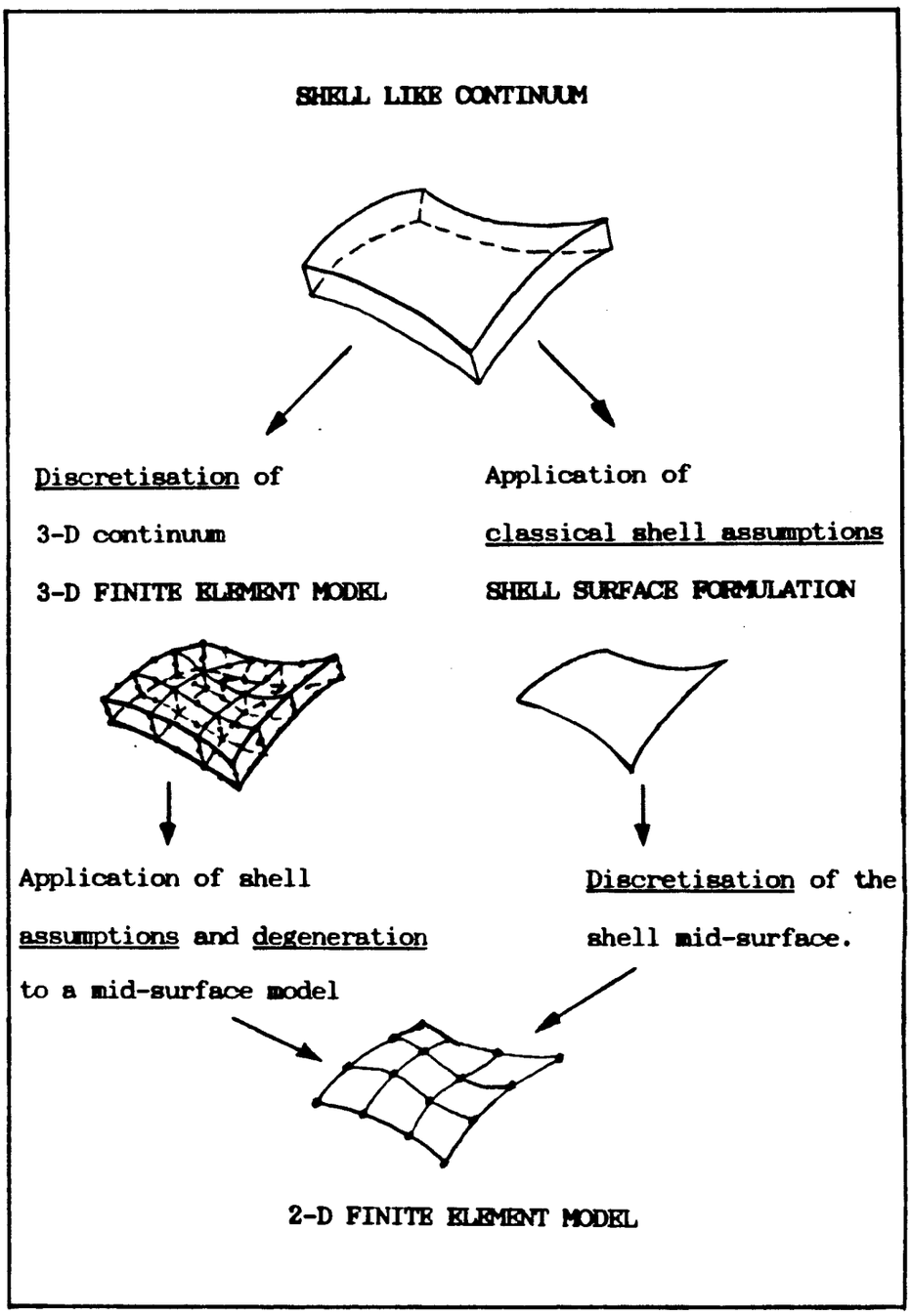

Figure 1.2.: Degeneration and Classical approaches to Shell Element Formation

phenomenon is known as shear locking and arises due to dominance of the transverse shear energy terms which are of the order $(L/h)^2$ (L = element length, h = shell thickness) and thus blow up as shell thickness decreases. Several techniques which reduce the effect of shear locking have been studied; among these the use of reduced integration has proved the most effective (Salomen, Hinton and Bicanic 1978).

Present Study Thin elastic shells of arbitrary geometry, the behaviour of which is described by classical shell theory are the subject of this thesis. Ciarlet (1976) has proposed an interesting way of posing such shell problems. The shell is mapped from three-dimensional space onto a flat two-dimensional domain where the shell problem is posed. Covariant components of mid-surface displacement and the geometric quantities used in the shell problem formulation are given by independent functions on this two-dimensional domain. The finite element method is applied to each of the functions on the domain, and coupling of transverse bending and membrane actions is included in the formulation with the use of the geometric properties of the shell mid-surface. This method is suited to conforming finite element methods. Ciarlet has only formulated the problem of determining the shell deformation under static loading; he has formulated an asymptotic error estimate for a conforming finite element analysis of this problem which includes an approximation of the shell geometry, but he has not studied the detailed implementation of his proposals. Some aspects of the implementation of Ciarlet's proposals have been investigated by other researchers, notably Bernadou (1980).

The objective of this study is to extend Ciarlet's formulation to include the eigenvalue problem which arises in the analysis of free vibration of the shell, and then to implement both the static and eigenvalue problems. Arbitrary shell geometry is catered for and some particular attention has been paid to the implementation of approximate geometry. The "mass term" in the eigenvalue problem is formulated in terms shell mid-surface displacement components, therefore tensor quantites which describe the mid-surface geometry enter into the formulation. As a consequence of this the calculation of the mass matrix for the finite element approximation of this problem does not follow standard procedures.

The use of curvilinear coordinate systems and associated tensorial quantities are essential to the shell formulations studied; these are described in chapter 2. The formulation of the shell problems using classical Kirchhoff-Koiter shell theory is presented in chapter 3. The finite element method and its application to these problems is discussed in chapter 4. Methods for the implementation of the finite element formulations are then presented in chapter 5. Some details of the FORTRAN computer program in which these methods are used are given in chapter 6. Several aspects of the shell formulations and their implementation have been investigated by using this program to analyse a series of shell examples. The results of these investigations are presented in chapter 7. In chapter 8 the results of the study are discussed, conclusions are drawn and recommendations for further study are made.

differentiable function. To achieve this inclusion with the application of the finite element method requires the use of large numbers of element degrees of freedom, including derivative degrees of freedom. Such elements are termed conforming finite elements. Much work has been done in an effort to circumvent this C^1 continuity requirement and many non-conforming elements have proved successful (for examples see Zienkiewicz 1977). Most of the work done on both conforming and non-conforming elements has been carried out in the context of flat plates where only the transverse displacement is of interest (Bell 1969, Hsieh, Clough and Toucher 1965).

Degeneration Concept Shell formulations are obtained by modifying three-dimensional elements to comply with shell assumptions. The shell continuum is first discretised, a single layer of continuum elements being used. Nodal displacements are then replaced by mid-surface nodal displacements and rotations. It is assumed that normals to the shell's mid-surface remain straight but not necessarily normal through deformation (Mindlin 1951). The three-dimensional field equations are thus reduced or "degenerated" to be dependent only on mid-surface displacements and rotations. These are independent variables, hence the resulting set of equations describing the behaviour of the shell are a set of second order differential equations, requiring only C^0 continuity of the finite element basis functions. Transverse shear is taken into account since no Kirchhoff-Love hypothesis is used. These elements are thus applicable to thick shells, but when applied in thin shell situations excessive stiffness characteristics are observed. This

CHAPTER 2

VECTORS AND TENSORS IN CURVILINEAR COORDINATES.

2.1 Introductory Remarks.

The tensor analysis and differential geometry required for an analysis of elastic shells are described here since many engineers are not familiar with these topics. The intention is to provide the minimum of information required to follow later discussion; therefore, where convenient, the ideas are presented directly in the context of curved surfaces. A shell example is also developed to illustrate the concepts and to give meaning to the various quantities as they are defined. Alternative and more comprehensive presentations of these ideas are to be found in standard texts on tensor analysis or shell theory (Flugge 1972, Ciarlet 1976, and Koiter 1970).

Notation and symbols are defined where required, and are also listed in Appendix A. Bold type is used to denote vectors, as in Gibbs type vector algebra which is independent of coordinates. Einstein's indicial summation convention is used, with range convention as follows: latin letters i,j,k,... take values {1,2,3}, and greek letters $\alpha,\beta,\ldots$ values {1,2}.

2.2 General Coordinate Systems

Euclidean space, E^3, is the 3-dimensional space in which all physical bodies are considered to reside. This space can be described using any coordinate system. A vector or tensor quantity may be associated with any point in the space. For a general coordinate system the components of such a vector, or tensor, are described relative to a basis associated with the point. Cartesian coordinates form the simplest description of E^3. This simplicity arises from the use of an orthonormal set of basis vectors, $\underline{e}_i$, which are parallelly propagated throughout the space. Hence in the cartesian system the basis is constant throughout the space. For curvilinear coordinate systems every point has a different set of tangent basis vectors associated with it. The position of any point in E^3 can be defined by a vector from the origin of the coordinate system. This vector can be uniquely defined by its components in the cartesian system since there is only one basis, $\underline{e}_i$, for all points along the vector.

2.3 Curvilinear Surface Cordinate System

A shell is a 3-dimensional body embedded in E^3 ; however, since it is thin its geometry is completely described by its mid-surface, S. This surface is a curved 2-dimensional subset of E^3. Due to the curvature of this subspace a cartesian coordinate system can not be used to describe it. The position of any point on the shell is defined by a pair of coordinates (ξ^1,ξ^2), where $\{\xi^\alpha\}$ are in a coordinate system inscribed on the surface. The position vector $\underline{s}$, in E^3 of this point has components determined by specfication of ξ^α, as shown below (also see figure 2.1.).

$$\underline{s} = \underline{s}(\xi^1,\xi^2) = s^1(\xi^1,\xi^2)\underline{e}_1+s^2(\xi^1,\xi^2)\underline{e}_2+s^3(\xi^1,\xi^2)\underline{e}_3$$

2.4 Surface Tangent Basis Vectors

The surface cordinates ξ^α have associated tangent basis $\underline{a}_i$, $(i = 1,2,3)$. Vectors $\underline{a}_\alpha$, $(\alpha = 1,2)$ are tangential to the surface and are defined by ;

$$\underline{a}_\alpha = \underline{a}_\alpha(\xi^1,\xi^2) = \frac{\partial \underline{s}}{\partial \xi^\alpha} \qquad (2.4.1)$$

The third basis vector is associated with coordinate z, the normal distance off the surface; $\underline{a}_3$ is defined normal to the surface by

$$\underline{a}_3 = \frac{\underline{a}_1 \times \underline{a}_2}{|\underline{a}_1 \times \underline{a}_2|} \quad . \qquad (2.4.2)$$

Note that $\underline{a}_3$ by this definition has unit length. It is a function of the vectors $\underline{a}_\alpha$ and therefore also a function of ξ^α.

2.5 Surface Mapping.

The shell mid-surface, S , is a bounded open subset of E^3. It may be mapped to a similar subset in E^2; however it is more convenient to consider the inverse mapping.

Let Ω be a bounded open subset in E^2 with boundary Γ. Then $\bar{S}$ is the image of Ω under the mapping $\underline{\phi}$ (Ciarlet 1976):

$$\underline{\phi} : \bar{\Omega} \subset E^2 \rightarrow \bar{S} \subset E^3 \qquad (2.5.1)$$
$$\underline{\phi} = \phi_i(\xi^1,\xi^2)\underline{e}^i$$

The component functions of the position vector are then simply the components of this mapping, ie. $s_i = \phi_i(\xi^\alpha)$. The tangent basis vectors are thus

$$\underline{a}_\alpha = \frac{\partial \underline{\phi}}{\partial \xi^\alpha} = \underline{\phi}_{,\alpha} \quad . \tag{2.5.2.}$$

All the geometric quantities associated with the shell mid-surface can be written in terms of the mapping $\underline{\phi}$, so that the shell problems can then be formulated on Ω in E^2.

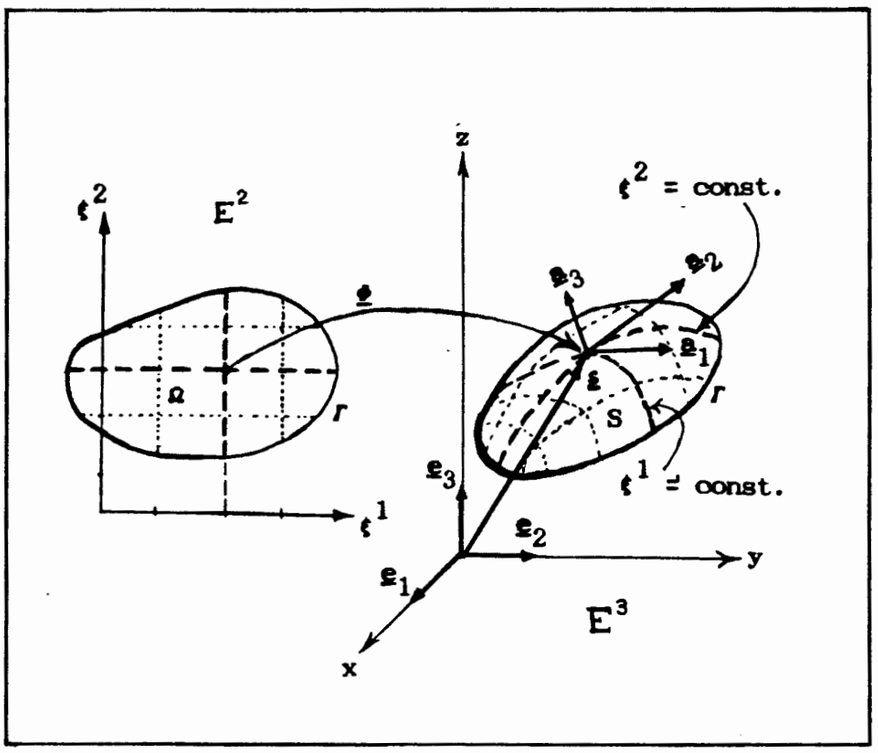

Figure 2.1.: Shell mid-suface mapping.

Example : Cylindrical Shell.

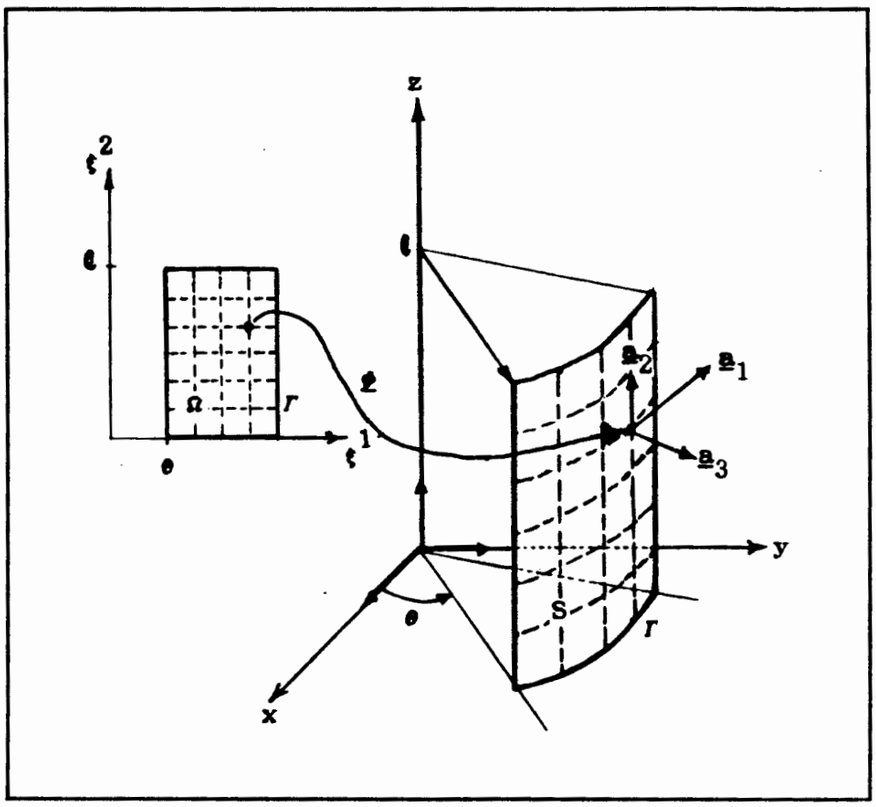

Surface coordinates ; $\xi^1 = \theta$, $\xi^2 = x_3$

Mapping ; $\phi_1 = R\cos\theta = R\cos(\xi^1)$

$\phi_2 = R\sin\theta = R\sin(\xi^1)$

$\phi_3 = x_3 = \xi^2$

Basis vectors (covariant components) ;

$\underline{a}_1 = -R\cos(\xi^1)\,\underline{e}_1 + R\sin(\xi^1)\underline{e}_2$

$\underline{a}_2 = \underline{e}_3$

$\underline{a}_3 = \sin(\xi^1)\underline{e}_1 + \cos(\xi^1)\underline{e}_2$

2.6 Covariant, and Contravariant Components.

Every coordinate basis has a reciprocal basis. Up to now this alternative basis has been ignored. For the familiar cartesian system the basis $\underline{e}_i$, and the reciprocal basis $\underline{e}^i$ are identical, so, that for any vector $\underline{v}$;

$$\underline{v} = v^i \underline{e}_i = v_i \underline{e}^i \quad ; \quad v^i = v_i \text{ (no sum)} \tag{2.6.1}$$

Generally the surface reciprocal basis $\underline{a}^i$ is defined by

$$\underline{a}_i . \underline{a}^j = \delta_i^j \quad \text{where} \quad \delta_i^j = \begin{matrix} 1 & i = j \\ 0 & i \neq j \end{matrix} \; . \tag{2.6.2}$$

Note that $\underline{a}_3 = \underline{a}^3$

In general, lack of orthonormality of the tangent basis vectors implies $\underline{a}_\alpha \neq \underline{a}^\alpha$ so that for vector $\underline{v}$,

$$\underline{v} = v^\alpha \underline{a}_\alpha + v^3 \underline{a}_3 = v_\alpha \underline{a}^\alpha + v_3 \underline{a}^3$$

$$v^\alpha \neq v_\alpha \text{ (no sum)} \quad \text{and} \quad v^3 = v_3$$

The components v_i are called the covariant components, and components v^i are the contravariant components of $\underline{v}$. In the finite element formulation the component functions of the displacement field are discretised. It becomes important to use a consistent description of the displacement for all terms in the formulation. The difference between the two descriptions is therefore discussed further. To show clearly the differerce between the two possible bases a set of skew coordinates in E^2 is used, figure 3.2. (Flugge 1972).

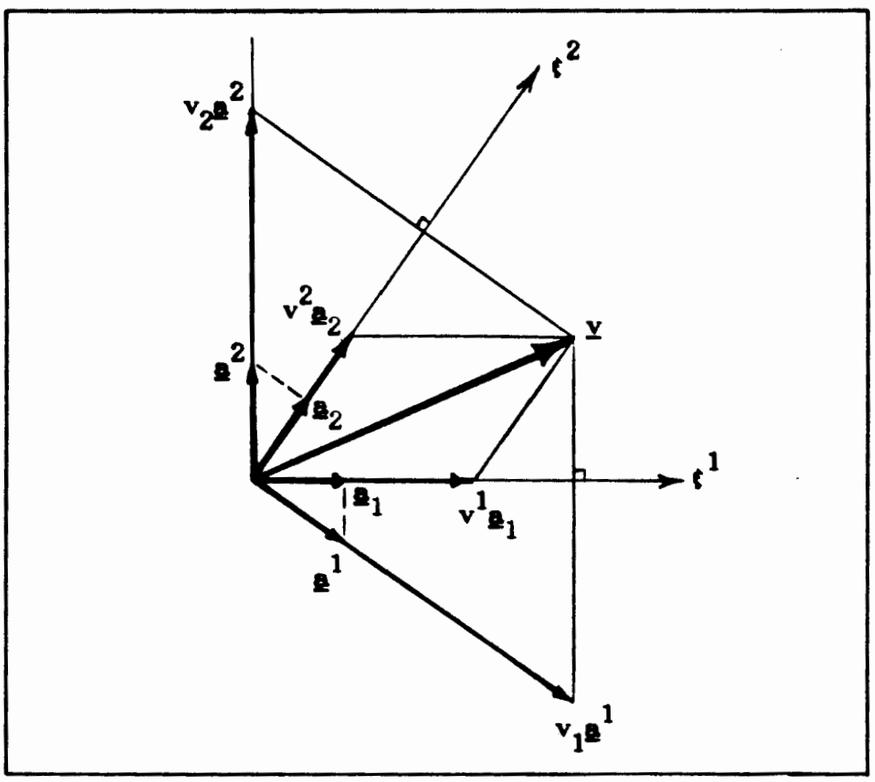

Figure 2.2.: Co- and contravariant components.

Figure 3.2 shows how component vectors in either description give the vector $\underline{v}$ via the usual paralleogram construction. Note $\underline{a}^1$ is normal to $\underline{a}_2$. The basis vectors $\underline{a}_\alpha$ are chosen to be of unit length for the skew coordinate system shown. It can be seen that the basis vectors $\underline{a}^\alpha$ are therefore not of unit length which implies that the v_α are not the length of the components of $\underline{v}$ in the directions $\underline{a}^\alpha$.

Since $\underline{a}_\alpha$ for a surface are given by expression (2.4.1) they are in general not of unit length and may have dimension. This is seen

more easily by looking at the case of polar coordinates in E^2, Figure 2.3. (Flugge 1972)

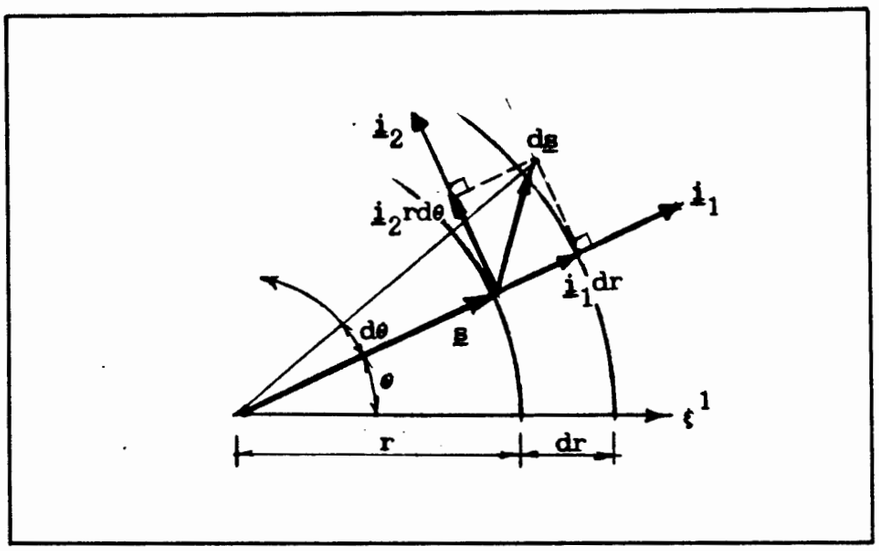

Figure 2.3.: Basis vectors in a polar coordinate system.

The vectors $\underline{i}_\alpha$ are unit vectors in the directions of the coordinate lines ξ^α, $\xi^1 = r$, $\xi^2 = \theta$, and hence the line element $d\underline{s}$ is such that

$$d\underline{s} = \underline{i}_1 dr + \underline{i}_2 r d\theta \quad ,$$

but

$$d\underline{s} = ds^1 \underline{a}_1 + ds^2 \underline{a}_2$$

The components of $d\underline{s}$ are most naturally chosen as $d\theta$ and dr, hence $\underline{a}_1$ is a unit vector in this example but $\underline{a}_2 = \underline{i}_2 r$, has length r and dimensions of length.

2.7 Metric Tensor.

The metric tensor is used to measure lengths in terms of the coordinate system (ξ^i). It is a second order tensor, the components of which are defined by

$$a_{ij} = \underline{a}_i \cdot \underline{a}_j \quad \text{(covariant components) or} \qquad (2.7.1)$$

$$a^{ij} = \underline{a}^i \cdot \underline{a}^j \quad \text{(contravariant components).} \qquad (2.7.2)$$

Note that the metric is symmetric, ie.

$$a_{ij} = a_{ji} \quad \text{or} \quad a^{ij} = a^{ji}.$$

The shell tangent basis has monoclinic nature, since only the angle between $\underline{a}_1$ and $\underline{a}_2$ may vary, the angle between $\underline{a}_\alpha$ and $\underline{a}_3$ being fixed as a right angle by the definition (2.3.2). This allows simplification of many of the tensor quantities associated with the surface. The full set of metric components is given in matrix form by

$$[a_{ij}] = \begin{bmatrix} a_{11} & a_{12} & 0 \\ a_{21} & a_{22} & 0 \\ 0 & 0 & 1 \end{bmatrix}$$

which reduces to

$$[a_{\alpha\beta}] = \begin{bmatrix} a_{11} & a_{12} \\ a_{21} & a_{22} \end{bmatrix} .$$

This latter set of components is called the "surface metric", or first fundamental form of the surface. It contains all the variable information of the full metric tensor. The determinant, a , of the metric is given by ;

$$a = a_{11}a_{22} - a_{12}a_{21} \tag{2.7.3}$$

Contravariant components of the surface metric may be found by inverting $[a_{\alpha\beta}]$, ie.

$$\left[a^{\alpha\beta}\right] = \left[a_{\alpha\beta}\right]^{-1} \tag{2.7.4}$$

The role of the metric tensor in determining lengths can be appreciated by considering the length of a line element $d\underline{s}$ in the surface (i.e. $d\underline{s} = d\xi^{\alpha}\underline{a}_{\alpha}$ component $ds_3 = z = 0$). Hence

$$|d\underline{s}| = (d\underline{s}.d\underline{s})^{\frac{1}{2}} = \sqrt{|\ \underline{a}_{\alpha}d\xi^{\alpha}.\underline{a}_{\beta}d\xi^{\beta}\ |} = \sqrt{|\ a_{\alpha\beta}\ d\xi^{\alpha}d\xi^{\beta}\ |}$$

An element of area on the surface ds is given by ;

$$ds = \sqrt{a}\ d\xi^1 d\xi^2 \tag{2.7.5}$$

Another important use of the metric tensor is to raise and lower indices. Consider the vector $\underline{v} = v_i\underline{a}^i = v^j\underline{a}_j$, and take the product with $\underline{a}_k$;

$$v_i\underline{a}^i.\underline{a}_k = v^j\underline{a}_j.\underline{a}_k$$

which is

$$v_i\delta^i_k = v^j a_{jk} \qquad \text{since } \delta^i_k = \begin{matrix} 0 & i \neq k \\ 1 & i = k \end{matrix}$$

set $i = k$ to get

$$v_i = v^j a_{ji} \ .$$

Similarly

$$v^i = v_j a^{ij} \ . \tag{2.7.6}$$

Example : Cylindrical Shell

Metric tensor components ;

(covariant) ; $a_{11} = R^2$, $a_{12} = a_{21} = 0$, $a_{22} = 1$

(contravariant) ; $a^{11} = \frac{1}{R^2}$, $a^{12} = a^{21} = 0$, $a^{22} = 1$

Basis vectors (contravariant components) ;

$$\underline{a}^1 = \frac{1}{R}\cos(\xi^1)\underline{e}_1 + \frac{1}{R}\sin(\xi^1)\underline{e}_2$$

$$\underline{a}^2 = \underline{e}_3 \quad .$$

2.8 Spatial Derivatives.

The rate of change of a function $\underline{v}(\xi^\alpha, z)$ with respect to ξ^α is given by

$$\frac{\partial \underline{v}}{\partial \xi^\alpha} = \underline{v}_{,\alpha} = (v_i \underline{a}^i)_{,\alpha} = v_{i,\alpha}\, \underline{a}^i + v_i\, \underline{a}^i{}_{,\alpha} \qquad (2.8.1)$$

where ξ^i are the surface coordinates, and a comma is used to denote partial derivatives.

The last term on the right hand side of this expression contains the derivative of the basis vectors. In the cartesian system this term would be zero since the basis vectors, $\underline{e}_i$ or $\underline{e}^i$, are invariant. The Christoffel symbols, $\Gamma_{ij}^{\ k}$, are used to express the derivatives of basis vectors; they are defined by

$$\Gamma_{ij}^{\ k} = \underline{a}_{i,j} \cdot \underline{a}^k \qquad (2.8.2a)$$

or

$$\underline{a}_{i,j} = \Gamma_{ij}^{k}\, \underline{a}_{k} \qquad (2.8.2.b)$$

or

$$\underline{a}^{i}{}_{,j} = -\Gamma_{jk}^{i}\, \underline{a}^{k} \qquad (2.8.2.c)$$

Substituting in (2.8.1) above

$$\underline{v}_{,i} = v_{j,i}\, \underline{a}^{j} + v_{j}\, \Gamma_{ik}^{j}\, \underline{a}^{k} \qquad (2.8.3)$$

Some relationships and expressions relating to the use of Christoffel symbols are listed below:

$$\Gamma_{ij}^{k}\, a_{km} = \Gamma_{ijm} \quad \text{(lower index with metric)} \qquad (2.8.4a)$$

$$\Gamma_{ij}^{k} = \Gamma_{ji}^{k} \quad \text{(symmetric w.r.t. first 2 indices)}$$
$$\Gamma_{ijm} = \Gamma_{jim} \qquad (2.8.4b)$$

The monoclinic nature of the tangent basis implies that

$$\Gamma_{\alpha 33} = \Gamma_{33\alpha} = \Gamma_{333} = 0 \quad \text{and} \quad \Gamma_{\alpha 3}^{3} = \Gamma_{33}^{\alpha} = \Gamma_{33}^{3} = 0$$

and that,

$$a_{\alpha,\beta} \cdot a_{3} + a_{3,\beta} \cdot a_{\alpha} = 0 \quad ;$$

hence

$$\Gamma_{\alpha\beta 3} = -\Gamma_{3\beta\alpha} = \Gamma_{\beta\alpha 3} = -\Gamma_{3\alpha\beta} = -\Gamma_{\alpha 3\beta}$$

and

$$\Gamma_{\alpha\beta}^{3} = -\Gamma_{3\beta}^{\alpha} = \Gamma_{\beta\alpha}^{3} = -\Gamma_{3\alpha}^{\beta} = -\Gamma_{\alpha 3}^{\beta} \quad .$$

2.9 Surface Curvature.

Surface curvature along some path on the surface is the rate of change of the direction of the surface normal along that path. The direction but not the length of the surface normal vector, $\underline{a}_3$, depends on the coordinates ξ^α. The Curvature at any point on the surface is expressed in components along the coordinate lines on the surface. These components are given by

$$\underline{a}^3{}_{,\alpha} \cdot \underline{a}_\beta = -\Gamma^3_{\alpha\beta} = -b_{\alpha\beta} \quad , \tag{2.9.1}$$

where the $b_{\alpha\beta}$ are the components of the surface curvature tensor, also known as the second fundamental form of the surface. The above components are the covariant components, but the curvature tensor may also be defined by its mixed components b^β_α , by

$$\underline{a}_{3,\alpha} \cdot \underline{a}^\beta = -\Gamma^\beta_{3\alpha} = -b^\beta_\alpha \tag{2.9.2}$$

The third fundamental form of the surface, $c_{\alpha\beta}$, is defined by

$$c_{\alpha\beta} = b^\lambda_\alpha \, b_{\lambda\beta} \tag{2.9.3}$$

Two scalar invariants of the curvature tensor are sometimes used to as measures of curvature ; these are

mean curvature : $\quad b^\alpha_\alpha$;

Gaussian curvature : $\quad \det\left[b^\alpha_\beta \right]$.

2.10 Covariant Derivative.

The derivative of vector $\underline{v}$ with respect to ξ^α (see 2.8.1) can be written as

$$\underline{v}_{,\beta} = v_\alpha \|_\beta \underline{a}^\alpha + v_3 \|_\beta \underline{a}^3 \qquad (3.10.1)$$

where $v_i \|_\beta$ are the covariant derivatives of components v_i.

By using the relations and definitions of section 2.9.

$$v_\alpha \|_\beta = v_{\alpha,\beta} - v_\lambda \Gamma_{\alpha\beta}^{\lambda} - v_3 b_{\alpha\beta} \qquad (2.10.2)$$

and

$$v_3 \|_\beta = v_{3,\beta} + v_\lambda b_\beta^\lambda \qquad (2.10.3)$$

Components of derivatives tangential to the surface are often of interest. The tangential covariant derivative is defined by

$$v_\alpha |_\beta = v_{\alpha,\beta} - v_\lambda \Gamma_{\alpha\beta}^{\lambda} \qquad (2.10.4)$$

so that

$$v_\alpha \|_\beta = v_\alpha |_\beta - v_3 b_{\alpha\beta} \qquad (2.10.5)$$

and

$$\underline{v}_{,\beta} = (v_\alpha |_\beta - v_3 b_{\alpha\beta})\underline{a}^\alpha + (v_{3,\beta} + v_\lambda b_\beta^\lambda)\underline{a}^3 \qquad (2.10.6)$$

Note that "$\|$" is used for the full covariant derivative and "$|$" for the surface tangent or "planar" covariant derivative ; in some texts, notably Flugge (1972), the opposite convention is used, but Koiter (1970) is followed here.

2.11 Concluding Remark.

The cylindrical surface example used in this chapter has many zero components in the tensors describing its geometry. This is because it is a developable, single curvature, surface. A doubly curved surface has also been studied the details of the specific geometries used may be found in Table 7.1.

CHAPTER 3

FORMULATION OF SHELL PROBLEMS.

3.1. Introductory Remarks.

The degree and distribution of deformation which an elastic shell undergoes under any particular set of conditions is governed by a variational or energy principle. The variational principle is presented and two special problems, deformation due to static loading and free vibration modal analysis are extracted. A strain energy functional is required for both of these problems. Formulation of the strain energy functional for shells follows that given by Ciarlet due to Koiter (Ciarlet 1976, Koiter 1970). The free vibration problem is obtained by consideration of kinetic and potential energy. In the resulting eigenvalue problem the kinetic energy functional is reduced to a "mass term", the formulation of which is given.

Thin shell theory arising from the Kirchhoff-Koiter assumptions is used. The kinematic relations for the shell are developed using these assumptions. Displacements and strains through the thickness of the shell are related to shell mid-surface quantities. Strain measures are derived in terms of mid-surface displacement covariant components and their derivatives. Boundary conditions are briefly discussed, and expressions for stress resultants are given.

3.2 The Energy Princple Governing Elastic Shell Behaviour.

The energy principle governing the full transient behavior of an elastic body is Hamilton's Principle, where the functional considered is ;

$$J = \int_{t_1}^{t_2} (T - V) \, dt + \int_{t_1}^{t_2} W \, dt \qquad (3.2.1a)$$

or

$$J = \int_{t_1}^{t_2} (T - \Pi) \, dt \qquad (3.2.1b)$$

with

J is the total energy

T is the total kinetic energy

V is the internal potential energy of the body, the strain energy

W is the potential of externally applied conservative forces i.e.loading and damping forces.

Π is the total potential energy, $\Pi = V - W$

The principle states that all paths of configurations that a body takes up as it goes from configuration 1, at time t_1, to configuration 2, at time t_2, satisfy Newton's law (conservation of momentum) at every instant during the interval (t_2-t_1). The actual path is thus a locus of configurations, and is the path which extremizes the functional J for the interval (Dym and Shames 1973).

The energy of an elastic body is characterised by its deformation described by its displacement field, $\underline{v} = \underline{v}(\xi^{\alpha},z,t)$. Determination of the displacements is a boundary value problem, BVP. The energy functionals used in the energy principle are global measures of energy for the body. The energy functionals have the following form :

Kinetic Energy Functional ;

$$T(\underline{v}) = \frac{1}{2}\int_{\hat{\Omega}} \rho\ \dot{\underline{v}}.\dot{\underline{v}}\ \partial\Omega = C(\dot{\underline{v}},\dot{\underline{v}}) \qquad \text{a bilinear form.}$$

Strain Energy Functional ;

$$V(\underline{v}) = \frac{1}{2}\int_{\hat{\Omega}} \sigma(\underline{v})\ .\ \epsilon(\underline{v})\ \partial\Omega = D(\underline{v},\underline{v}) \qquad \text{a bilinear form.}$$

External Work (damping assumed zero) ;

$$W(v) = \int_{\hat{\Omega}} P(\xi^{\alpha},z,t).\underline{v}\ \partial\Gamma \qquad \text{a linear form,}$$

where $P(\xi^{\alpha},z,t)$ is the loading function.

Extremization of the functional $J(\underline{v})$ implies that its Gateaux derivative is zero for some displacement configuration $\underline{u} \in \underline{V}$, ie. ;

$$DJ(\underline{u})\underline{v} = 0 \qquad \forall\ \underline{v} \in \underline{V} \qquad (3.2.2)$$

where $\underline{V}$ is the space of admissible configurations for the body.

It is assumed that displacement field for a shell has the form

$$\underline{v}(\xi^{\alpha},z,t) = \underline{v}(\xi^{\alpha},z)\ e^{-\imath\omega t} \qquad \dot{\underline{v}} = -\imath\omega\ \underline{v} \tag{3.2.3}$$

where $\imath = \sqrt{-1}$

and ω is a natural frequency a mode of vibratuion of the shell.

The functional $J(\underline{v})$ to be extremised can then be written as ;

$$J(\underline{v}) = \int_{t_1}^{t_2} (-\omega^2 C(\underline{v},\underline{v}) - (D(\underline{v},\underline{v}) - W(\underline{v}))\ e^{-\imath\omega t}\ dt \tag{3.2.4}$$

The special cases of this extremisation problem considered are outlined below.

3.2.1 Displacement under static loading.

Loading is constant with respect to time and no vibration is considered ($\omega = 0$). Performing the time integration in (3.2.4) the functional $J(\underline{v})$ becomes ;

$$J(\underline{v}) = -(t_1 - t_2)\ (D(\underline{v},\underline{v}) - W(\underline{v})) \tag{3.2.5}$$

The second term on right hand side of this expression is the total potential energy, a positive definite quantity. Since the interval is arbitrary, but non-zero, the extremisation problem is equivalent to a minimization of total potential energy. Minimum total potential energy is the energy state associated with equilibrium of a body. This minimisation problem implies the

following variational boundary value problem (VBVP) see for example Reddy (1987) ;

$$\text{Find } \underline{u} \in V \mid D(\underline{v},\underline{v}) = W(\underline{v}) \quad \forall\ \underline{v} \in \underline{V} \ . \tag{3.2.6}$$

3.2.2 Free vibration modal analysis.

Where no loading or damping forces are applied, a displacement configuration, or mode shape, corresponding every natural frequency of the shell can be found which satisfies Hamilton's Principle. Performing the time integration the functional to be extremised becomes

$$J(\underline{v}) = \frac{1}{\imath\omega}(e^{-\imath\omega t_2} - e^{-\imath\omega t_1}) \left(-\omega^2 C(\underline{v},\underline{v}) - D(\underline{v},\underline{v}) \right) \ . \tag{3.2.7}$$

For non trivial cases ie. $\omega \neq 0$, the first term is non-zero for any arbitrary time interval. On application of the Gateaux derivative the extremisation problem reduces to the following eigenvalue problem ;

$$D(\underline{u},\underline{v}) - \lambda\, C(\underline{u},\underline{v}) = 0 \qquad \forall\ \underline{v} \in \underline{V} \tag{3.2.8}$$

where

λ are the eigenvalues of the system

$\lambda = -\omega^2$ and,

$\underline{u}$ are mode shapes, eigenfunctions, corresponding to the natural frequencies ω found for the shell from the characteristic equation (3.2.8).

An alternative method of obtaining this eigenvalue problem has been presented by Eve and Reddy (1987).

3.3 Shell Kinematics Using Thin Shell Assumptions.

The assumptions used for thin shell theory are ;

a) Normals to the undeformed shell mid-surface remain normal after deformation.

b) The state of stress in the shell is approximately planar and parallel to the shell mid-surface.

These assumptions effectively imply that the shear stress through the thickness of the shell is negligible. The thickness, h, of the shell will be assumed constant throughout this study. All points in the shell have coordinate z such that $-\frac{h}{2} \leq z \leq \frac{h}{2}$.

Any point in the shell lies on a surface distance z from the shell mid-surface and parallel to it, as shown in figure 3.1. Thin shell problems are simplified by relating all quantities of interest to the mid-surface. This is done by relating the geometry of the general surface described above to that of the shell mid-surface.

In figure 3.1 points A and B have the same coordinates ξ^α. The surfaces through these points are parallel so that they have the same normal vector, ie. $\underline{a}_3(\xi^\alpha) = \underline{g}_3(\xi^\alpha)$, and their position vectors are related by

$$\underline{r}(\xi^\alpha) = \underline{s}(\xi^\alpha) + z\underline{a}_3(\xi^\alpha) \quad . \tag{3.3.1}$$

Hence

$$\underline{r}_{,\alpha} = \underline{s}_{,\alpha} + z_{,\alpha}\underline{a}_3 + z\underline{a}_{3,\alpha} \quad . \tag{3.3.2}$$

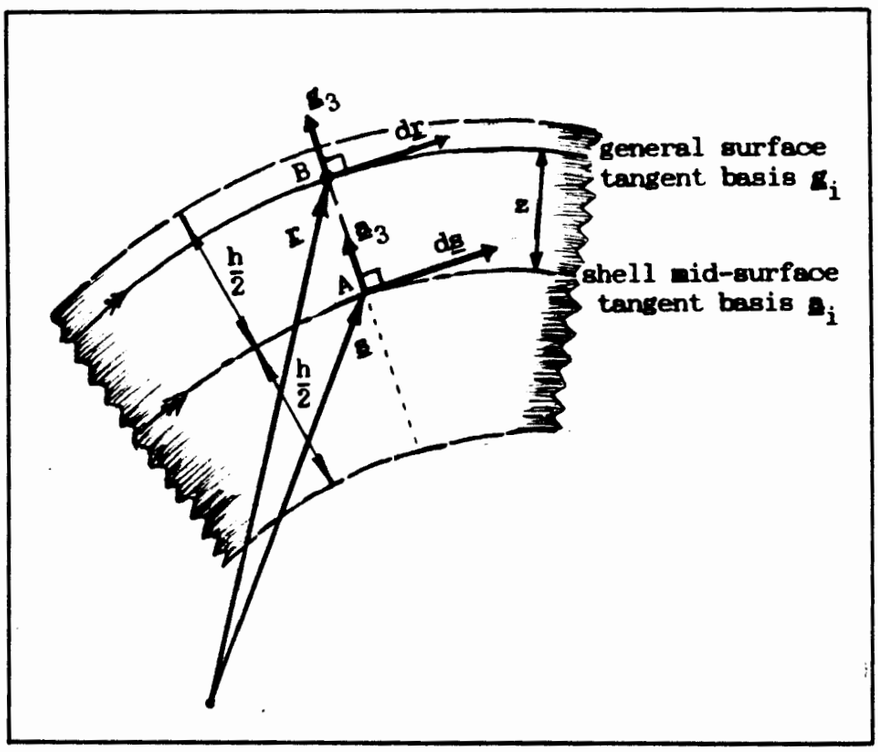

Figure 3.1.: Points off the shell mid-surface.

Noting the relationships given in chapter 2,

$$\underline{g}_\alpha = \underline{a}_\alpha - z b_\alpha^\lambda \underline{a}_\lambda \qquad (3.3.3)$$

and

$$g_{\alpha\beta} = a_{\alpha\beta} - z2b_{\alpha\beta} + z^2 c_{\alpha\beta} \qquad (3.3.4)$$

Deformation of the shell mid-surface is described by the displacement field $\underline{u}(\xi^\alpha)$ with components $u_i(\xi^\alpha)$, relative to the undeformed surface tangent basis $\underline{a}_i$. Figure 3.2 (Flugge 1972) shows how the deformed shell is related to the undeformed shell through the displacement $\underline{u}$.

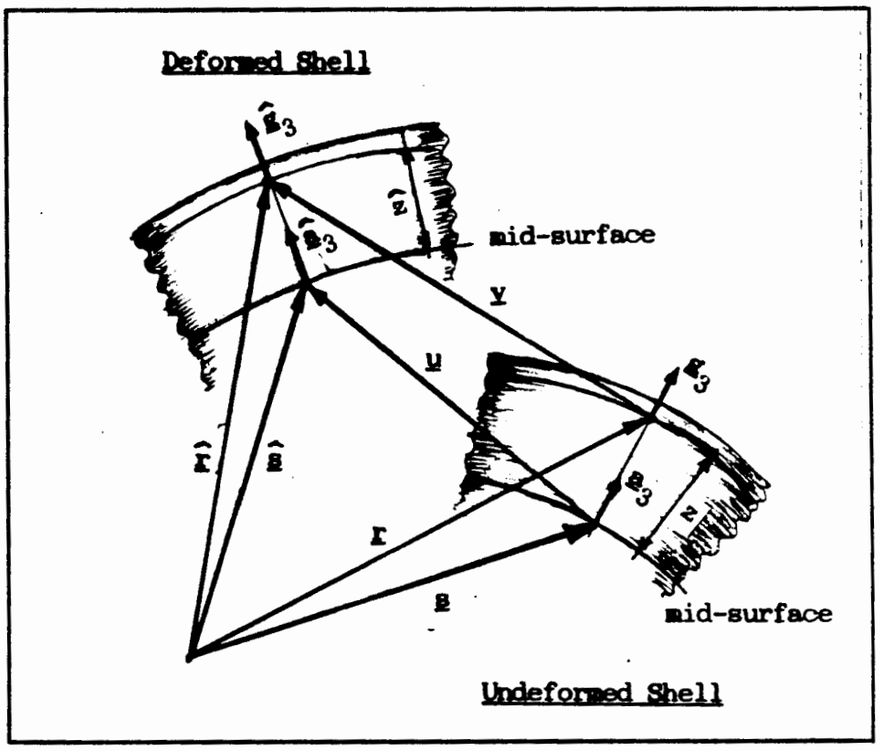

Figure 3.2.: Shell kinematics.

From figure 3.2 it is seen that $\hat{\underline{s}} = \underline{s} + \underline{u}$, so that

$$\hat{\underline{s}}_{,\alpha} = \underline{s}_{,\alpha} + \underline{u}_{,\alpha} \tag{3.3.5}$$

which is,

$$\hat{\underline{a}}_{\alpha} = \underline{a}_{\alpha} + (u_{\lambda}|_{\alpha} - u_3 b_{\lambda\alpha}) \underline{a}^{\lambda} + (u_{3,\alpha} + u_{\lambda} b^{\lambda}_{\alpha}) \underline{a}^{3} \quad . \tag{3.3.6}$$

The displacement $\underline{v} = \underline{v}(\xi^{\alpha},z)$ at any point, is related to the mid-surface displacement $\underline{u}(\xi^{\alpha})$ by assuming $\hat{z} \approx z$, and $u_3 = v_3$ (by an assumption of small displacements),

$$\underline{v} = \underline{u} + z(\hat{\underline{a}}_3 - \underline{a}_3) \quad . \tag{3.3.7}$$

From figure 3.2,

$$\hat{\underline{r}} = \underline{r} + \underline{v} \tag{3.3.8}$$

and

$$\hat{\underline{r}}_{,3} = \underline{r}_{,3} + \underline{v}_{,3} \quad . \tag{3.3.9}$$

By conservation of normals,

$$u_{\alpha,3} + u_{3,\alpha} = -2u_{\lambda}b_{\alpha}^{\lambda}$$

so that

$$u_{\alpha,3} + u_{\lambda}b_{\alpha}^{\lambda} = -(u_{3,\alpha} + u_{\lambda}b_{\alpha}^{\lambda}) \quad . \tag{3.3.10}$$

Letting z tend to zero in (3.3.9),

$$\hat{\underline{s}}_{,3} = \underline{s}_{,3} + \underline{u}_{,3} \tag{3.3.11}$$

which is,

$$\hat{\underline{a}}_3 = \underline{a}_3 + (u_{\alpha,3} + u_{\lambda}b_{\alpha}^{\lambda})\underline{a}^{\alpha} + u_{3,3}\underline{a}^{3} \tag{3.3.12}$$

using (3.3.10), and since $u_{3,3} = 0$ by the small displacement assumption,

$$\hat{\underline{a}}_3 - \underline{a}_3 = -(u_{3,\alpha} + u_{\lambda}b_{\alpha}^{\lambda})\underline{a}^{\alpha}$$

therefore from (3.3.7),

$$\underline{v} = u_{\alpha}\underline{a}^{\alpha} + u_3\underline{a}^{3} - z(u_{3,\alpha} + u_{\lambda}b_{\alpha}^{\lambda})\underline{a}^{\alpha} \quad . \tag{3.3.13}$$

3.4 Shell Strain Tensors.

Starting with the full strain tensor ϵ_{ij} it is first noted that the components $\epsilon_{3\alpha} = \epsilon_{\alpha 3}$ are zero. This results from the assumption of conservation of normals. The component ϵ_{33} is non-zero by the plane stress assumption, however the strain energy terms involving ϵ_{33} are zero since $\sigma_{33} = 0$. It is therefore only necessary to find expressions for the strain components $\epsilon_{\alpha\beta}$.

Strains are given by the change in length of infinitesimal line elements. The strains in such line elements situated through the shell thickness are related to those on the mid-surface. To do this consider the line elements shown in figure 3.1, $d\underline{r}$ at point B tangent to the general surface, and $d\underline{s}$ at A tangent to the mid-surface. The line element $d\underline{r}$ is related to $d\underline{s} = d\xi^{\alpha}\underline{a}_{\alpha}$.

$$d\underline{r} = (\underline{a}_{\alpha} - zb^{\lambda}_{\alpha}\underline{a}_{\lambda}) \, d\xi^{\alpha} \tag{3.4.1}$$

with length

$$d\underline{r}.d\underline{r} = (a_{\alpha\beta} - z2b_{\alpha\beta} + z^2 c_{\alpha\beta}) \, d\xi^{\alpha} d\xi^{\beta} \tag{3.4.2}$$

Considering the strain of any line element parallel to the mid-surface the general strain tensor $\epsilon_{\alpha\beta}$ is obtained.

$$\epsilon_{\alpha\beta} = \frac{1}{2} (\hat{g}_{\alpha\beta} - g_{\alpha\beta}) \tag{3.4.3}$$

By using (3.3.4) and expressing $\hat{z}$ as $\hat{z} = z (1 + \epsilon_{33})$, $\epsilon_{\alpha\beta}$ is expressed in terms of mid-surface quantities and ϵ_{33} :

$$\epsilon_{\alpha\beta} = \frac{1}{2} \left[(\hat{a}_{\alpha\beta} - a_{\alpha\beta}) - 2z(\hat{b}_{\alpha\beta} - b_{\alpha\beta}) + z^2(\hat{c}_{\alpha\beta} - c_{\alpha\beta}) \right] + z2\hat{b}_{\alpha\beta}\epsilon_{33} + z^2((1 + \epsilon_{33}) - 1) \, \hat{c}_{\alpha\beta} \quad . \tag{3.4.4}$$

Note superscripts to z imply powers since z is a scalar quantity.

This expression is simplified by linearising with respect to z. This is reasonable since $|z| \leq \frac{h}{2}$ and h is considered small, $\frac{h}{R} << 1$ by the "thin" shell assumption (R is the radius of curvature of

the shell). Terms in ϵ_{33} are dropped for the purposes of energy calculations. The strain tensor $\epsilon_{\alpha\beta}$ is then given in two parts, the mid-surface strain tensor $\gamma_{\alpha\beta}$, and the mid-surface change of curvture tensor $\rho_{\alpha\beta}$:

$$\epsilon_{\alpha\beta} = \gamma_{\alpha\beta} + z\ \rho_{\alpha\beta} \tag{3.4.5}$$

where

$$\gamma_{\alpha\beta} = \frac{1}{2}\ (\hat{a}_{\alpha\beta} - a_{\alpha\beta}) \tag{3.4.6}$$

and

$$\rho_{\alpha\beta} = \ (\hat{b}_{\alpha\beta} - b_{\alpha b}) \tag{3.4.7}$$

The strain energy functional is required in terms of displacements. To achieve this the strain quantities, identified above, are related to the displacement components and their derivatives, using the relationships (3.3.4) and (3.3.13). Assuming displacements to be small, terms which are non-linear in components u_i and their derivatives can be considered negligible. Using this simplification in the expansion of $\hat{a}_{\alpha\beta}$ and $\hat{b}_{\alpha\beta}$, the strain tensors $\gamma_{\alpha\beta}$ and $\rho_{\alpha\beta}$ may be given in the following form :

$$\gamma_{\alpha\beta} = \frac{1}{2}\ (\ u_\alpha|_\beta + u_\beta|_\alpha\ ) - u_3 b_{\alpha\beta}\ , \tag{3.4.8}$$

$$\rho_{\alpha\beta} = u_3|_{\alpha\beta} - c_{\alpha\beta}u_3 + b^\lambda_\alpha u_\lambda|_\beta + b^\lambda_\beta u_\lambda|_\alpha + b^\lambda_\alpha|_\beta u_\lambda\ . \tag{3.4.9}$$

Note the relationships ;

$$\gamma^\alpha_\beta = \gamma_{\lambda\beta}\ a^{\lambda\alpha} \quad \text{and} \quad \rho^\alpha_\beta = \rho_{\lambda\beta}\ a^{\lambda\alpha}\ . \tag{3.4.10}$$

Alternative expanded expresions for these tensors are

$$\gamma_{\alpha\beta} = \frac{1}{2} \left(u_{\alpha,\beta} + u_{\beta,\alpha} \right) - u_\lambda \Gamma^{\lambda}_{\alpha\beta} - u_3 b_{\alpha\beta} \qquad (3.4.11)$$

and

$$\rho_{\alpha\beta} = u_{3,\alpha\beta} + u_{\lambda,\beta} b^{\lambda}_{\alpha} + u_{\lambda,\alpha} b^{\lambda}_{\beta} - u_{3,\lambda} \Gamma^{\lambda}_{\alpha\beta} + u_3 c_{\alpha\beta} + \frac{1}{2} \left(b^{\lambda}_{\alpha,\beta} + b^{\lambda}_{\beta,\alpha} - 2\Gamma^{\eta}_{\alpha\beta} b^{\lambda}_{\eta} \right) u_\lambda \quad . \qquad (3.4.12)$$

3.5 Shell Strain Energy Functional.

Koiter summarises the assumptions made for stress and strain in the shell with the following three statements :

a) The material of the shell is elastic, homogenous and isotropic.

b) Strains are small everywhere in the shell.

c) The state of stress is approximately plane and parallel to the middle surface.

The constitutive law for linear elastic plane strain relates the stresses to the strains by :

$$\sigma^{\alpha}_{\beta} = \frac{E}{(1-\nu^2)} \left[(1-\nu)\epsilon^{\alpha}_{\beta} + \nu\epsilon^{\eta}_{\eta}\delta^{\alpha}_{\beta} \right] \qquad (3.5.1)$$

where E is Youngs modulus of elasticity,

and ν is Poisons ratio.

The strain energy functional, $D(\underline{v},\underline{v})$, is then written as ;

$$D(\underline{v},\underline{v}) = \int_{\hat{\Omega}} \left(\bar{\sigma}^{\alpha}_{\beta}\gamma^{\beta}_{\alpha} + \hat{\sigma}^{\alpha}_{\beta}\rho^{\beta}_{\alpha} \right) \partial\hat{\Omega} \qquad (3.5.2)$$

Substituting for the stresses using (3.4.1) ,

$$D(\underline{v},\underline{v}) = \int_{\hat{\Omega}} \frac{E}{(1-\nu^2)} \Big[((1-\nu)\gamma^{\alpha}_{\beta}\gamma^{\beta}_{\alpha} + \nu\gamma^{\alpha}_{\alpha}\gamma^{\beta}_{\beta}) + z^2((1-\nu)\rho^{\alpha}_{\beta}\rho^{\beta}_{\alpha} + \nu\rho^{\alpha}_{\alpha}\rho^{\beta}_{\beta}) \Big] \partial\hat{\Omega} \tag{3.5.3}$$

where,

$$\gamma^{\alpha}_{\beta} = \gamma^{\alpha}_{\beta}(\underline{v}(\xi^{\alpha})) \quad , \quad \rho^{\alpha}_{\beta} = \rho^{\alpha}_{\beta}(\underline{v}(\xi^{\alpha})) \ ,$$

and

$$\partial\hat{\Omega} = \partial s \partial z = \sqrt{a}\ \partial\xi^1\partial\xi^2\partial z \quad .$$

Integration is easily divided into that through the thickness and that over the shell midsurface. It is convinient but not necessary to preform the z integration analytically. All remaining terms in the integral are then functions of ξ^1,ξ^2, and the intergration may be performed over the domain $\Omega \subset \Lambda^2$.

$$D(\underline{v},\underline{v}) = \int_{\Omega} \frac{Eh}{(1-\nu^2)} \Big[((1-\nu)\gamma^{\alpha}_{\beta}\gamma^{\beta}_{\alpha} + \nu\gamma^{\alpha}_{\alpha}\gamma^{\beta}_{\beta}) + \frac{h^2}{12}((1-\nu)\rho^{\alpha}_{\beta}\rho^{\beta}_{\alpha} + \nu\rho^{\alpha}_{\alpha}\rho^{\beta}_{\beta}) \Big] \sqrt{a}\partial\xi \tag{3.5.4}$$

3.6 Stress Resultants.

"Stress resultant" is the term used for the effect over unit length on the mid-surface of the stresses through the thickness of the shell. Using the stress strain relation (3.5.1) and the strain displacement relations (3.4.6) and (3.4.7), the membrane

$$C(\underline{u},\underline{v}) = \rho \int_{\Omega} \Big[h\, u_\alpha v_\beta a^{\alpha\beta} + \frac{h^3}{12} (u_{3,\eta} v_{3,\lambda} + u_\zeta b^\zeta_\eta v_{3,\lambda} + u_{3,\eta} v_\mu b^\mu_\lambda + u_\zeta v_\mu b^\zeta_\eta b^\mu_\lambda)\, a^{\eta\lambda} + u_3 v_3 \Big] \partial\Omega \,. \tag{3.7.3}$$

3.8. External Work.

Externally applied conservative forces and couples are assumed to act on the shell mid-surface. The work done on the shell is therefore the product of these forces and couples with the corresponding mid-surface displacements and rotations, integrated over the surface. A linear functional, $W(\underline{v})$, is the measure of external work; it is given in full by

$$W(\underline{v}) = \int_{\Omega} (p^\alpha v_\alpha + p^3 v_3)\, \partial s + \int_{\Gamma_N} N^\alpha v_\alpha\, \partial\Gamma + \int_{\Gamma_Q} Q v_3\, \partial\Gamma + \int_{\Gamma_{M_n}} M_n n^\alpha \theta_\alpha\, \partial\Gamma + \int_{\Gamma_{M_t}} M_t t^\alpha \theta_\alpha\, \partial\Gamma$$

where

θ_α are shell mid-surface rotations along coordinate lines ξ^α

$\theta_\alpha = v_{3,\alpha} + b^\lambda_\alpha v_\lambda$

p^α, p^3 are components of load prescribed on Ω.

N^α, Q are components of forces acting on portions of the boundary Γ_N and Γ_Q, ($Q = N^3$ a shearing force).

M_n, M_t are the normal (bending) and tangential (twisting) moments prescribed on portions of the boundary Γ_{M_n} and Γ_{M_t} in the directions of unit normal and tangential vectors, $\underline{n}$ and $\underline{t}$.

3.8 Boundary Conditions.

In order to fully specify the boundary conditions either the forces or couples acting on the boundary or displacements or rotations on the boundary must be specified. The boundary is described in parts on which different conditions apply ;

Γ_N known in-plane force $\underline{N} = N^\alpha \underline{a}_\alpha$ acting,

$\Gamma - \Gamma_N$ prescribed in-plane displacements u_α

Γ_Q known transverse, shearing, force $Q = N^3$,

$\Gamma - \Gamma_Q$ prescribed transverse displacement u_3

Γ_{M_n} known boundary normal bending moment M_n

$\Gamma - \Gamma_{M_n}$ prescribed rotation $\theta_n = \underline{n} \cdot \underline{\ell}$

Γ_N known twisting moment M_t

$\Gamma - \Gamma_N$ prescribed twist $\theta_t = \underline{t} \cdot \underline{\ell}$

"Essential" boundary conditions are those for which displacements or rotations are prescribed. On these portions of the boundary the reaction forces acting are unknown. Where loads are applied on the boundary, the boundary conditions are "natural".

3.10 The Space V of Admissible Displacements.

In this chapter the energy functionals have been formulated in terms of displacement components and their derivatives, for the VBVPs derived in section 3.2. to be valid the functionals must be defined. That is it must be possible to evaluate the required integrals. This places a restriction on the displacement

component functions.

First partial derivatives of tangential components u_α, $u_{\alpha,\beta}$, and first and second partial derivatives of the normal component u_3, $u_{3,\alpha}$, $u_{3,\alpha\beta}$ appear in functions to be integrated. Hence ;

$$\underline{V} = \{(u_1,u_2,u_3) \in (H^1(\Omega)xH^1(\Omega)xH^2(\Omega)) :$$
$$u_i \text{ satisfy essential boundary conditions.}\}$$

where,

$H^m(\Omega)$ is a Hilbert space on Ω, that is u and derivatives of order $\leq m \in L_2(\Omega)$, $u \in L_2(\Omega)$ if $\int_\Omega u^2 < \infty$.

The requirement that u_3 should belong to $V_3 \subset H^2(\Omega)$ has consequences effecting the finite element discretization of displacements.

3.11 Concluding Remarks.

An important aspect of this chapter has been the formulation of expressions for the bilinear forms $D(\underline{v},\underline{v})$ and $C(\underline{v},\underline{v})$. These will form the basis of the finite element formulation to be discussed in the next chapter. All the infomation specific to shells is contained in these two terms. A full transient analysis of shells only requires the addition of a time integration scheme and a calculation for damping.

C H A P T E R 4

FORMULATION OF A CONFORMING FINITE ELEMENT APPROXIMATION FOR SHELL PROBLEMS.

4.1. Introductory Remarks.

Exact solutions to shell problems have only been found for a very few special cases. Such special cases involve shells of simple geometry under simple loadings. To obtain solutions to shell problems of a more general nature recourse is made to approximate methods, in particular the Finite Element Method. The displacement of a shell is described by the displacement field, $\underline{u}(\xi^1,\xi^2)$, defined on the domain $S \subset E^3$ (see Ch. 3.). It has an infinite number of degrees of freedom, and may also be described by a set of three functions, u_i on the domain $\Omega \subset E^2$, which have the form ;

$$u_i : \xi \in \bar{\Omega} \rightarrow u_i(\xi) \in$$

These functions are the components of the displacement vector $\underline{u} = \underline{u}(\xi^1,\xi^2)$ of a point $\underline{\phi}(\xi^1,\xi^2)$ on $S \in E^3$, in this case the covariant components :

$$\underline{u}\,(\xi^\alpha) = u_i(\xi^\alpha)\underline{a}^i(\xi^\alpha) \ , \qquad \text{where} \qquad \underline{a}^i = \underline{a}^i(\underline{\phi}(\xi^\alpha)) \ .$$

Simplification of the problem is achieved by discretisation of the continuous functions $u_i(\xi^\alpha)$. Each of the displacement components is thus constrained to a finite number of degrees of freedom.

The finite element method provides a systematic method of discretising any function over a given domain. A brief description of the method is given in this chapter. This description contains definition of notation and terminology to be used in later discussion. Attention is paid to 2-dimensional cases, and the use of derivative degrees of freedom. The concept of conforming finite elements is presented, and particular reference is made to the application of the finite element method to shell problems. Detailed treatments of finite element theory can be found in a number of texts, for example Bathe (1982), Cook (1981), Datt and Touzot (1984), Carey and Oden(1979), and Zienkiewicz (1977).

In this chapter the functionals identified in chapter 4 are presented in a form particularly suited to the use of conforming finite elements. Approximation of the geometry, using an approximate mapping is discussed. The consequences of discretization of the displacements, and the approximation of geometry, are outlined with respect to the energy principle.

4.2 The Finite Element Method

4.2.1 Introduction

The finite element method is a particular case of the Galerkin approximation to a variational boundary value problem, VBVP. The Galerkin Method makes use of the following notions.

By Fourier series theory any function v belonging to a Hilbert space V on a domain Ω, can be expressed as a linear combination of infinitely many basis functions $\Lambda_i(\xi)$ defined on Ω ;

$$v = \sum_{i=1}^{\infty} a_i \Lambda_i \qquad v, \Lambda_i \in V \quad a_i \in R \qquad (4.2.1.)$$

The coeffficients a_i form an infinite set of degrees of freedom for the function v, in the infinite-dimensional space V, which is spanned by $\{\Lambda_i\}_{i=1}^{\infty}$.

An approximation v_h to v is obtained by choosing a finite number of linearly independant functions Λ_i such that

$$v_h = \sum_{i=1}^{N} a_i \Lambda_i \qquad v_h , \Lambda_i \in V_h , \qquad (4.2.2)$$

where V_h is a finite dimensional space defined by

$$\text{span}\{ \Lambda_i \}_{i=1}^{N} = V_h \quad ,$$

and the coefficients a_i are the N degrees of freedom of the approximate function v_h.

A VBVP of the form ;

$$\text{Find} \quad u \in V \mid B(u,v) = l(v) \ , \ \forall \ v \in V \tag{4.2.3}$$

has approximate solution $u_h \in V_h$ which satisfies

$$B(u_h,v_h)=l(v_h) \ , \ \forall \ v_h \in V_h \tag{4.2.4}$$

Substituting for u_h and v_h, in (4.2.4) using the form (4.2.2) with dofs. a_i and b_j for the functions u_h and v_h respectively, the VBVP is expressed as ;

Find $\{a_i\}$ such that

$$\sum_{i=1}^{N} \sum_{j=1}^{N} B(\Lambda_i,\Lambda_j)a_i b_j = \sum_{j=1}^{N} l(\Lambda_j)b_j \quad , \quad \forall \ b_j \in R$$

Since the v_h are arbitrary, the coefficients b_j may be cancelled, leaving N linear equations in the N coefficients a_i. This set of linear equations is often written in the form ;

$$[K] \{a\} = \{f\} \tag{4.2.5}$$

where,

[K] is an NxN matrix, coefficients $K_{ij} = B(\Lambda_i,\Lambda_j)$

{a} is an N-tuple vector of degrees of freedom a_i

{f} is an N-tuple vector, entries $f_j = l(\Lambda_j)$.

The finite element method is a systematic method for choosing the interpolation functions Λ_i which form a basis for the space V_h. The space V_h is then called the finite element space or the discrete space of the problem. The continuity requirements for the functions $v_h \in V_h$ are discussed in section 4.3.

4.2.2 Elements and Nodes.

To choose the Λ_i the domain Ω is first subdivided into E subdomains, Ω_e, called finite elements, such that

$$\Omega_e \cap \Omega_f = 0 \qquad e \neq f \qquad e,f = 1,E \tag{4.2.6}$$

and

$$\bigcup_{e=1}^{E} \bar{\Omega}_e = \bar{\Omega} \quad .$$

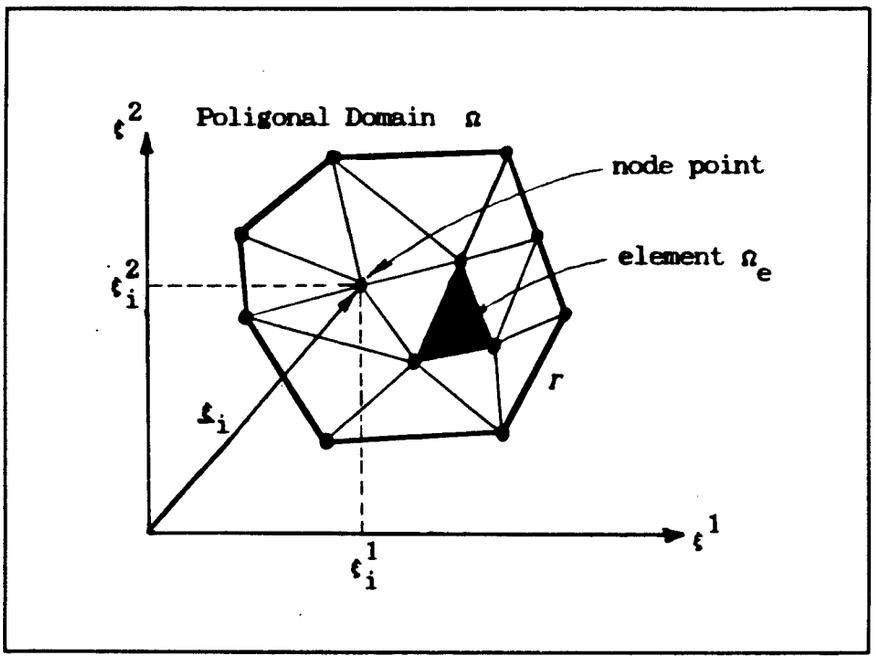

Figure 4.1.: Discretization of the domain Ω.

For the shell problem the domain $\Omega \in E^2$ is assumed to be polygonal. It may therefore be covered, in the sense of (4.2.6) above, by a triangulation. The triangles are used as the finite elements Ω_e as shown in figure 4.1.

Non-polygonal domains may be mapped to polygonal shape via mappings applied to curved boundaries (Bernadou 1980). This added complication is not included in this study.

4.2.3 Basis Functions and Degrees of Freedom.

Basis functions Λ_i are chosen as piecewise polynomials on Ω. Each Λ_i is associated with an interpolation point $\underline{\xi}_i = (\xi^1, \xi^2)$, called a node point. At each node point a set of nodal degrees of freedom is chosen. Function values $(v)_i$ and or values of the functions derivatives $(v_{,\alpha})_i$, $(v_{,\alpha\beta})_i$...etc. at the nodes are used. The basis functions have the following properties :

(i) The restrictions $\Lambda_i\big|_{\Omega_e} = \psi_i^{(e)}$ are polynomials, ie.

$$\psi_i^{(e)} \in X_e \subset P^k(\Omega_e)$$

where X_e is a subspace of the space P^k of all polynomials of order $\leq k$ defined on the element Ω_e.

(ii) $$\psi_i^{(e)}(\underline{\xi}_j) = \delta_{ij}$$

(iii) For the case with only function values $(v)_i$ as dof.s ,

$$v_h = \sum_{i=1}^{N} (v)_i \, \Lambda_i \qquad (4.2.7a),$$

with first partial derivatives ;

$$v_{h,\beta} = \sum_{i=1}^{N} (v)_i (\Lambda_i)_{,\beta} \, .$$

The basis functions are such that ,

$$\Lambda_i(n_j) = \begin{matrix} 0 & i \neq j \\ 1 & i = j \end{matrix} .$$

In this case each node has only one basis function associated with it. The total number of degrees of freedom N is equal to the total number of nodes n.

Figure 4.2 shows a basis function of this type ;

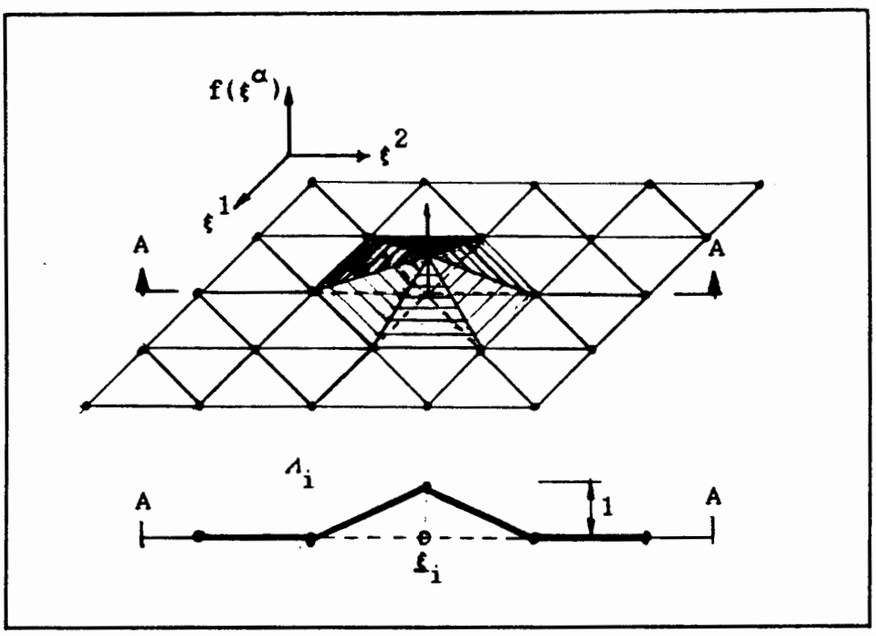

Figure 4.2.: Simple Lagrangian type basis function.

For the 2D case with function values $(v)_i$ and first partial derivatives $(v,_\alpha)_i$ as dofs. , the sets of basis functions Λ_i and Λ^α_i are used. Each node has 3 dofs. and the total number of dof.s, N = 3 x n . The function v_h, and its first derivatives are then given by

$$v_h = \sum_{i=1}^{n} (v)_i \Lambda_i + (v_{,\alpha})_i \Lambda^\alpha_i \qquad (4.2.8a)$$

and

$$v_{h\ ,\beta} = \sum_{i=1}^{n} (v)_i (\Lambda_i)_{,\beta} + (v_{,\alpha})_i (\Lambda_i^{\alpha})_{,\beta} \ . \qquad (4.2.8b)$$

The basis functions Λ_i and Λ_i^{α} are chosen such that

$$\Lambda_i(n_j) = \begin{matrix} 0 & i \neq j \\ 1 & i = j \end{matrix}$$

$$\text{and} \quad (\Lambda_i(n_j))_{,\beta} = 0 \quad \forall\ i,j \quad \beta = 1,2$$

$$\Lambda_i^{\alpha}(n_j) = 0 \qquad \forall\ i,j \quad \alpha = 1,2$$

$$\text{and} \quad (\Lambda_i^{\alpha}(n_j))_{,\beta} = \begin{matrix} 0 & \forall\ i,j & \alpha \neq \beta \\ 0 & i \neq j & \alpha = \beta \\ 1 & i = j & \alpha = \beta \end{matrix}$$

The finite element space for this case is defined by

$$\text{span}\{\ \Lambda_i\ ,\ \Lambda_i^{\alpha}\ \}_{i=1}^{n} = V_h \qquad \alpha = 1,2$$

Figure 4.3 shows a basis function of this type ;

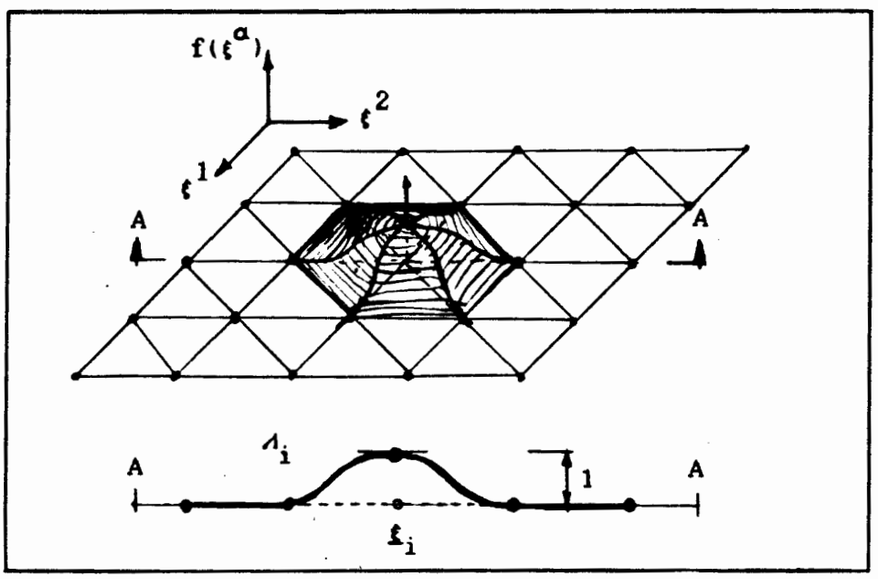

Figure 4.3.: Hermite type basis function.

Not all nodes need have the same set of degrees of freedom. Conditions for setting up basis functions where second or higher derivatives are to be used as nodal dof.s can be obtained by an extension of those shown above.

4.2.4 Element Calculations.

The functions $\psi_i^{(e)} = \Lambda_i\big|_{\Omega_e}$ are known as local basis functions or element shape functions. Since $\psi_i^{(e)} = 0$ outside Ω_e, only those shape functions corresponding to degrees of freedom at nodes on $\bar{\Omega}_e$ need be considered on Ω_e. Referring back to equation (4.2.5), the matrix [K] may be evaluated as the sum of element contributions, $[k_{ij}]^{(e)}$ from elements e = 1,E . These contributions arise by the following argument :

$$K_{ij} = B(\Lambda_i , \Lambda_j)$$

$$= \int_{\Omega} \ldots\ldots\ldots$$

$$= \sum_{e=1}^{E} \int_{\Omega_e} \ldots\ldots\ldots$$

$$= \sum_{e=1}^{E} k_{ij}^{(e)}$$

$$= \sum_{e=1}^{E} B^{(e)}(\psi_i^{(e)}, \psi_j^{(e)}) \quad .$$

$[k]^{(e)}$ is thus an N_e x N_e matrix, N_e the total number of dofs. at nodes on $\bar{\Omega}_e$.

4.2.5 Shells

For shell problems the three functions $u_i(\xi^\alpha)$ are independent on the domain Ω, their discretisation may therefore be carried out separately, using different triangulations. In practice numerical integration is used to evaluate terms involving products of different components or their derivatives. To perform this integration efficiently it is convenient or even necessary to use the same triangulation.

4.3. Conforming Finite Element Approximations

The VBVPs of the form (4.2.3) arrise from BVPs of order 2m. In the derivation of the VBVP assumtions are made as to the nature of the funtions $v \in V$. The space $\underline{V} = \{ \underline{v} \in H^m(\Omega) : \underline{v}$ satisfies all essential boundary conditions $\}$ is a subspace of the Hilbert space $H^m(\Omega)$, (see Ch.3.). The basis functions used to define the finite element space V_h determine the nature of its elements v_h. A reasonable condition on the approximation would seem to be that ;

$$V_h \subset V \subset H^m(\Omega)$$

which implies

$$v_{h,\lambda} \in V_{h\ ,\lambda} \subset H^{m-1}(\Omega)$$

$$v_{h,\lambda\mu} \in V_{h\ ,\lambda\mu} \subset H^{m-2}(\Omega) \ \ldots\text{etc.}$$

where,

$$V_{h\ ,\lambda} = \text{span}\{(\Lambda_i)_{,\lambda}, (\Lambda_i^\alpha)_{,\lambda}, (\Lambda_i^{\alpha\beta})_{,\lambda}, \ldots\ldots\}_{I=1}^{n}$$

$$V_{h\ ,\lambda\mu} = \text{span}\{(\Lambda_i)_{,\lambda\mu}, (\Lambda_i^\alpha)_{,\lambda\mu}, (\Lambda_i^{\alpha\beta})_{,\lambda\mu}, \ldots\}_{I=1}^{n}$$

A finite element approximation with choice of basis functions defining V_h such that $V_h \subset V \subset H^m(\Omega)$ is called a conforming

approximation. It is not necessary to make the choice of V_h in this way. Where V_h is not a subspace of V the term non-conforming is used. Existence and uniqueness of solutions to the VBVP (4.2.3) can be shown for conforming approximations if the bilinear functional B(.,.) is elliptic which is the case for shell formulations of the type presented in chapter 3 (Ciarlet 1975). For non-conforming methods a solution may be obtained but spurious solutions also arise since ellipticity of the functional is lost .

For a conforming approximation $v_h = \Lambda_i a_i \in V \subset H^m(\Omega)$, hence $\Lambda_i \in H^m(\Omega)$ and since $\Lambda_i\big|_{\Omega_e}$ is piecewise polynomial this is satisfied if $\Lambda_i \in C^{m-1}$.

For problems where $m \geq 2$ and piecewise polynomial interpolation is to be used, it can be shown that derivative degrees of freedom are required if the above conditions are to be met. For the 2-dimensional case with m=2 the set of nodal degrees of freedom function value, first and second partial derivatives corresponds to a set of basis functions which give C^1 continuity to v_h. The need for second derivatives arises from the need to uniquely define the derivative $v_{,n}$ normal to the interface Γ_{ij} between two elements Ω_i and Ω_j.

Proof that these degrees of freedom, defined at nodes, yield a C^1 continuous, piecewise polynomial function over a domain $\Omega \in R^2$ is given by Ciarlet (1980) ; where Ω is covered by a triangulation and nodes are chosen at the corners of the triangles. On each

triangle, Ω_e, the space X^e is defined such that;

$$P^4(\Omega_e) \subset X^e(\Omega_e) \subset P^5(\Omega_e).$$

The element using this scheme is the Bell triangle (see Ch.6).

The three unknown functions to be approximated in the shell problem, $u_\beta(\xi^\alpha)$ and $u_3(\xi^\alpha)$, belong to the spaces $V_\alpha \subset H^1(\Omega)$ and $V_3 \subset H^2(\Omega)$ respectively. In this study only conforming approximations are considered. For the approximation to be conforming for displacements,

$$\underline{V}_h \subset \underline{V} = V_1 \times V_2 \times V_3 \subset (H^1(\Omega) \times H^1(\Omega) \times H^2(\Omega)).$$

Since the same triangulation is to be used for interpolation of each of the three displacement component functions the set of displacement degrees of freedom at corner nodes must contain the set;

$$\{ (v_\alpha)_i , (v_3)_i , (v_{3,\alpha})_i \}. \qquad (4.3.1)$$

4.4 Shell Energy Functionals For The Direct Application Of Conforming Finite Element Approximations.

The bilinear and linear forms appearing in the shell VBVPs are rewritten in matrix form. The static probelm formulated in chapter 4 can be written in the alternative form below, proposed by Ciarlet (1976) ; note D_{IJ} is used here where Ciarlet uses A_{IJ}.

$$J(V_J) = \int_\Omega V_I D_{IJ} V_J \sqrt{a}\partial\xi - \int_\Omega F_J \sqrt{a}\partial\xi \qquad I,J = 1,12 \qquad (4.4.1)$$

where

$$V_I = \{ v_1 , v_{1,1} , v_{1,2} , v_2 , v_{2,1} , v_{2,2} , v_3 , v_{3,1} , v_{3,2} , v_{3,11} , v_{3,12} , v_{3,22} \} \quad (4.4.2)$$

F_J is a consistant forcing function or "load" vector.

The coefficients of the 12x12 matrix $[D_{IJ}]$ are all functions of shell mid-surface geometry, thickness h and material constants, ν and E. The geometry is characterised by the values, $a^{\alpha\beta}$, $b_{\alpha\beta}$, $c_{\alpha\beta}$, b^{β}_{α}, $b^{\beta}_{\alpha,\lambda}$, $\Gamma^{\lambda}_{\alpha\beta}$. These parameters are functions of ξ^{α} on $\Omega \subset E^2$, and are related to the partial derivatives of the mapping $\underline{\phi}(\xi^{\alpha})$, as defined in chapter 3. Hence

$$D_{IJ} = D_{IJ}(\phi_{,\alpha}, \phi_{,\alpha\beta}, \phi_{,\alpha\beta\lambda}, h, \nu, E) \quad ,$$

where the functions D_{IJ} are algebraic in their arguments, that is only the operations, +,-,x,÷,$\sqrt{\ }$, are used. They are obtained by substitution of (4.4.11) and (4.4.12) into the bilinear form given by (4.5.4), expanding the resulting expression, and collecting coefficients of like terms. This is a rather laborious process ; the 78 expressions obtained are given in Appendix B, together with some notes on the algebra described above. No reference was found containing the D_{IJ}, expressed in terms of the arguments indicated above, with which to preform an independent check on this work. Bernadou (1980) shows the matrix $[D_{IJ}]$ for the special case of a cylindrical shell in terms of the radius R, and this provided a partial check on some of the D_{IJ}.

It is observed that the set of components in V_I evaluated at a point i on Ω contains the set of nodal degrees of freedom required for a conforming finite element approximation. This suggests the suitability of this form of the shell minimisation problem to approximation by such a method. It has been used as a basis for this study. The $v_{\alpha,\beta}$ values are not nesessarily required as nodal degrees of freedom and can be obtained form partial derivatives of v_{α_h} see (4.2.7b).

Rewriting of the mass term functional in matrix form is considerably simpler than for the strain energy functional. A 12x12 matrix $[C_{IJ}]$ is formed so that the same vector V_I can be used. Only 11 of the coefficients are potentially non-zero ; these are also given in Appendix B. The eigen value problem is rewritten as

$$\int_{\Omega} V_I \left[D_{IJ} - \lambda C_{IJ} \right] U_J = 0 \quad . \qquad (4.4.3)$$

4.5 Approximate Mapping.

Description of geometry is essential input to any scheme designed to analyse shells of arbitrary shape. In chapter 3 it was shown how the geometry of the shell mid-surface $S \in E^3$ could be defined as the image of a domain $\Omega \in E^2$ under the mapping $\underline{\phi}$. The intergrands of the functional J contain terms involving the partial derivatives of $\underline{\phi}$. It is necessary therefore to define the 27 functions, $\phi_{i,\alpha}$, $\phi_{i,\alpha\beta}$, $\phi_{i,\alpha\beta\lambda}$ in order to be able to evaluate the bilinear forms in these problems. In practice it is inconvenient to provide specific expressions of these quantities

for each geometry to be used. An attractive alternative is an approximate mapping which can be used to define any given geometry. The form of such an approximate mapping $\underline{\phi}_h$ is given by Ciarlet (1976) as ;

$$\underline{\phi}_h = \phi_{hi}\underline{e}^i \qquad \text{with} \quad \phi_{hi} = \Theta_h\phi_i$$

where Θ denotes an interpolation operator.

The interpolation scheme of interest is the finite element method. The piecewise polynomial basis functions discussed in section 4.2 are used to interpolate geometric data provided at node points. A space $\underline{\mathbf{S}}_h$ is defined as the finite element space of the mapping in a way similar to that by which $\underline{\mathbf{V}}_h$ is defined for the approximate displacements.

The three components of the mapping are independant functions ; theoretically different triangulations and interpolation functions could be used to approximate each component. In practice the approximate mapping should provide an approximation for any particular surface which is independant of the orientation of the surface in E^3. To achieve this all the components of the mapping must be defined by the same interpolation scheme.

Example ; Linear interpolation of the geometric mapping functions of a circular cylinder.

Mapping components ; $\phi_1 = R \cos \theta$

$\phi_2 = R \sin \theta$

$\phi_3 = z$

Looking at components 1 and 2 (3 is exact)

At $\theta = 0^\circ$	$\phi_1 = R$	$\phi_2 = 0$
At $\theta = 45^\circ$	$\phi_1 = \frac{1}{\sqrt{2}} R$	$\phi_2 = \frac{1}{\sqrt{2}} R$
At $\theta = 90^\circ$	$\phi_1 = 0$	$\phi_2 = R$

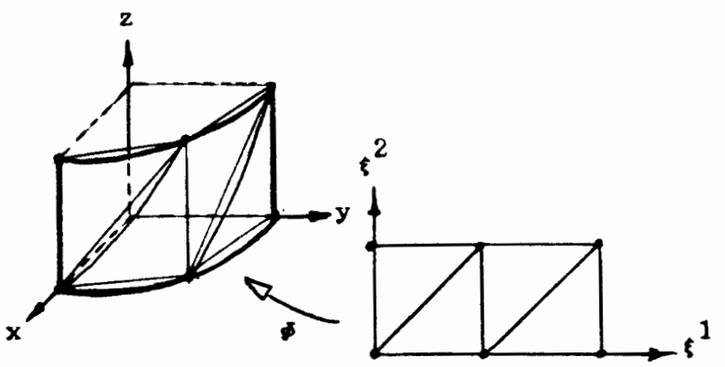

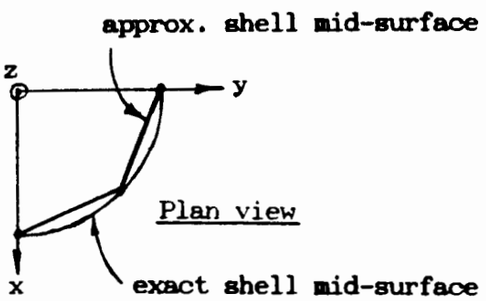

4.6 Continuity Requirements For The Mapping.

Requirements for the space $\underline{\underline{\Phi}}_h$ are not as easily defined as those for the space V_h. Displacements, stresses, and strains on the surface are of interest ; these quantities are calculated and expressed with direct reference to the surface mapping and its partial derivatives. In section 4.3 the continuity requirements for the displacements have been discussed. They are derived from the need to evaluate the bilinear form of the strain energy functional. The conditions on an approximate mapping are also derived from this need. They may be set up from two different approaches.

In the first approach the surface S is approximated by S_h obtained via the mapping $\underline{\phi}_h$ and the shell problems are posed on S_h. The VBVPs for the shell are formulated in terms of displacement components v_i with respect to the tangent basis $\underline{a}^i$. In defining the problem the shell surface $S = \underline{\phi}(\bar{\Omega})$ was assumed to be regular, that is the two tangent basis vectors $\underline{a}_\alpha = \underline{\phi}_{,\alpha}$, from which the $\underline{a}^i$ are derived, are uniquely defined and linearly independent for all points on $\bar{\Omega}$. In order to maintain this condition it is necessary to make the inclusion $\underline{\phi}_h \in \underline{\underline{\Phi}}_h \subset \underline{\underline{\Phi}} \subset (C^1)^3$. The shell formulations on S_h are commonly said to "conform for geometry" if the approximate mapping has this property.

Ciarlet places a different interpretation on the description "conforming for geometry" ; he proposes that $\underline{\phi}_h$ requires C^3 continuity only on the interior of elements and that no inter-element continuity is necessarily required. This

interpretation is obtained by considering the main objective as obtaining a good approximation to the energy functionals, and arises in the following way. The approximate mapping is theoretically independant of the displacement field discretisation, for which a single triangulation is assumed. Terms of the form $V_I D_{IJ} V_J$ are to be intergrated over the elements of the displacement discretisation. If the geometric mapping is not C^3 continious and the edge of an element of the geometric discretisation passes through the interior of the displacement discretisation element, then some of the terms to be integrated will be discontinious since third derivatives of the mapping appear in some of the D_{IJ}. By choosing the displacement triangulation such that elements in the geometric discretisation are exactly covered by a subset of displacement elements the above high continuity requirement on the approximate mapping can be relaxed. The requirement becomes for C^3 continuity only on the interior of geometry discretisation elements. By choosing the same triangulation for both displacement and geometric discretisation, as is done by Ciarlet, the above condition is easily met. Convergence of the finite element approximation of the total potential energy minimisation problem is proved by Ciarlet using this approach to the approximation of geometry. Note that ϕ_h is defined only on the union of the interiors of elements if it is not of the class C^0.

The requirements indicated by both approaches are met if C^1 continious finite elements using simple polynomial element shape functions in 2-dimensions are used to interpolate the geometry. Simple C^0 third order schemes should however suffice.

4.7 Summary ; Conforming discrete shell problems.

In this chapter the components for a finite element approximation of the VBVPs identified in section 3.2 have been formulated. The approximation involves discretisation of displacements and,or geometry, the conditions on these discretisations which lead to conforming approximation of the VBVPs have been set out. In the following chapter the numerical methods required to implement a conforming finite element analysis for shells using these ideas is presented.

This chapter is summarised by looking at the conceptual consequences of the introduction of the discretisations into the energy principle.

(i) Consider only approximation of the geometry. The surface $\mathbf{S}_h$ is the approximate mid-surface of the shell or the mid-surface of an approximate shell, and $J_h(\underline{v})$ is the functional measuring the exact energy of the approximate shell. The displacement associated with a stationary value of this functional retains an infinite number of degrees of freedom and the problem is therefore no more solvable in this form than the exact one. This consideration serves only to clarify the meaning of approximate geometry.

(ii) Consider only approximation of displacements. The energy functional $J(v_h)$ is a measure of the energy of the shell due to the approximate displacements, and it is therefore an approximate measure of the energy of the exact shell.

(iii) Considering both approximations simultaneously $J_h(v_h)$ can be thought of as the approximate energy of the approximate shell.

C H A P T E R 5

METHOD OF IMPLEMENTATION.

5.1 Introductory Remarks

Numerical methods are used to implement finite element approximations. In this chapter application of these methods to the conforming finite element formulation presented is discussed. Numerical integration is performed on the real elements and not on a master element because of the way derivatives of the shell mid-surface mapping enter into the problem. A method of constructing element shape functions on an arbitrarily shaped element is therefore discussed in detail. Reference to the FORTRAN program in which the ideas presented in this chapter are used is kept to a minimum to avoid clouding the discussion with coding details.

The choice of the discretisation scheme, i.e. element shapes, nodal positions, nodal degrees of freedom and hence element shape functions, is a first step in the implementation of any finite element analysis. In formulating the conforming finite element approximation for shells in chapter 4 a set of conditions for the required interpolation schemes has been built up. The choice of interpolation schemes used in this study are identified at the outset since much of the following discussion refers directly to this choice. In conclusion some remarks are made about the decision to perform element calculations on the real element rather than a master.

5.2 Discretisation Schemes

For the shell problem considered the functions to be discretised are the displacement covariant component functions $u_i(\xi^\alpha)$ i=1,3 , and, if geometry is to be approximated, the geometric mapping components $\phi_i(\xi^\alpha)$ =1,3 . The use of straight sided triangular elements is assumed (see section 4.2.2.), and the same triangulation over the domain $\Omega \in \mathbb{R}^2$ is used to form the finite elements for all the functions to be interpolated. The inter-element continuity requirements for a conforming approximation have been identified in sections 4.3 and 4.6 ; the in-plane displacement components $u_\alpha(\xi^\alpha)$ α=1,2 require C^0 interpolation functions, the transverse displacements $u_3(\xi^\alpha)$ must have C^1 continuity, and the mapping components $\phi_i(\xi^\alpha)$ require C^3 continuity only on each individual element.

Properties of finite element basis functions and hence element shape functions have been described in sections 4.2.3 and 4.2.4. In addition to these rules it can be shown that the use of complete polynomials for element shape functions is desirable (Dhatt and Touzot 1984). Several classical triangular element schemes exist for both C^0 and C^1 continuous interpolation. For the interpolation of in-plane displacement components Lagrange elements types 1,2 and 3 were implemented, their basic features being shown in Table 5.1. The Hermite triangles shown in Table 5.1 are used in the approximation of geometry (see section 5.6.). Schemes for C^1 continuous interpolation are in general fairly complicated, the four C^1 triangular elements studied by Bernadou (1980) where considered ; the Argyris element, the Bell element,

and the two Hsieh-Clough-Toucher elements. It is convenient to use the same scheme for both the transverse displacements and the geometric mapping components. The Bell element was chosen for this study ; its basic features are also summarised in Table 5.1 and it is discussed in more detail later in this chapter.

ELEMENT	no. nodes	no. dofs	m $C^m(\Omega)$	m' $C^{m'}(\Omega_e)$	k P_k
BELL 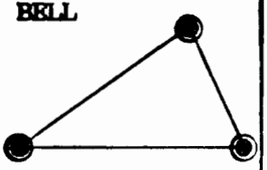	3	18	1	5	4
HERMITE 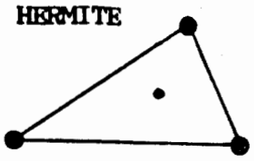	4	10	0	3	3
LAGRANGE type 1 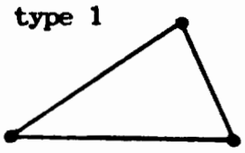	3	3	0	1	1
type 2 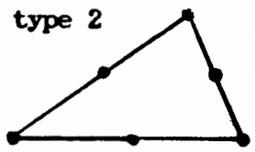	6	6	0	2	2
type 3 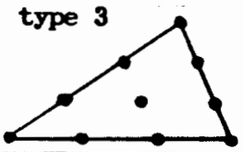	10	10	0	3	3

• = function value degree of freedom

o = 1st partial derivative degree of freedom

O = 2nd partial derivative degree of freedom

Table 5.1 : Finite element interpolation schemes used.

5.3 Displacement Discretisation

The Lagrange-Bell scheme chosen has 2n+18 degrees of freedom on each element where n is the number of Lagrange element nodes, n=(k+1)(k-1)/2 and k is the order of in-plane interpolation. The order and number of nodal displacement degrees of freedom for the shell element are shown in Table 5.2.

Element dofs.	Displacement quantity	Nodes
a_i	$(u_1(\underline{\xi}_i))$	i=1,n
a_{n+i}	$(u_2(\underline{\xi}_i))$	i=1,n
$a_{2n+(i-1)+1}$	$(u_3(\underline{\xi}_i))$	i=1,3
$a_{2n+(i-1)+2}$	$(u_{3,1}(\underline{\xi}_i))$	i=1,3
$a_{2n+(i-1)+3}$	$(u_{3,2}(\underline{\xi}_i))$	i=1,3
$a_{2n+(i-1)+4}$	$(u_{3,11}(\underline{\xi}_i))$	i=1,3
$a_{2n+(i-1)+5}$	$(u_{3,12}(\underline{\xi}_i))$	i=1,3
$a_{2n+(i-1)+6}$	$(u_{3,22}(\underline{\xi}_i))$	i=1,3
nodes 1 to 3 are the corner nodes		

Table 5.2.: Shell element nodal degrees of freedom.

Displacement component functions and their derivatives appear in the shell formulations presented in Chapter 4 as components of the vector (V_I) , see section 4.4.2. Since the displacement components are discretised this vector is related to displacement degrees of freedom via the element shape functions and their derivatives. On an element

$$(V_I) = [B](a) \qquad (5.3.1)$$

where

[B] is a matrix relating displacement component functions and their derivatives to the nodal displacement degrees of freedom

(a) is a vector of nodal degrees of freedom of nodes on the element.

The matrix [B] has the form,

$$[B] = X[N] \qquad (5.3.2)$$

where

[N] is a diagonal matrix of element shape functions

X is an operator which defines the derivatives required.

The set (V_I) can be partitioned into three parts each assocated with one of the three displacement components. These subsets correspond to subsets of the element displacement degrees of freedom.

$$(V_I)_1 = (v_1, v_{1,1}, v_{1,2}) \quad I=1,3 \qquad (a_i)_1 \quad i=1,n$$

$$(V_I)_2 = (v_2, v_{2,1}, v_{2,2}) \quad I=4,6 \qquad (a_i)_2 \quad i=1,n+1,2n$$

$$(V_I)_3 = (v_3, v_{3,1}, v_{3,2}, v_3, v_{3,11}, v_{3,12}, v_{3,22}) \quad I=7,12 \qquad (a_i)_3 \quad i=2,n+1,2n+18$$

Hence.

$$[B] = \begin{bmatrix} [B_1] & & \\ & [B_2] & \\ & & [B_3] \end{bmatrix}$$

where

$$[B_1] = [B_2] = X_1[N_{(L)}]$$
$$(3xn) \qquad (3xn)(nxn)$$

$$X_1 = \begin{bmatrix} 1 & , & 1 & , & \ldots\ldots \\ \partial/\partial\xi^1 & , & \partial/\partial\xi^1 & , & \ldots\ldots \\ \partial/\partial\xi^2 & , & \partial/\partial\xi^2 & , & \ldots\ldots \end{bmatrix}$$

$[N_{(L)}]$ is a matrix with Lagrange shape functions on its diagonal and

$$[B_3] = X_3[N_{(B)}] \quad ,$$
$$(6x18) \quad (6x18)(18x18)$$

$$X_3 = \begin{bmatrix} 1 & ,\ldots\ldots\ldots \\ \partial/\partial\xi^1 & ,\ldots\ldots\ldots \\ \partial/\partial\xi^2 & ,\ldots\ldots\ldots \\ \partial^2/\partial\xi^1\partial\xi^1 & ,\ldots\ldots\ldots \\ \partial^2/\partial\xi^1\partial\xi^2 & ,\ldots\ldots\ldots \\ \partial^2/\partial\xi^2\partial\xi^2 & ,\ldots\ldots\ldots \end{bmatrix}$$

$[N_{(B)}]$ is a matrix with Bell shape functions on its diagonal.

5.4 The Construction of Element Shape Functions

The method of constructing polynomial element shape functions described here can be used for elements of any shape. The essence of this method was used by Bell (1969) in developing the stiffness matrix for his conforming C^1 plate bending element. This general systematic method is also described in a recent book by French authors Dhatt and Touzot (1984). For classical elements the formulae for element shape functions on simple master elements are well known, since element calculations are usually done on the master element the method of constructing the element shape functions is not of much concern.

A polynomial element shape function ψ_i^e belongs to the space $X^{(e)}$ $P^k(\Omega_e)$ since space is defined as the span of element shape functions, see section 4.2.3. Any basis of the space $P^k(\Omega_e)$ is also a basis for $X^{(e)}$. The simple basis of mononomial functions for any polynomial in two dimensions is obtained from Pascal's triangle figure 5.1. The function being interpolated over the element, u_n can be written as

$$u_n(\xi^\alpha) = \mu_1(\xi^\alpha)\, q_1 + \mu_2(\xi^\alpha)\, q_2 + \ldots \mu_r(\xi^\alpha)\, q_r = \langle \mu_i \rangle\, q_i \qquad (5.4.1)$$

where

- q_i are generalised parameters
- μ_i are mononomial basis functions
- r is the number of possible terms in the polynomial
- r-n the number of nodal degrees of freedom unless additional conditions are used to relate generalised parameters to each other, as in the Bell element (if $r \neq n$ the shape functions are not complete polynomials) $r=(k+1)(k-1)/2$.

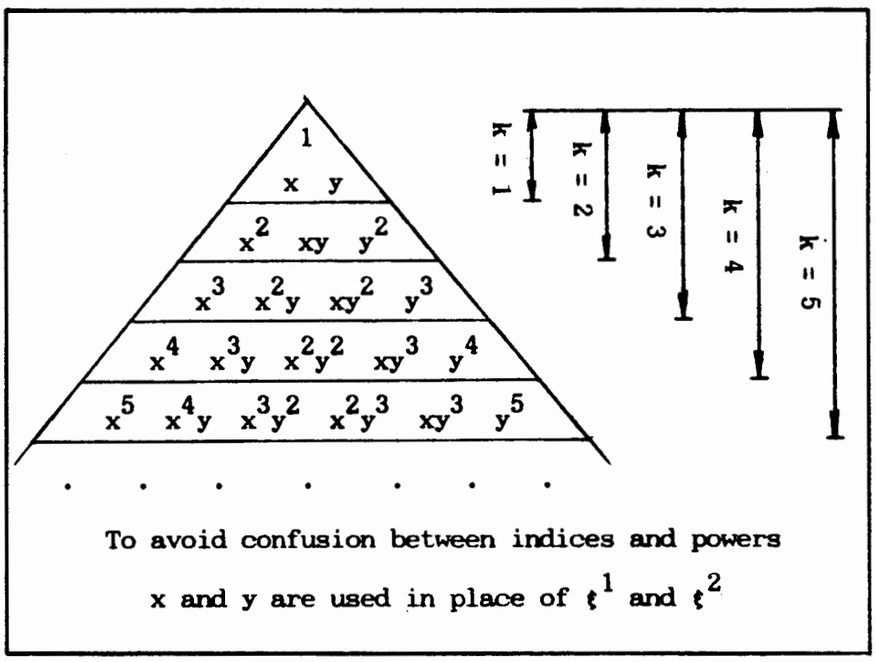

Figure 5.2.: Pascals triangle.

Generalised parameters and nodal displacement degrees of freedom can be related since

$$u_i = \psi_i \, a_i = \mu_i \, q_i \qquad i=1,n \quad . \tag{5.4.2}$$

The conditions on finite element basis functions are defined at nodes, noting that nodal degrees of freedom a_j are chosen as function values or function derivatives at the nodes $\underset{\sim}{\xi}_i$

$$a_j = (u(\underset{\sim}{\xi}_i)) = \langle \mu_\ell(\underset{\sim}{\xi}_i) \rangle \, q_\ell \tag{5.4.3a}$$

or

$$a_{j+\alpha} = (u_{,\alpha}(\underset{\sim}{\xi}_i)) = \langle \mu_{\ell,\alpha}(\underset{\sim}{\xi}_i) \rangle \, q_\ell \tag{5.4.3b}$$

Using such relationships for all the degrees of freedom at nodes on an element

$$\{a\} = [A]\{q\} \quad \text{or} \quad [A]^{-1}\{a\} = \{q\} \quad . \tag{5.4.4a,b}$$

The rows of the matrix [A] are formed using the method shown in (5.4.3a and b).

Substituting back into (5.4.1)

$$u_n(\xi_i^{\alpha}) = <\mu(\xi_i^{\alpha})> [A]^{-1}\{a\} \tag{5.4.5a}$$

and noting (5.4.3b)

$$u_{n,\alpha}(\xi_i^{\alpha}) = <\mu(\xi_{i,\alpha}^{\alpha})> [A]^{-1}\{a\} \quad . \tag{5.4.5b}$$

The functions $\mu_{i,\alpha}$, $\mu_{i,\alpha\beta}$, etc. are easily obtained since μ_i are simple mononomials.

Substituting (5.4.5) into (5.4.2) the element shape functions are defined by

$$\{\psi_i^e\} = <\mu(\xi^{\alpha})> [A]^{-1}\{a\} \quad . \tag{5.4.6}$$

The [B] matrices obtained earlier for the shell displacement nodal degree of freedom relations are easily formed since the operator X will only effect the polynomial basis, $[A]^{-1}$ being constant on any particular element. A matrix [P...] is defined,

$$[P_{0,1}^{k}] = X_1 <\mu_i> \qquad i=1,n \quad , \tag{5.4.7}$$

where the superscript k is the polynomial order of the basis $<\mu_i>$ and the subscripts indicate the order of derivatives formed by the operator X .

Example

Lagrange elements type 1 used for interpolation of in plane components of displacement, i.e. k=1 , r=n=3 and only function values as degrees of freedom at nodes

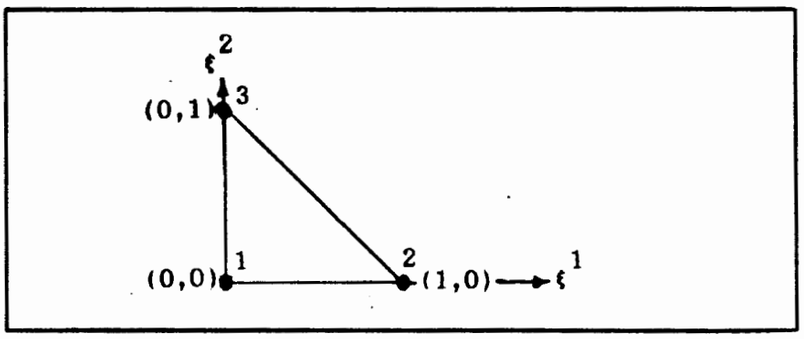

$$\langle \mu \rangle = \langle 1 \ , \ \xi^1 \ , \ \xi^2 \rangle$$

$$[A] = \begin{bmatrix} 1 & 0 & 0 \\ 1 & 1 & 0 \\ 1 & 0 & 1 \end{bmatrix} \qquad [A]^{-1} = \begin{bmatrix} 1 & 0 & 0 \\ -1 & 1 & 0 \\ -1 & 0 & 1 \end{bmatrix}$$

$$[N] = \begin{bmatrix} (1-\xi^1-\xi^2) & & \\ & (\xi^1) & \\ & & (\xi^2) \end{bmatrix}$$

$$[P^1_{0,1}] = \begin{bmatrix} 1 & \xi^1 & \xi^2 \\ 0 & 1 & 0 \\ 0 & 0 & 1 \end{bmatrix} \qquad [B] = \begin{bmatrix} (1-\xi^1-\xi^2) & (\xi^1) & (\xi^2) \\ -1 & 1 & 0 \\ -1 & 0 & 1 \end{bmatrix}$$

Note the element geometry used in this example is that usually used for master elements and the diagonal terms of [N] are the well known formulae for the master element shape functions.

5.5 The Bell Triangle Interpolation Scheme

The formulation of shape functions for the Bell triangle is based on a complete fifth order polynomial. The 21 degrees of freedom of the comparable fifth order polynomial are reduced to the 18 values indicated in Table 5.1. This reduction in the number of degrees of freedom is done by forcing the edge normal slope of the interpolated function to vary cubically along the edge. To do this the mid-side normal slopes are written in terms of the nodal degrees of freedom at the corner nodes defining the edge. The resulting shape functions are then complete in fourth order terms but retain some terms of fifth order. The full details of this process are not given here ; they may be found in Bell's paper (1969). An outline of the steps required to obtain the shape functions in the same form as described in section 5.3 is presented.

The relationship between mid-side normal slopes and corner node degrees of freedom is contained in a matrix [H] such that

$$\{a_{21}\} = \begin{bmatrix} I_{18} \\ \hline H \end{bmatrix} \{a_{18}\} \qquad (5.5.1)$$

where

[H] is a (3x18) matrix.

Figure 5.2 shows the full set of 21 degrees of freedom used to obtain a complete fifth order C^1 interpolation.

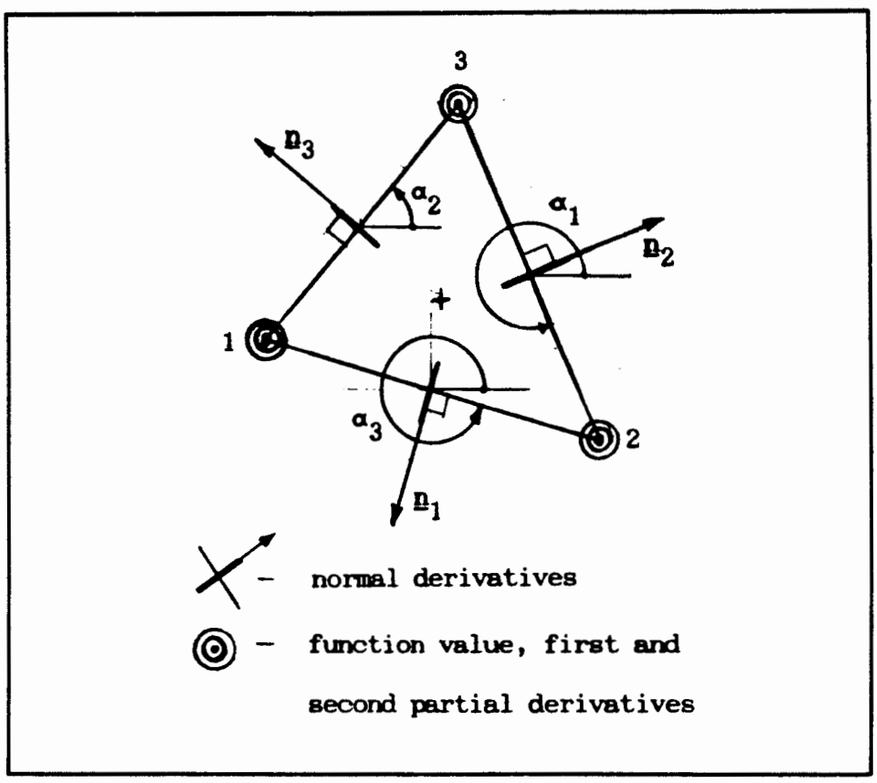

Figure 5.2.: Degrees of freedom used to derive the Bell Triangle interpolation scheme.

The set of degrees of freedom $\{a_{21}\}$ is related to generalised parameters in the way described in section 5.4. The last three rows of matrix [A] correspond to the mid-side derivative degrees of freedom and involve sines and cosines of the angles α indicated in figure 5.2. The approximate function u_h is given by

$$u_h(\xi) = \langle \mu_i(\xi) \rangle [A]^{-1} \left[\begin{array}{c} I_{18} \\ \hline H \end{array}\right] \{a_{18}\} \qquad (5.5.2)$$

$$(1x21)(21x21)(21x18)(18x1)$$

A generalised parameters-nodal degree of freedom transformation matrix [T] is defined,

$$[T] = [A]^{-1} \begin{bmatrix} I_{18} \\ \tilde{H} \end{bmatrix} \quad . \qquad (5.5.3)$$

(21x18)

Hence for the transverse displacements in the shell formulation :

$$\begin{aligned} \{V\}_3 &= \{v_3, v_{3,1}, v_{3,2}, v_{3,11}, v_{3,12}, v_{3,22}\}^T \\ &= [B]_3\{a\} \quad , \\ &= [P^5_{0,1,2}]\,[T]\{a\} \quad , \end{aligned}$$

where

$$[P^5_{0,1,2}] = X_3 \langle \mu_i \rangle = \begin{bmatrix} \langle \mu_i \rangle \\ \langle \mu_{i,1} \rangle \\ \langle \mu_{i,2} \rangle \\ \langle \mu_{i,11} \rangle \\ \langle \mu_{i,12} \rangle \\ \langle \mu_{i,22} \rangle \end{bmatrix} \quad i = 1,21$$

(6x21)

An alternative method for setting up the Bell triangle shape functions is described by Dhatt and Touzot (1984). The six mononomial fifth order terms in the polynomial basis are replaced by three binomials. The polynomial basis is then that of the element space $X^{(e)}$; it has 18 components corresponding to 18 generalised parameters. These can then be directly related to the 18 nodal degrees of freedom by inversion of the matrix [A] obtained using this set of polynomial basis functions.

5.6 Approximate Geometry Interpolation Schemes.

Three interpolation schemes for the approximation of geometry are used ; Bell triangles, Hermite trinagles, and Lagrange type 3 trinagles. All three of these meet the requirement for C^3 continuity of the mapping component functions on each element.

To specify the shell geometry values corresponding to the nodal degrees of freedom of the interpolation scheme must be supplied for each of the three components of the mapping : these are, for the Bell scheme the 18 values $\phi_i(\underline{\xi}_j)$, $\phi_{i,a}(\underline{\xi}_j)$, $\phi_{i,\alpha\beta}(\underline{\xi}_j)$ at all element corner nodes $(\underline{\xi}_j)$, for the Hermite scheme the 9 values $\phi_i(\underline{\xi}_j)$, $\phi_{i,\alpha}(\underline{\xi}_j)$ at corner nodes and the 3 values $\phi_i(\underline{\xi}_j)$ at element interior nodes, and for the Lagrange scheme the 3 values $\phi_i(\underline{\xi}_j)$ at all nodes. By way of example the use of the Bell scheme is decribed. The use of the other schemes follows a similar pattern.

Example : Bell Scheme.

On each element 54 input values are used, made up of 6 values for each of the 3 components at each of the 3 corner nodes. The input data is grouped into three sets $\{s\}_i$ corresponding to the nodal degrees of freedom of the three mapping components ϕ_{hi}

$$\{s_{18}\}_i = \{\ \phi_i(\underline{\xi}_j),\ \phi_{i,1}(\underline{\xi}_j),\ \phi_{i,2}(\underline{\xi}_j),\ \phi_{i,11}(\underline{\xi}_j),\ \phi_{i,12}(\underline{\xi}_j),\ \phi_{i,22}(\underline{\xi}_j)\ \}. \qquad (5.6.1)$$

The values in these sets correspond to the element shape functions of the Bell element

$$\phi_{hi}(\xi^{\alpha}) = (\psi^{e}_{(\beta)})(s_{18})_i \quad . \tag{5.6.2}$$

From (5.5.2)

$$\phi_{hi} = < \mu_i(\xi^{\alpha}) > [T] \, (s_{18})_i \tag{5.6.3}$$

and hence the generalised parameters of the approximate mapping component over the element $(q)_i$ are given by

$$(q_{21})_i = [T](s_{18})_i \tag{5.6.4}$$

These may be used with the polynomial basis $<\mu_{21}(\xi^{\alpha})>$ and its derivatives to give the mapping components and their derivatives (see equation 5.4.6).

5.7 Element Calculations

Global stiffness and mass matrices [k] and [m] are formed by assembly of element contributions, see section 4.2.4. The element matrices required are the element stiffness matrix $[k]^{(e)}$ and the element mass matrix $[m]^{(e)}$. These are calculated by the same procedure since in formulating the matrix form of the energy functional bilinear forms the same set of displacement components and their derivatives have been used i.e. (V_I), see section 4.4. These are related to element nodal degrees of freedom for the Lagrange-Bell element by the matrix [B], in sections 5.3 and 5.4. The element matrices have the form

$$[k_{ij}]^{e} = [D^{e}(\psi_i, \psi_j)] = \int_{\Omega_e} [B]^{T}[D][B] \sqrt{a} \partial\xi^{1} \partial\xi^{2} \tag{5.7.1}$$

$$[m_{ij}]^e = [C^e(\psi_i,\psi_j)] = \int_{\Omega_e} [B]^T[C][B] \sqrt{a}\partial\xi^1\partial\xi^2 \qquad (5.7.2)$$

where $[D] = [D_{IJ}]$ (12x12) formulated from strain energy functional in section 4.4

$[C] = [C_{IJ}]$ (12x12) formulated from kinetic energy functional in section 4.4.

The integration is carried out numerically using a quadrature rule. The rules used have the following form ;

$$[k]^{(e)} = \sum_{ipt=1}^{nipt} [B(\underset{\sim}{\xi}_{ipt})]^T[D(\underset{\sim}{\xi}_{ipt})][B(\underset{\sim}{\xi}_{ipt})] \sqrt{a(\xi_{ipt})}\, W_{ipt} \qquad (5.7.3)$$

where $\underset{\sim}{\xi}_{ipt}$ is the position vector of an integration point, ipt

nipt is the number of integration points used.

W_{ipt} is the weighting of the integration point.

By substituting expression (5.4.7), (5.6.3) and (5.6.4) into the matrix [B] the element matrix can be rewritten in the form

$$[k] = [S]^T [k_q] [S] \qquad (5.7.4)$$

where

$[k_q]$ is the stiffness matrix with respect to generalised parameters (q)

$$[k_q] = \sum_{ipt=1}^{nipt} {}^{m}_{o}[\bar{P}(\underset{\sim}{\xi}_{ipt})]^T[D(\underset{\sim}{\xi}_{ipt})][\bar{P}(\xi_{ipt})] \sqrt{a(\underset{\sim}{\xi}_{ipt})}\, W_{iptp}$$

$$((2n+21)x12)(12x12)(12x(2nx21)) \qquad (5.7.5)$$

where

$$[\tilde{P}] = \begin{matrix} n + n + 21 \\ \left[\begin{matrix} \left[P^k_{0,1}\right] & & \\ & \left[P^k_{0,1}\right] & \\ & & \left[P^5_{0,1,2}\right] \end{matrix}\right] \begin{matrix} 3 \\ 3 \\ 6 \end{matrix} \end{matrix} \qquad (5.7.6)$$

(12x(2n+21))

and

$$[S] = \begin{matrix} n + n + 18 \\ \left[\begin{matrix} [A_{(L)}]^{-1} & & \\ & [A_{(L)}]^{-1} & \\ & & [T] \end{matrix}\right] \begin{matrix} n \\ n \\ 21 \end{matrix} \end{matrix} \qquad (5.7.7)$$

((2n+21)x(2n+18)).

By partitioning the [D] matrix and taking into account symmetry of the element matrices only 6 small matrices need to be evaluated to give the full element matrix.

$$[D_{IJ}] \begin{matrix} 3 + 3 + 6 \\ \left[\begin{matrix} [D_1] & [D_2] & [D_4] \\ \text{sym.} & [D_3] & [D_5] \\ & & [D_6] \end{matrix}\right] \begin{matrix} 3 \\ 3 \\ 6 \end{matrix} \end{matrix}$$

$$[k_q] = \left[\begin{matrix} \left[[P^k]^T[D_1][P^k]\right] & \left[[P^k]^T[D_2][P^k]\right] & \left[[P^k]^T[D_4][P^5]\right] \\ & \left[[P^k]^T[D_3][P^k]\right] & \left[[P^k]^T[D_5][P^5]\right] \\ \text{sym.} & & \left[[P^5]^T[D_6][P^5]\right] \end{matrix}\right] \qquad (5.7.8)$$

5.8 Concluding Remarks

In this chapter the process of making real element calculations has been decribed. Most finite element implementations make use of a master or reference element on which element shape functions are obtained directly from formulae and the numerical integration scheme is specified. The master element $\hat{\Omega}$ is considered in a nondimensional space with coordinates η^1, η^2. It maps under a geometric transformation τ to the real element as is shown in figure 5.3.

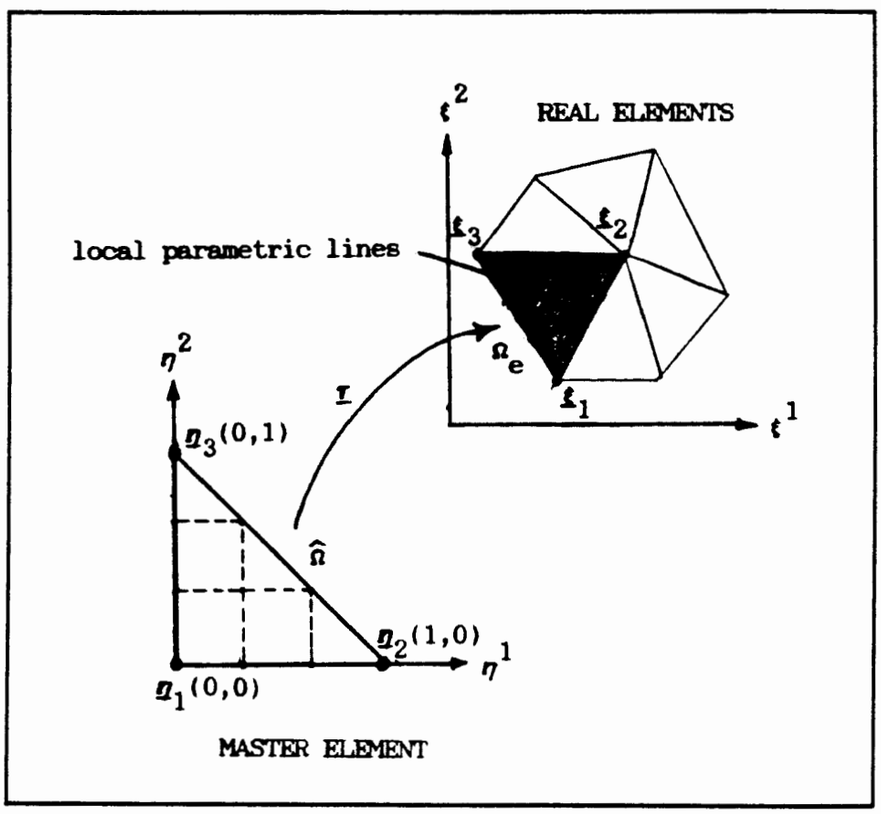

Figure 5.3.: Master element mapping.

Where derivative degrees of freedom are used, calculations

performed on the master correspond to functional derivatives with respect to the η^{α} and not ξ^{α}. The element matrices must therefore be transformed, and all directional quantites used in the calculations must be described with respect to the same coordinate system. The complexity of these transformations increases with the order of derivatives to be transformed.

In this study shell surface geometry is evaluated either using the exact mapping $\boldsymbol{\phi}$ or using an approximate mapping $\boldsymbol{\phi}_h$. The values $\phi_{i,\alpha}, \phi_{i,\alpha\beta}, \phi_{i,\alpha\beta\lambda}$ are required at each integration point. These are specified relative to the global coordinates ξ^{α} for exact mapping functions. Thus, if a master element were used with an exact specification of geometry a transformation τ^{-1} for up to third derivatives would have to be calculated at each integration point. An approximate mapping is defined in terms of the element shape functions which if a master element is used are given with respect to the coordinates η^{α}. The input nodal values which specify the geometry are however given with respect to the coordinates ξ^{α}. The Bell and Hermite interpolation schemes use derivative degrees of freedom, and input values must therefore be transformed.

The implementation of the finite element analysis of shell problems decribed in this thesis, which allows flexibility in the manner in which the geometry is obtained, is greatly simplified by the choice to perform element calculations on the real element. This simplification is a result of the elimination of the need to accomodate the different transformations decribed above.

Considerable extra computational effort is used in the inversion of the generalised parameter - nodal degree of freedom relation matrices (see section 6.4.2). In some cases this loss is to some extent cancelled in that the many transformations which would be required if a master element were to be used need not be calculated.

C H A P T E R 6

FINITE ELEMENT PROGRAM.

6.1 Introductory Remarks

The conforming finite element formulations presented in this thesis were implemented in a FORTRAN computer program using the methods described in chapter 5. This program was developed on a UNIVAC 1100 mainframe computer at the University of Cape Town. It was written with the intention of investigating the following aspects of the shell formulations and their implementation.

(i) The effectiveness in modelling shells for the determination of ; (a) displacements and stresses under static loading, and (b) mode shapes and frequencies of free vibrational modes.

(ii) The use of different orders of Lagrange interpolation schemes for in-plane displacement components.

(iii) The choice of a suitable integration scheme.

(iv) The use of approximate mappings on the results obtained for shells of arbitrary geometry.

Several options were implemented to enable the program to be capable of the range of problems required for the investigations indicated above. These options are described. The program's main structure is shown, and those modules of particular interest are described in more detail. Special attention is paid to the way in which the shell surface mapping enters into the calculations.

6.2 Options.

6.2.1 Analysis Type.

The option, static or free vibration analysis is self explanatory. The processes required for the two types of analysis are essentially the same with the exception of the solution procedures. This is reflected in the program structure shown in figure 6.1. The calculation of element and global mass matrices is performed at the same time as the calculation of the stiffness matrices. For a static analysis a range of different types of loading was allowed including, self weight (gravitational field direction specified in the global Cartesian system, i.e. in E^3), uniform pressure (in the direction of the outward normal to the surface, i.e. $\underline{a}_3$), and point loads (specified in components with respect to the global Cartesian basis vectors $\underline{e}_i$).

6.2.2 In-Plane Displacement Interpolation Scheme.

This option has been mentioned in chapter 5. The specification of any one of the three Lagrange interpolation schemes allowed is done purely by entering the type, i.e. 1, first order, 2, second order, 3, third order. From this value the number of nodes, n , is obtained. This number is then used as a control parameter for all the element calculations as outlined in chapter 5.

6.2.3 Integration Schemes

It is well known that a quadrature rule of polynomial degree k specified for a triangular region may be transferred into a quadrature rule of the same degree for any other triangular region (Stroud 1975). This notion is used by Lyness and Jespersen (1976)

in developing a set of numerical integration schemes for triangles. These rules use different arrangements and numbers of integration points. Transformation of the rules from the equilateral reference triangle to a triangle of any shape is easily achieved by supplying corner node coordinates and the triangles area (the area is obtained from the corner coordinates). The calculation of integration point coordinates and weight functions is not complex and is based on values, or expressions, tabulated by Lyness and Jespersen. A wide range of schemes were implemented, it was found that those with negative weighting functions did not work. The number of integration points required for each of the rules implemented are given in Table 6.1.

Rule	31	32	41	42	44	51	52	61	62	64	72	81
nipts.	4 *	3	6	10 *	9	7	10	12	16 *	13	16	16

Rule 51

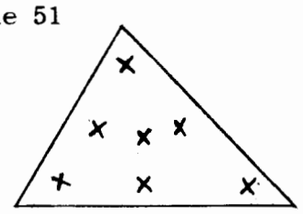

Rule 52

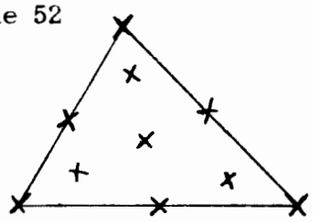

* rules with negative weightings

Table 6.1 : Integration Rules (Lyness and Jespersen)

The choice of integration rule is specified by entering its identification number. The first digit of this number indicates

the degree of polynomial for which the rule is exact. The second digit gives some information about the type of rule, even numbers being Cytolic rules and odd being Holistic rules; these terms are explained by Lyness and Jespersen. Cytolic rules make use of integration points on the edges of the triangular region over which integration is carried out. The integration points of Holistic rules are all on the interior of an element.

6.2.4 Shell Surface Geometric Mapping.

Subroutines, which return for a given point the exact values of geometric mapping functions and their derivatives, have been written for the shell geometries used in program verification or as examples (see chapter 7). Each geometry explicitly given in this way is allocated an identification number, the number zero being indicating that an approximate mapping is to be used. The explicit mapping functions used shown in Table 7.1. They are specific to particular orientations of the required surfaces with respect to the global coordinate scheme; for example, the flat plate mapping is given in the plane x_1, x_2 i.e. $\underline{e}_3$ is the unit normal. Input of additional "known geometry parameters" for each mapping allows some variation of the geometry, for example the radius is required for a cylindrical mapping. For shell mid-surface geometries having single constant curvature the matrices $[D_{IJ}]$ and $[C_{IJ}]$ are independent of the position on the surface and need only be calculated once where such exact mappings are specified. The program is coded to recognise this from the geometry identification number.

If geometry is to be approximated choice between the three schemes implemented (see section 5.6) is also made via specification of an identification number. Approximate geometry is calculated from the approximate mapping using nodal input and interpolation functions as described in section 5.4.

6.3 Program Structure.

Figure 6.1 shows the global flow chart for the program. Those modules to be discussed in more detail are marked with an asterisk.

6.3.1 Input.

All input is read in by the input module at the start of the program. The input consists of the following :

- control data; number of nodes, number of elements, in plane interpolated order, integration rule, geometry ID, static/eigenvalue analysis,
- material data; E, ν, ρ , and shell thickness,
- element topologies;
- nodal coordinates (ξ^1, ξ^2); only corner nodes are required
- surface geometry; either nodal data for approximate mapping or known geometric mapping parameters
- boundary conditions; number of fixed degrees of freedom nodes and fixed degrees of freedom
- loading or frequency analysis data; load type intensity direction, or numbers of frequencies tolerence and maximum frequence.

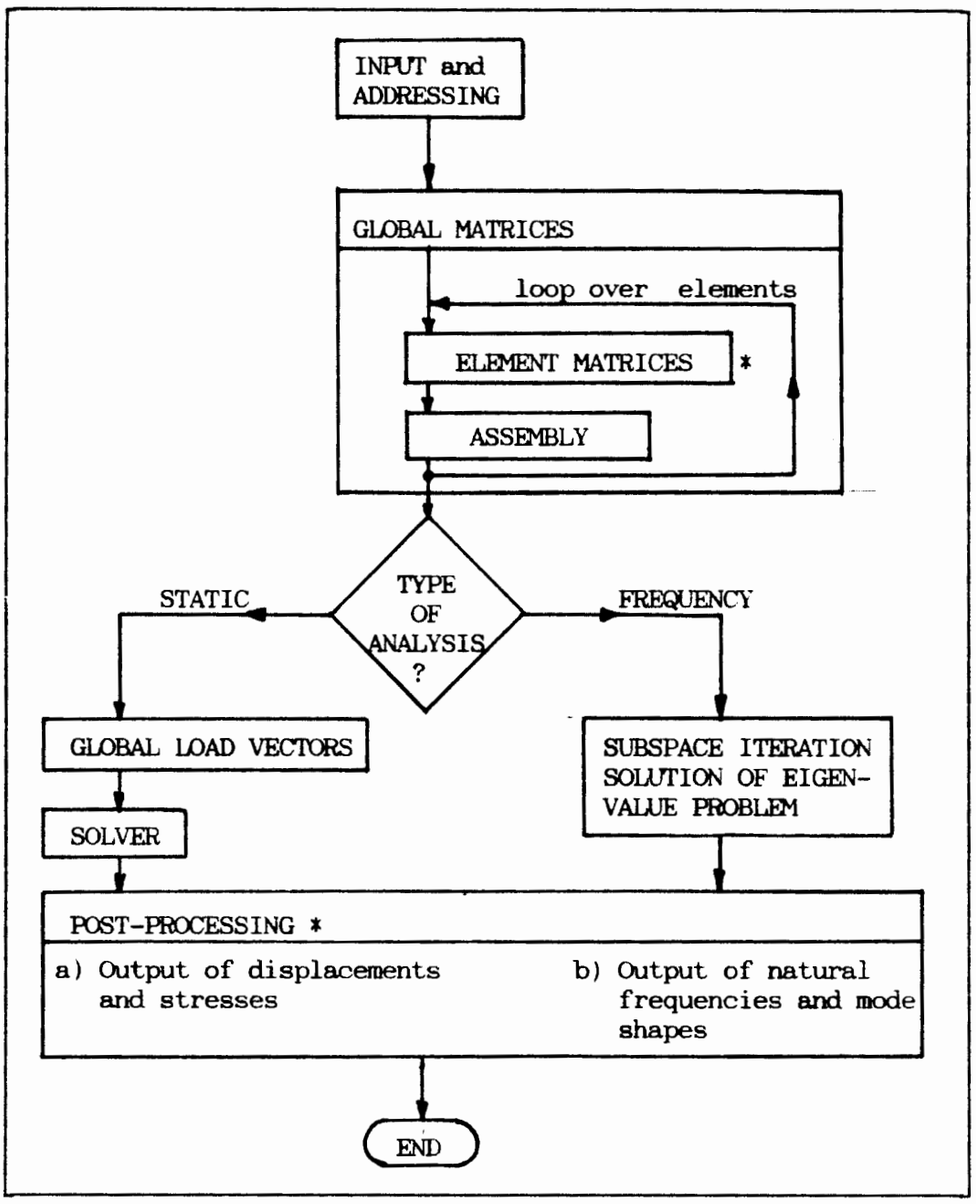

Figure 6.1 : Global Flow Chart.

The element topology is read in before other nodal information and is used to identify "corner nodes". This information is then used to allocate storage for other input. The number of degrees of freedom at a particular node is obtained from the in plane interpolation choice and the topology. Boundary condition data is used to determine degree of freedom equation numbers and hence the total number of equations.

6.3.2 Solvers.

The solvers used are the skyline profile solver and the subspace iteration eigenvalue solver, which makes use of the profile solver. Details of both these processes and their implementation are given by Bathe (1982).

6.4 Element Matrix Calculation Module.

6.4.1 Element Prolife.

The need to perform element calculations on a real element, i.e. a triangle of arbitrary shape, has been discussed in section 5.4. To do this what may be called an "element profile" must first be set up. This profile consists of the generalised parameter-nodal degree of freedom transformation matrices for the chosen interpolation schemes, an integration rule (i.e. a set of integration points on the element and their weighting factors), and, if an approximate surface geometric mapping is to be used, a set of generalised parameters for this mapping. Flow charts for element calculations are shown in figures 6.3 and 6.4.

To set up this profile, a local coordinate system with origin at the centroid of the element is used. This coordinate transformation is a pure shift, shown in figure 6.2. Since there is no distortion or rotation of the element there is no change in derivatives, and the Jacobian of such a shift transformation is the identity matrix.

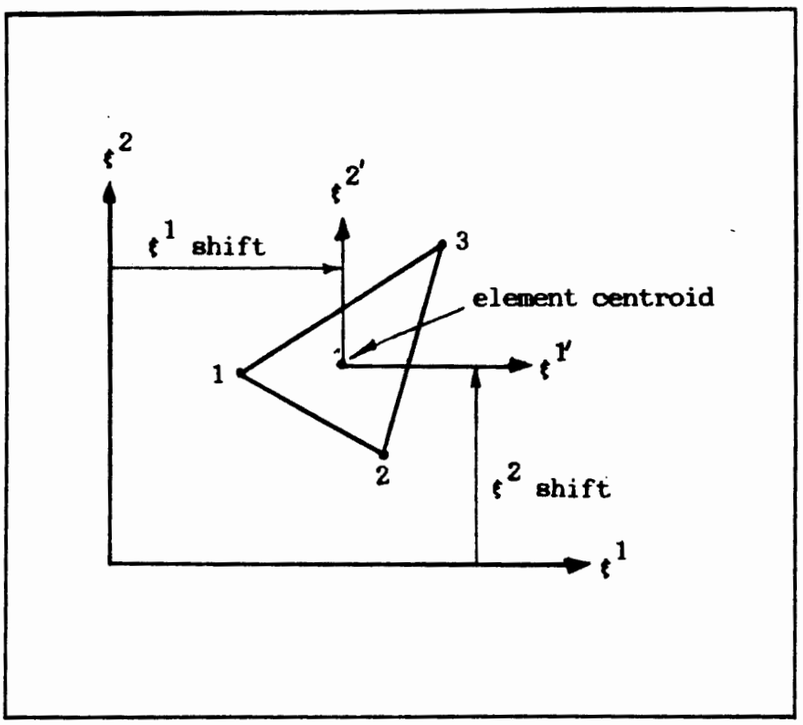

Figure 6.2. ; Element Local Coordinates.

The use of this local coordinate system avoids numerical problems which arise due to large variations in coordinate values between points on elements close to the origin and far from it. These problems are caused by rounding errors which appear both in

inverting the generalised parameter-nodal degree of freedom relationship matrices and evaluation of terms of the polynomial basis. For the Bell triangle fifth order terms appear both in the matrix to be inverted and the polynomial basis. The calculations on two elements of the same shape at different points in the mesh have exactly the same rounding errors when local coordinate systems are used. If all elements in the mesh are of similar size the rounding errors in element calculations are evenly distributed over the mesh.

The subroutine which sets up the local coordinate system calculates all the element's node positions in this system ; nodes other than corner nodes are not given in the global system. The element's area used in integration point calculations and the other characteristics of the triangle required to set up the Bell shape functions are also calculated.

The generalised parameter-nodal degree of freedom transformation matrices [T] and $[A_{(L)}]^{-1}$ are calculated as described in chapter 5. The matrix inversions required are discussed in section 6.4.2. If an approximate geometric mapping is to be used for the shell mid-surface geometry nodal input is transformed to a set of generalised parameters using the matrix [T]. Hence the calculation of this matrix before performing the integration loop.

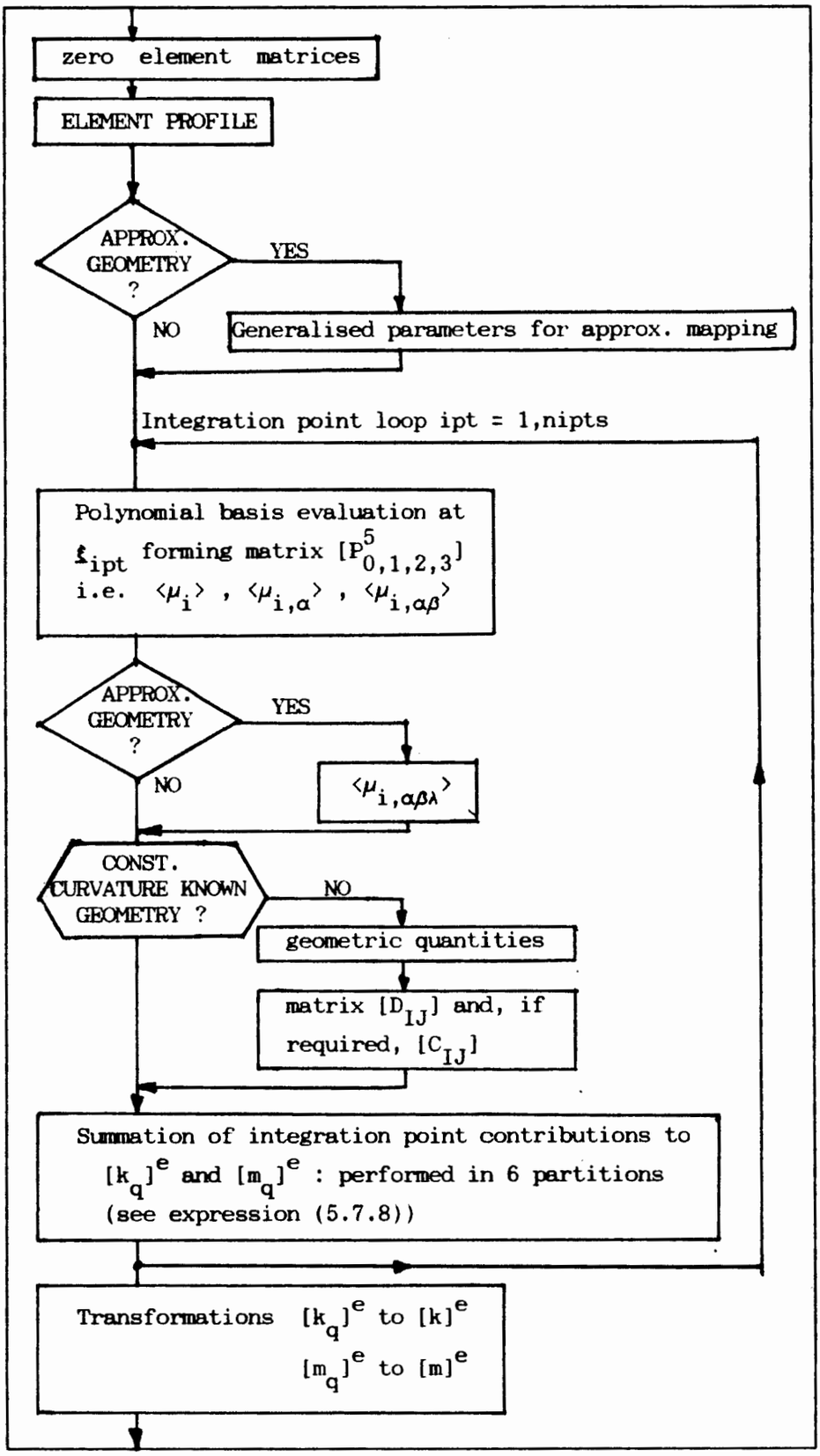

Figure 6.3 : Element Calculations Flow Chart.

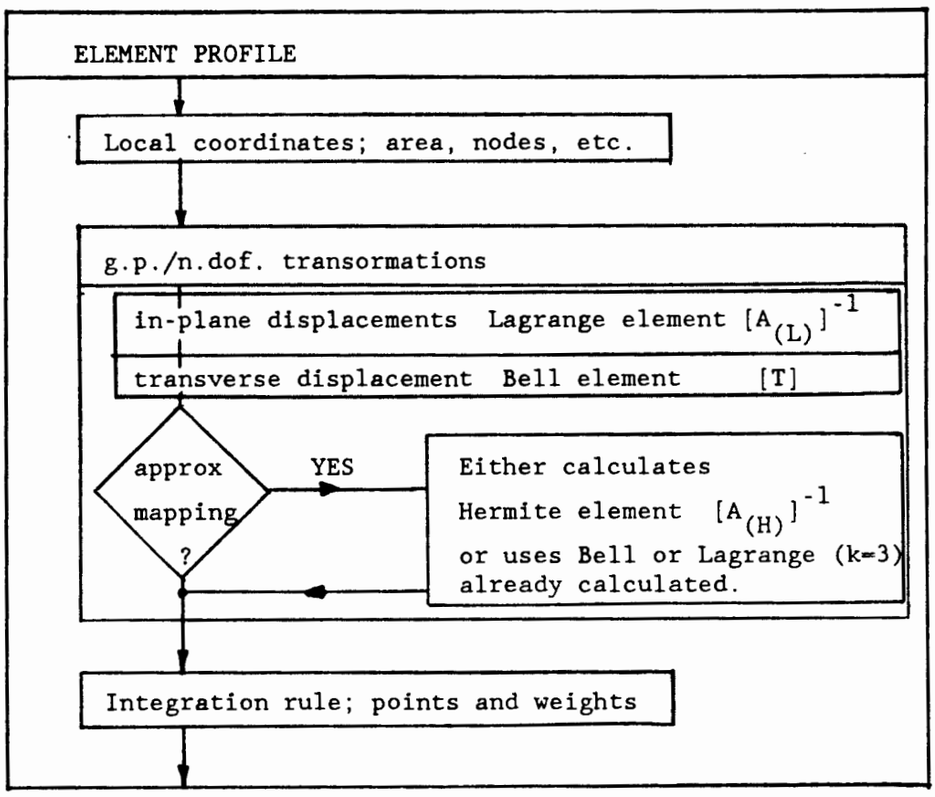

Figure 6.4 : Element Profile.

6.4.2 Matrix Inversions.

Matrices of a maximum order M=21 must be inverted to find the generalised parameter-nodal degree of freedom transformations for each element. These matrices are non-singular by definition but may have zeros on the diagonal, and a reasonably sophisticated inversion routine is therefore required. The inversion process is potentially time consuming ; it is possibly the largest contributing factor to the inefficiency of real element calculations. In the program written for this study a NAG-FORTRAN library package routine (F01AAF) was used for matrix inversions.

This routine uses Crout's method to calculate the approximate inverse of a real matrix. The time taken to invert a matrix using this routine is roughly proportional to M^3. The Bell element formulation used spends 1.6 times the time spent in inversion for the alternative formulation mentioned in section 5.5. This alternative formulation is thus recommended.

6.4.3 Integration Loop.

The matrix $[P^5_{0,1,2,3}]$ contains all the terms in ξ^1_{ipt} and ξ^2_{ipt} to be used in integration point calculations, with the exception of the functions in known geometric mapping routines. The components of this matrix are shown in figure 6.5. The matrices $[P^k_{0,1}]$ k=1 to 3 required for the calculation of Lagrange interpolation functions are contained in this matrix, as shown. The calculation of this matrix is performed once at each integration point and used in the calculation of each of the six partitions of the element matrix, shown in expression (5.7.8). The calculation of geometric quantities and the coefficients of matrices $[D_{IJ}]$ and $[C_{IJ}]$ is dealt with in section 6.5. The element matrix $[k_q]^{(e)}$ corresponds to generalised parameters and is calculated in the integration loop. After completion of the loop this matrix is transformed to $[k]^{(e)}$ which corresponds to nodal degrees of freedom, again this transformation is carried out in the six partitions. Element mass matrices are calculated at the same time, if required.

6.5 Calculation of Geometric Quantities.

All the geometric properties of the shell surface are functions of ξ^α on the domain $\Omega \in \mathbb{E}^2$ through their relationship to the

		1	2	3	4	5	6	7	8	9	10	11	12	13	14	15	16	17	18	19	20	21
$\langle\mu\rangle$	1	1	x	y	x^2	xy	y^2	x^3	x^2y	xy^2	y^3	x^4	x^3y	x^2y^2	xy^3	y^4	x^5	x^4y	x^3y^2	x^2y^3	xy^4	y^5
$\langle\mu\rangle_x$	2	0	1	0	2x	y	0	$3x^2$	2xy	y^2	0	$4x^3$	$3x^2y$	$2xy^2$	y^3	0	$5x^4$	$4x^3y$	$3x^2y^2$	$2xy^3$	y^4	0
$\langle\mu\rangle_y$	3	0	0	1	0	x	y^2	0	x^2	$2x^2$	$3y^2$	0	x^3	$2x^2y$	$3xy^2$	$4y^3$	0	x^4	$2x^3y$	$3x^2y^2$	$4xy^3$	$5y^4$
$\langle\mu\rangle_{xx}$	4	0	0	0	2	0	0	6x	2y	0	0	$12x^2$	6xy	$2y^2$	0	0	$20x^3$	$12x^2y$	$6xy^2$	$2y^3$	0	0
$\langle\mu\rangle_{xy}$	5	0	0	0	0	1	0	0	2x	2y	0	0	$3x^2$	4xy	$3y^2$	0	0	$4x^3$	$6x^2y$	$6xy^2$	$4y^3$	0
$\langle\mu\rangle_{yy}$	6	0	0	0	0	0	2	0	0	2x	6y	0	0	$2x^2$	6xy	$12y^2$	0	0	$2x^3$	$6xy^2$	$12xy^2$	$20y^3$
$\langle\mu\rangle_{xxx}$	7	0	0	0	0	0	0	6	0	0	0	24x	6y	0	0	0	$60x^2$	24xy	$6y^2$	0	0	0
$\langle\mu\rangle_{xxy}$	8	0	0	0	0	0	0	0	2	0	0	0	6x	4y	0	0	0	$12x^2$	12xy	$6y^2$	0	0
$\langle\mu\rangle_{xyy}$	9	0	0	0	0	0	0	0	0	2	0	0	0	6x	6y	0	0	0	$6x^2$	12xy	$12y^2$	0
$\langle\mu\rangle_{yyy}$	10	0	0	0	0	0	0	0	0	0	6	0	0	0	6x	24y	0	0	0	$6x^2$	24xy	$60y^2$

x and y are used in place of ξ^1 and ξ^2 to avoid confusion between indices and powers

* $[P^1_{0,1}]$ ** $[P^2_{0,1}]$ *** $[P^3_{0,1}]$ **** $[P^5_{0,1,2}]$

Figure 6.5 : Matrix $[P^5_{0,1,2,3}]$.

mapping $\underline{\phi}(\xi)$, see chapter 3. The basis vectors and their derivatives are obtained directly from derivatives of the components of the mapping, $\underline{\phi}_i$

$$\underline{a}_\alpha = \underline{\phi}_{,\alpha} \qquad \underline{a}_{\alpha,\beta} = \underline{\phi}_{,\alpha\beta} \qquad \underline{a}_{\alpha,\beta\lambda} = \underline{\phi}_{,\alpha\beta\lambda} \quad .$$

These vectors are then used to obtain all the geometric quantities for the shell by the relationships shown in chapter 3, either the approximate mapping or the exact mapping routines are used to calculate them. The remaining calculations are then independent of how the mapping was obtained. The following is a list of the geometric quantities used in various parts of the program

$$\underline{a}_\alpha,\ \underline{a}_\beta,\ a_{\alpha\beta},\ a^{\alpha\beta},\ a,\ b_{\alpha\beta},\ b^{\beta}_{\alpha}\ ,\ b^{\lambda}_{\alpha,\beta},\ c_{\alpha\beta},\ \Gamma^{\lambda}_{\alpha\beta} \quad .$$

These are all calculated in a single routine for a given point on an element.

Note that for the exact mapping calculations coordinates must be given in the global system on Ω and not the element local system.

6.6 Matrices $[D_{IJ}]$ and $[C_{IJ}]$.

The method used to obtain expressions for the components D_{IJ} in appendix B is followed. The 28 components of the matrices $[P_{IJ}]$ and $[Q_{IJ}]$ and the 78 components of matrices $[R_{IJ}]$ and $[S_{IJ}]$ are combined to give the 78 essential components of $[D_{IJ}]$ shown in Appendix B. The non-zero components of $[C_{IJ}]$ are calculated and inserted directly into a two dimensional array.

6.7 Post-Processing.

6.7.1 Nodal Displacements.

The static analysis displacement solution vector or, in the case of frequency analysis, the mode shape vectors contain covariant components of the nodal displacements. In chapter 2 it was shown that covariant components are not necessarily the actual lengths of component vectors since the tangent basis vectors are not necessarily of unit length. The displacement covariant components are therefore not of much practical use. Since shell displacements are often described relative to the global coordinate system in $\mathbf{E}^3$, the displacement solutions were transformed to components in the global system. This requires calculation of nodal tangent basis vectors which are obtained as described in section 6.5.

6.7.2 Integration Point Stress Resultants.

The shell mid-surface strains $\gamma_{\alpha\beta}$ and $\rho_{\alpha\beta}$, given by expressions (3.4.11) and (3.4.12) are evaluated and inserted into expressions (3.6.1) and (3.6.2) to obtain the doubly contravariant components of the stress resultants, $n^{\alpha\beta}$ and $m^{\alpha\beta}$. The strain quantities are functions of covariant displacement components and their derivatives. An element solution vector is formed and converted into a set of generalised parameters for each of the displacement component functions using the generalised parameter-nodal degree of freedom transformation matrices. These matrices are not recalculated but are read from a file to which they were written during element matrix calculations. The required displacement components and their derivatives are then obtained at points on

the element by multiplication of the generalised parameters with relevant rows of the matrix $[P^5_{0,1,2}]$ evaluated at the point. The geometric properties in the strain expression are also evaluated at these points. The doubly invariant components of the stress resultants obtained from the strains using tensor $K^{\alpha\beta\chi\mu}$ as shown in section 3.6 are then transformed to the values of the actual stress resultants and moments by multiplication with the components of the covariant components of the metric $a_{\alpha\beta}$.

6.7.3 Plotting.

The SACLAND Graphics Package was used to provide contour plots and 3-dimensional representations of various functions over the domain $\Omega \in \mathbf{E}^2$. For displacement plots the displacements at integration points were used to increase the number of data points. This is easily done since the processes for calculating these were already set up for the calculation of integration point stress resultants and for nodal point displacements. It is reasonable to do this since the information carried in the derivative degrees of freedom cannot be used directly.

CHAPTER 7

RESULTS

7.1 Introductory remarks

Three fundamentally different shell mid-surface geometries were used in the investigation of different aspects of the implementation of the formulation presented in earlier chapters. The three geometries used were a flat plate, a circular cylinder in the form of a barrel vault roof, and a hyperbolic parabaloid. Basic features of each of these geometries are discussed and relevant geometric quantities for all three are given in Table 7.1. Both static and eigenvalue analyses have been carried out for sets of examples involving the three different geometries.

A range of the integration rules discussed by Lyness and Jespersen as shown in figure 6.1 were used with static analysis problems to ascertain the most suitable rule for each geometry. Exact surface mappings were used for these investigations. The Lagrange type 1,2 and 3 interpolation schemes were used to approximate inplane displacement component functions. This variation of interpolation schemes was carried out with both static and eigenvalue analyses for the curved surface geometries; exact surface mappings were used for these investigations. The effect of including the approximation of shell mid-surface geometry was evaluated for each of the three approximate mapping interpolation schemes implemented.

GEOMETRIC QUANTITY	SURFACE		
	Flat Plate	Cylindrical Barrel Vault	Hyperbolic Parabaloid
Mapping Components			
ϕ_1	x	R cos θ	x
ϕ_2	y	R sin θ	y
ϕ_3	0	z	$\frac{xy}{c}$
Surface Metric Components and Determinant			
a_{11}	1	R^2	$1 + \left(\frac{y}{c}\right)^2$
a_{12}			xy/c
a_{22}	1	1	$1 + \left(\frac{x}{c}\right)^2$
a^{11}	1	$1/R^2$	$(c^2+x^2)(c^2+x^2+y^2)^{-1}$
a^{12}			$-xy(c^2+x^2+y^2)^{-1}$
a^{22}	1	1	$(c^2+y^2)(c^2+x^2+y^2)^{-1}$
$a=\det(a_{\alpha\beta})$	1	R^2	$(c^2+x^2+y^2)c^{-2}$
Curvature Tensor Components			
b_{11}		-R	
b_{12}			$(c^2+x^2+y^2)^{-1/2}$
b_{22}			
b_1^1		$-R^{-1}$	$-xy(c^2+x^2+y^2)^{-3/2}$
b_2^1			$(c^2+x^2)(c^2+x^2+y^2)^{-3/2}$
b_1^2			$(c^2+x^2)(c^2+x^2+y^2)^{-3/2}$
b_2^2			$-xy(c^2+x^2+y^2)^{-3/2}$
3rd Fundamental Form Components			
c_{11}		1	$(c^2+x^2)(c^2+x^2+y^2)^{-2}$
c_{12}			
c_{22}			$(c^2+x^2)(c^2+x^2+y^2)^{-2}$
Christoffel Symbols (Non-zero Components)			
Γ_{21}^1			$y(c^2+x^2+y^2)^{-1}$
Γ_{21}^2			$x(c^2+x^2+y^2)^{-1}$
Non-zero Derivatives of Curvature Components			
$b_{12,1}$			$-x(c^2+x^2+y^2)^{-3/2}$
$b_{12,2}$			$-y(c^2+x^2+y^2)^{-3/2}$

Table 7.1 : Geometric Quantities for Example Problems.

Results of all investigations are presented for each geometry in turn, and details of the example problems including the finite element meshes used are also given. Where available, independently obtained results are compared with those obtained in the present study; ABAQUS and ADINA packages are also used to provide independent numerical results. In all the analyses performed with ABAQUS use is made of the S8R element, a thick shell "degenerate" type shell element with eight nodes, and for which reduced integration is used (see ABAQUS Theoretical Manual, 1982). Both ABAQUS and ADINA use subspace iteration methods to obtain eigenvalue solutions, as does the present study.

7.2 Flat Plate Examples

A flat plate (FP) has the simplest possible shell geometry. The tangent basis is a constant orthonormal set of vectors, and the shell surface mapping $\underline{\phi}$ is the identity. Since all curvature quantities are zero (see Table 7.1) there is no coupling between membrane and transverse bending action and hence between in plane and transverse displacement components.

7.2.1 Static Analysis

A square plate with fully clamped boundary under uniformly distributed load was analysed. The finite element mesh, dimensions and material properties used are given in figure 7.1. The results obtained for the central deflection are compared with an analytical solution obtained for this problem via a formula derived by Timoshenko (1959). The integration rule investigation results are presented in figure 7.2. Moment stress resultant along the line AB are compared with those obtained using ABAQUS (figure 7.3).

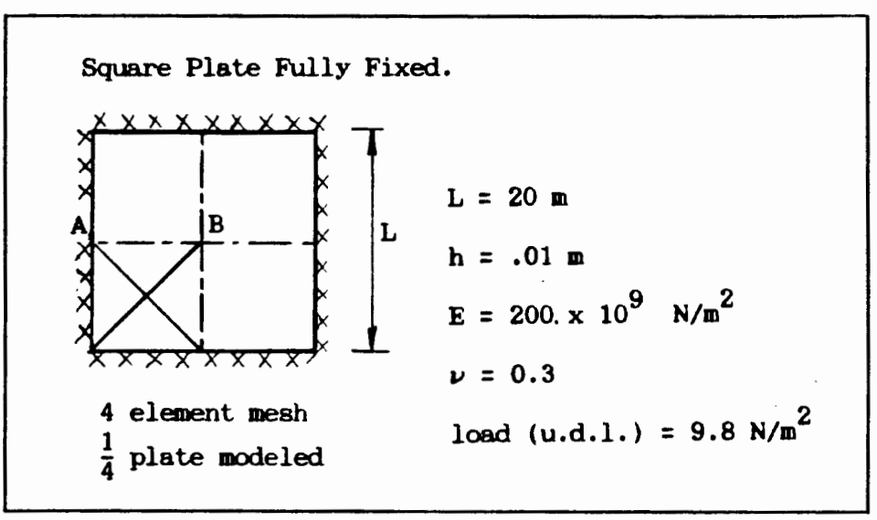

Figure 7.1.: Flat Plate Static Analysis Example

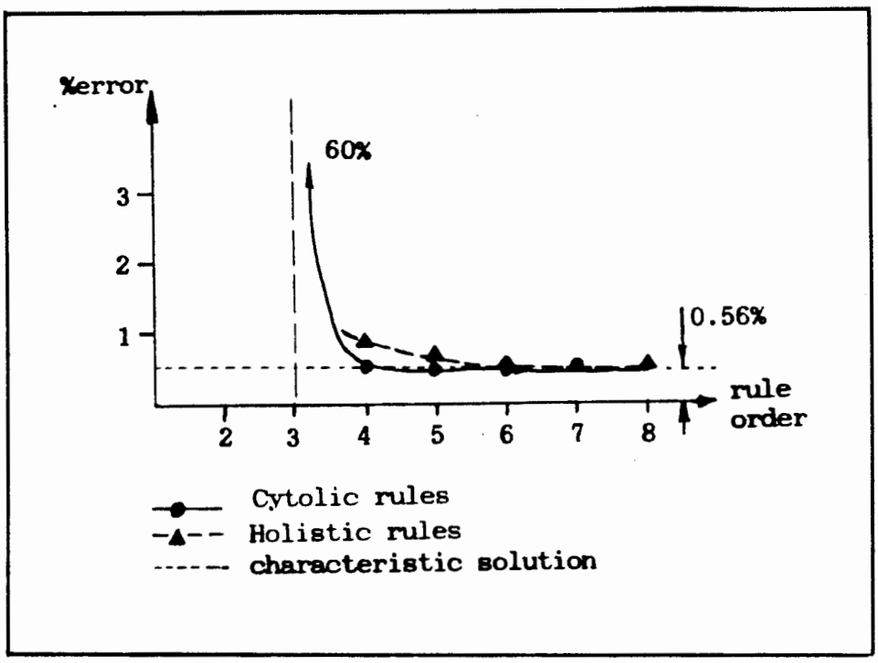

Figure 7.2.: FP integration rule investigation

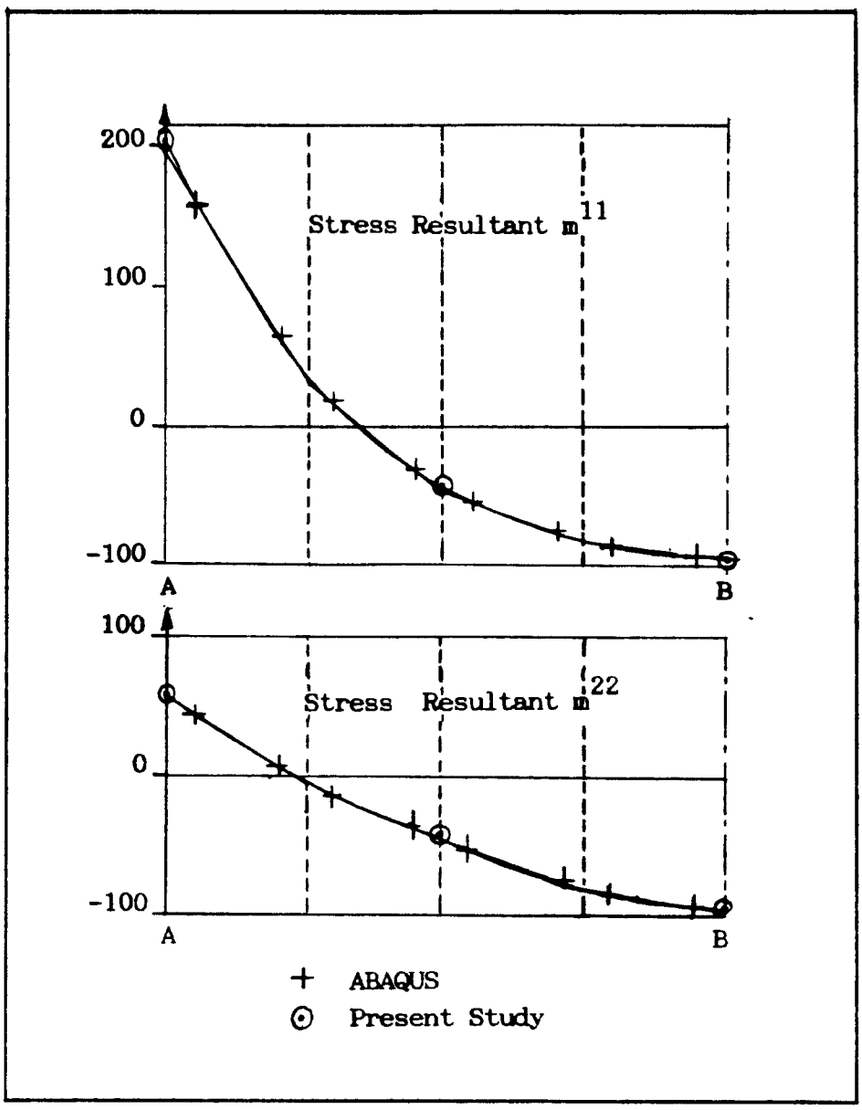

Figure 7.3 : FP Stress Resultants

7.2.2 Eigenvalue Analysis

Two examples are presented for eigenvalue analyses of flat plates;

(a) a simply supported square plate, and

(b) a triangular cantilever.

Both these examples are used for shell element verification by ADINA (see ADINA System Verification Manual, (1983)).

(a) Simply Supported Plate

Only the first natural frequency is shown; this is compared with an analytical result obtained via a formula due to Blevins (1979), and with a result obtained using ADINA. These results are given in Table 7.2 and a plot of the corresponding mode shape, or eigenfunction, is shown in figure 7.5. Details of this example and meshes used for both the present study and with ADINA are shown in figure 7.4.

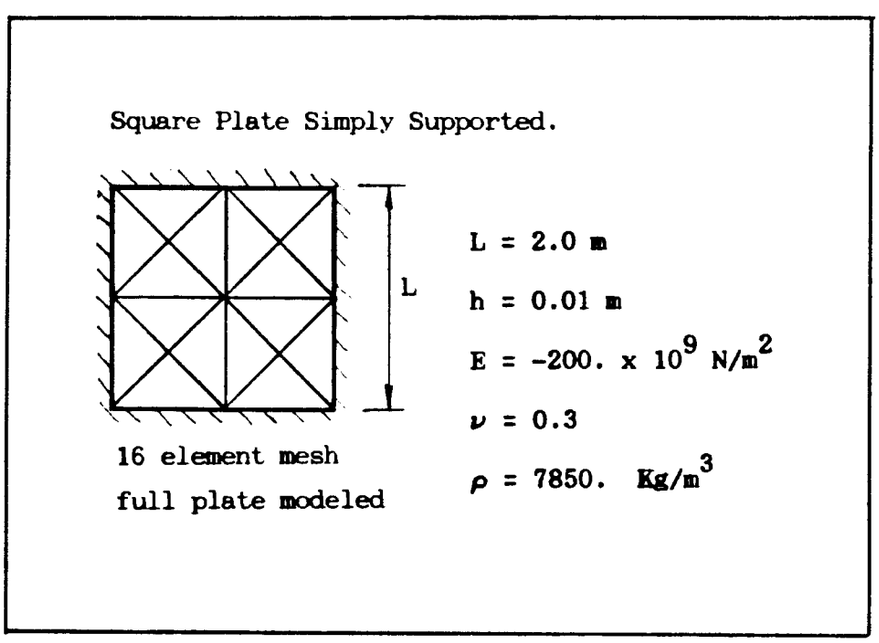

Figure 7.4 : FP Eigenvalue Analysis example (a)

	1^{st} natural freq. Hz
Blevins	12
ADINA	12,17
Present Study	11,99

Table 7.2 ; Results ; FP Eigenvalue Analysis example (a)

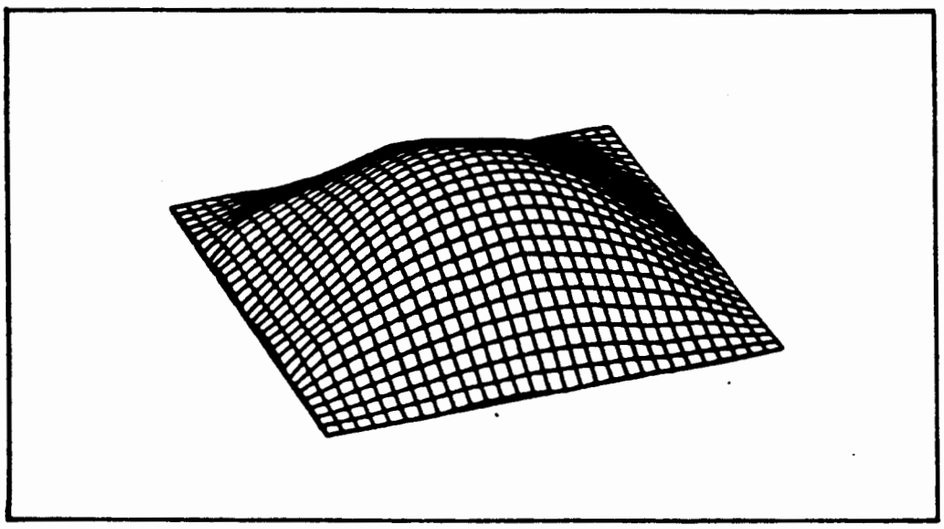

Figure 7.5 ; Mode Shape, mode 1 example (a)

(b) Triangular Cantilever

The first four natural frequencies are shown; these are compared with some experimental results and results obtained using ADINA. Several different meshes were used for the analyses performed on the basis of the present study, details of this example and all the meshes used are shown in Figure 7.6. The natural frequency results are given in Table 7.3.

TRIANGULAR CANTILEVER.

Present Study Meshes.

single element 2 element mesh 4 element mesh

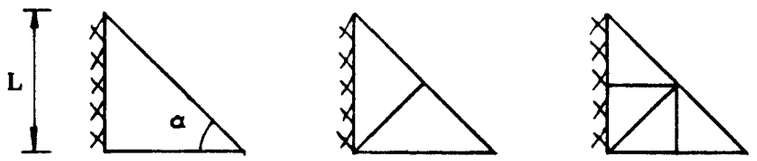

ADINA Mesh.

36 elements (Flat triangular shell facet elements linear interpolation)

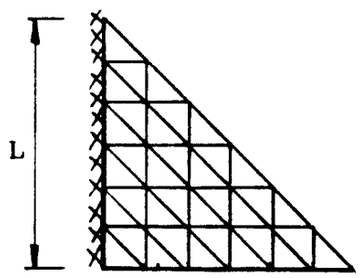

Material Properties and Dimensions.

$E = 2.0685 \times 10^{11}$ N/m^2 L = 0.254 m

$\nu = 0.3$ $h = 0.155 \times 10^{-2}$ m

$\rho = 7840$ Kg/m^3 $\alpha = 45^{\circ}$

Figure 7.6 : FP Eigenvalue Analysis example (b)

Mode	1	2	3	4
Experimental-Results (Cowper et al (1969)	34,5	136,0	190,0	325,0
ADINA 36 element mesh	36,4	143,3	194,9	366,7
Present Study : single element mesh	36,8	148,0	202,1	349,0
2 element mesh	36,8	140,7	203,1	350,7
4 element mesh	36,7	139,7	195,1	338,4

Table 7.3 : Results : eigenvalue analysis FP example (b)

7.2.3 Remarks

These flat plate examples serve to verify the calculation of transverse displacement shape functions, the static and eigenvalue analysis algorithims and solvers, and post processing calculations. Integration rule investigations show that for a given mesh all integration rules exact for polynomials > 3 are satisfactory for practical purposes; errors are less than 1% for the given mesh. The use of high order interpolation for transverse displacements is shown to be suited to the capturing of vibration modes with few degrees of freedom.

7.3 Barrel Vault Roof Examples

The barrel vault roof (BVR) is a portion of a circular cylinder, as shown in figure 7.7 The shell is free along its longitudinal edges and simply supported by a diaphram wall along the circumferential edges. The mid-surface of the shell has constant curvature and is a developable surface. It can be seen from Table 7.1. that many of the surface geometric quantities are zero and those which are non-zero are constant. The components of the surface mapping ϕ_i are trigonometric functions which, of course, cannot be represented exactly by polynomial functions. Since all the surface quantities are constants, use of the exact mapping leads to a form of the problem which is simpler than that obtained through the use of an approximate map (see Ciarlet (1975) and Bernadou (1980)). This situation is exceptional and applies only to cylindrical surfaces.

Very similar examples were used for both static and eigenvalue analyses for the circular cylinder shell geometry. The dimensions, angles and material properties used in each case are given in Table 7.4. The configuration used for the static analysis has been used extensively in the verification of shell element formulations. The meshes shown in figure 7.8 for the present study were used for both the static and eigenvalue analyses.

Static Analysis	Eigenvalue Analysis
$E = 206.8 \times 10^9$ N/m^2	$E = 3.0 \times 10^6$ 16/in^2
$\nu = 0.$	$\nu = 0.$
h = 0.762 m	h = 3 in
R = 7.62 m	R = 600 in
L = 7.62 m	L = 300 in
$\alpha = 40^\circ$	$\alpha = 20^\circ$
load = 478.24 N/m^2 (vertically down)	$\rho = 0.0868$ 16/in^3

Table 7.4 : Details for BVR examples

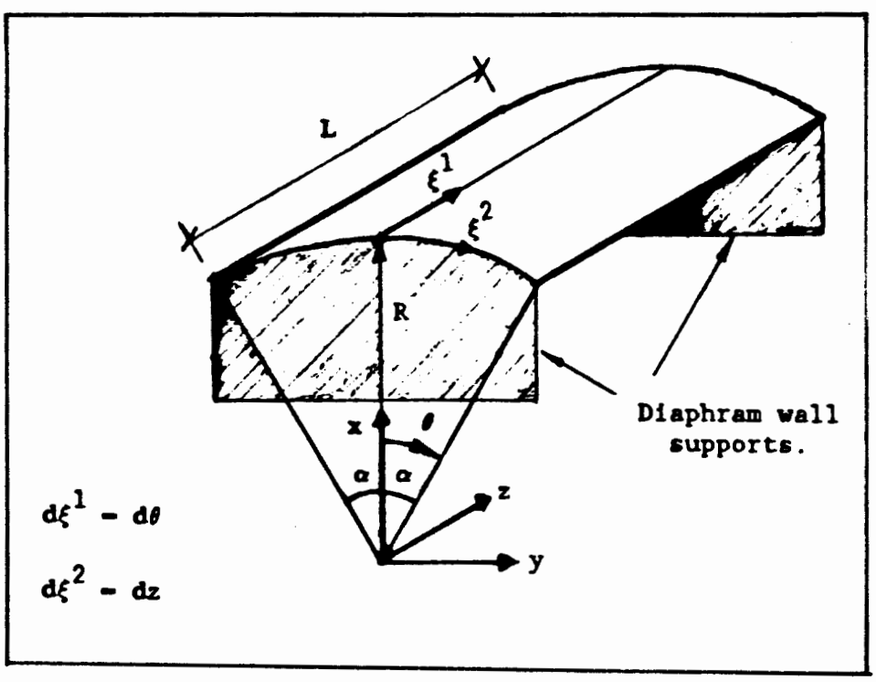

Figure 7.7 : Barrel Vault Roof

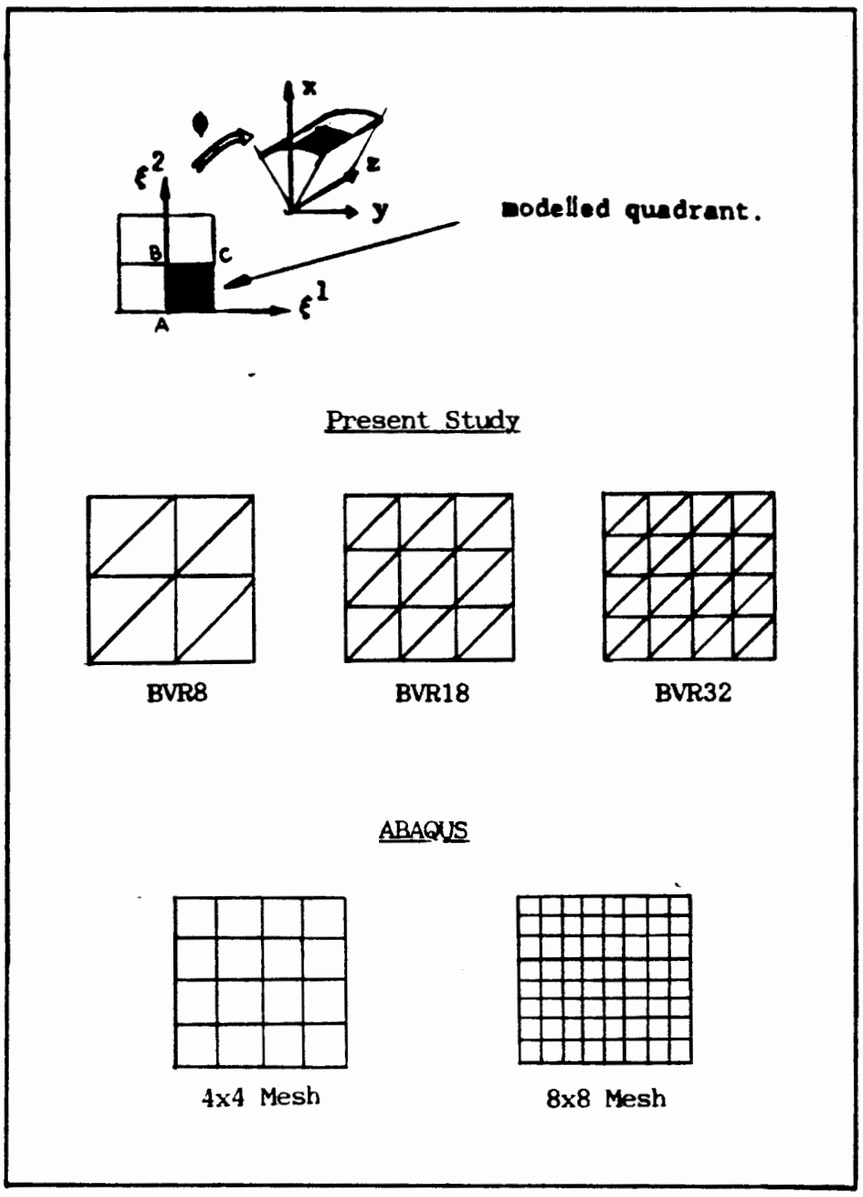

Figure 7.8 : Barrel Vault Meshes

7.3.1 Static Analysis

(a) Integration Rule Investigation Results

In figure 7.9 the results obtained with the present study for the veritcal displacement at C are compared with a generally accepted solution for this displacement given by Ashwell (1976).

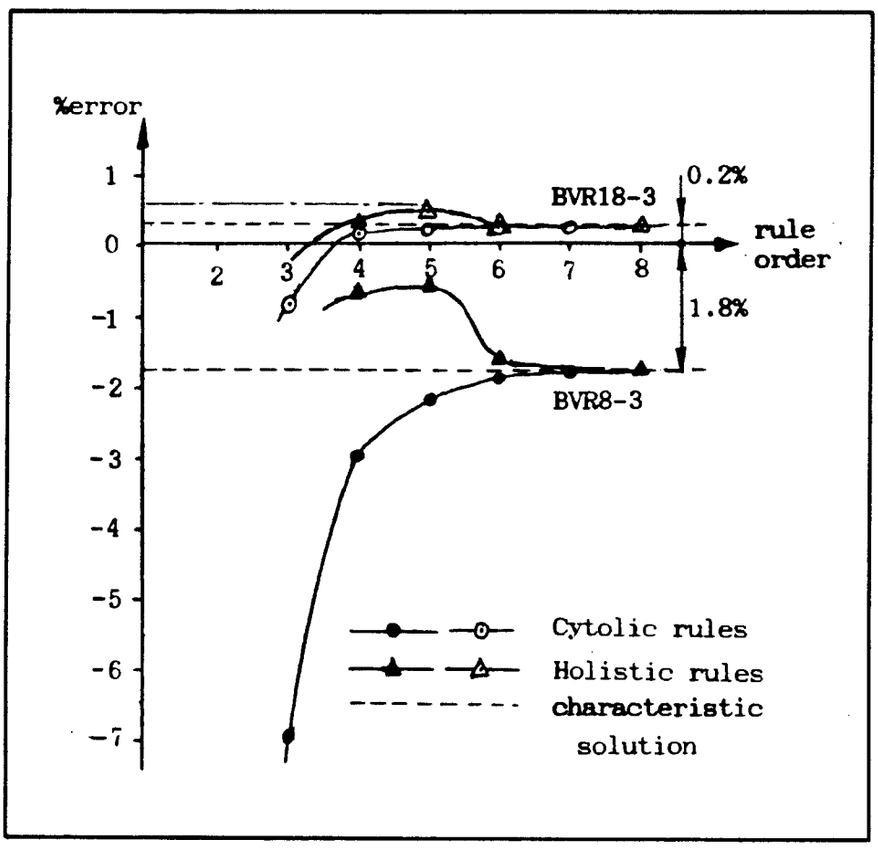

Figure 7.9 : BVR Integration rule Investigations

(b) In-Plane Displacement Interpolation Investigation

Results for the vertical deflection along BC are presented for analyses using the various meshes, see figures 7.10(a), (b) and (c). Figure 7.10(a) shows the effect of increasing the order of the in-plane displacement interpolation with a fixed mesh, while figures (b) and (c) show the effect of mesh refinement with the linear and quadratic schemes, convergence of the cubic scheme would not show up on a diagram of this type since errors are very small, as can be seen from figure 7.9 above. The interpolation order is indicated by "-1", "-2" or "-3" following the mesh discription. The ABAQUS result shown was obtained with the 8x8 mesh, for which deflection at C is within 1% of the accepted result.

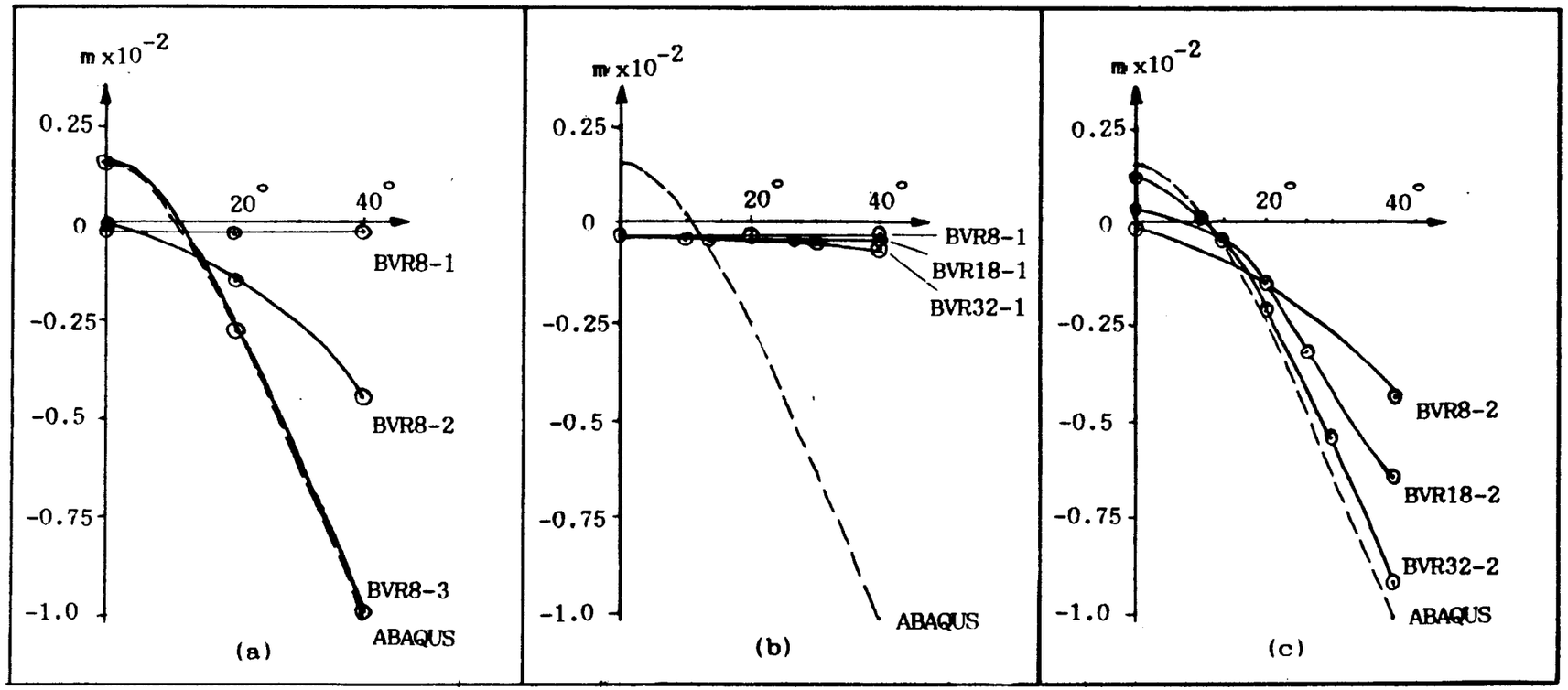

Figure 7.10 : BVR interpolation investigations

(c) Stress Resultants

No satisfactory results for stress resultants m^{11}, m^{22}, n^{11}, and n^{22} along lines AB and BC were obtained. The source of errors is not clear ; one possibility is mentioned in the conclusion in chapter 8.

(d) Approximation of Shell Surface Mapping

Results obtained with the BVR8-3 and BVR18-3 mesh, using integration rule 52 in conjunction with each of the approximate mapping schemes, are given in Table 7.5.

Mapping Approximation	Deflection at C ($x10^{-2}$)m	
	BVR18-3	BVR8-3
exact	0.990	1.015
Bell triangles	0.990	1.015
Hermite triangles	0.870	1.010
Lagrange type 3 triangles	0.992	1.015
Analytical solution	1.013×10^{-2} m	

Table 7.5 : Results : BVR approximate mappings

7.3.2 Eigenvalue Analysis

Table 7.6 shows the results obtained for the first five natural frequencies with the present study ABAQUS and by Clough and Wilson (1971). The results of Clough and Wilson appear to have been obtained with mass per unit area in different units from those quoted. This error is corrected here.

		NATURAL FREQUENCIES Hz				
		1	2	3	4	5
Clough-Wilson 8x8 mesh		0.808	2.010	2.84	3.83	5.81
ABAQUS 4x4		0.775	1.852	2.595	3.758	5.573
ABAQUS 8x8		0.775	1.852	2.572	3.732	5.283
PRESENT STUDY EXACT GEOMETRY	BVR-8 Mesh In-plane displacements approx by Lagrange					
	type 1	0.528	0.729	1.171	1.392	1.634
	type 2	0.168	0.331	0.608	0.746	1.152
	type 3	0.770	1.890	2.826	3.777	5.893
	BVR-18 Mesh In-plane displacements approx by Lagrange					
	type 1	0.425	0.585	0.979	1.198	1.336
	type 2	0.136	0.307	0.4937	0.636	0.968
	type 3	0.772	1.889	2.664	3.721	5.554
PRESENT STUDY APPROX. GEOMETRY	BVR-8 Mesh Geometry approx by					
	Bell	0.777	1.889	2.826	3.778	5.893
	Hermite	0.777	1.890	2.827	3.777	5.895
	Lagrange type 3	0.777	1.891	2.826	3.777	5.894

Table 7.6 : Results : BVR eigenvalue analysis .

7.3.3 Remarks

Integration rule investigations show the convergene of the results obtained for a given mesh with increasing order of the integration rules. A charateristic solution is obtained for the mesh. To provide some measure of the effectiveness of a rule the following error quantities are looked at.

(a) The percentage error of the characteristic solution E, given by

$E = |(\text{exact} - \text{charateristic})/\text{exact}|$.

(b) The difference between the result obtained with a particular rule and the characteristic solution, e, given by

$e = |(\text{characteristic} - \text{rule})/\text{exact}|$.

(c) The parameter by which a rule is judged D,defined by

$D = E + e$.

For example the fifth order rules used with the 8 element mesh.

$E = 1.8\%$; for rule 52 , $e = 0.5\%$, therefore $D = 2.3\%$

for rule 51 , $e = 1.0\%$, therefore $D = 2.8\%$

The rule 52 is therefore considered the better of the two, even though rule 51 gives the best result for this particular loading case and mesh. The error due to numerical integration dominates if $E > e$, as in the case of the third order rules. With slight mesh refinement results improve dramatically, $D < 0.5\%$. Note that the rule 51 yields the worst result, for rules of order > 3, with the 18 element mesh.

The order of interpolation used for inplane displacement component functions is shown to have a very marked effect on the results obtained for both static and eigenvalue problems. The first order scheme gives a very "stiff" result i.e. a form of membrane locking takes place,although some slight yielding of this is observed with mesh refinement. The solutions obtained with the second order scheme also improve with mesh refinement, but convergence to an acceptable solution with a pratical mesh is not found. The third order scheme is clearly shown to be effective ; good solutions are obtained even with the coarsest mesh used.

The shell surface mapping functions appear to be approximated equally well with each of the schemes implemented. Good results are obtained for bending stress resultants ; however, membrane stress results are poor.

7.4 Hyperbolic Parabaloid

Figure 7.12 shows the hyperbolic parabaloid (HYP) shell used.

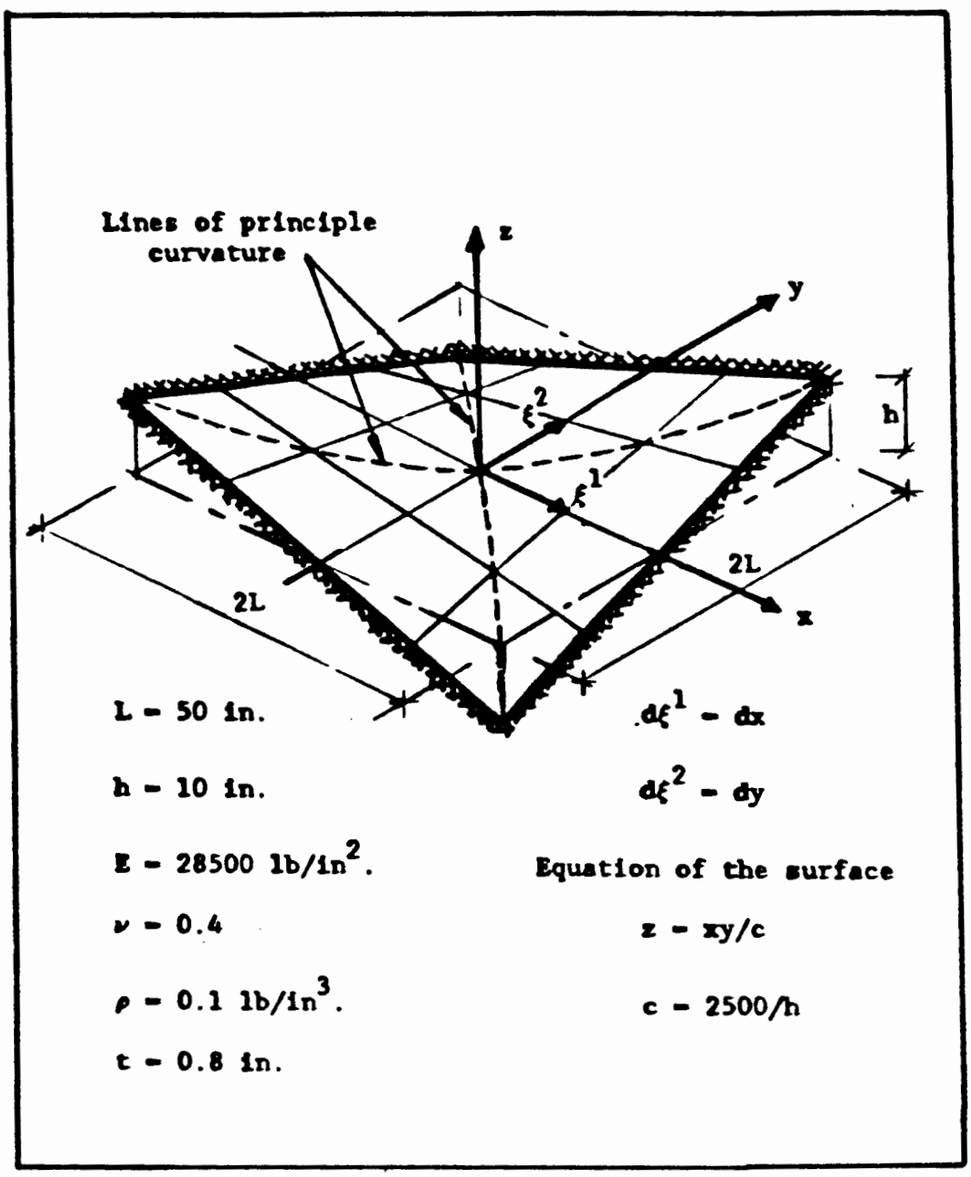

Figure 7.12 : Hyperbolic Parabaloid Example

This problem has been used by others for the verification of shell elements for static analysis (Kanok-Nukulchi 1978 and ADINA 1983), but not for eigenvalue analysis. The surface geometry is non-trivial although some of the geometric quantities used are zero (see Table 7.1). The tangent basis is not orthogonal so that off-diagonal terms of the surface metric are non-zero. The surface curvature tensor has zeros on the diagonal, hence the mean curvature is zero, but the off-diagonal terms are non-zero and dependent on surface coordinates. The functions ϕ_i and their derivatives are simple polynomial expressions which are exactly interpolated using any of the $\underline{\phi}_h$ schemes, so that approximation of the geometry is dependent only on the choice of the integration schemes.

The mesh used for present study analyses is shown below in figure 7.13. The meshes used for ABAQUS analyses are similar to those used for the Barrel Vault examples.

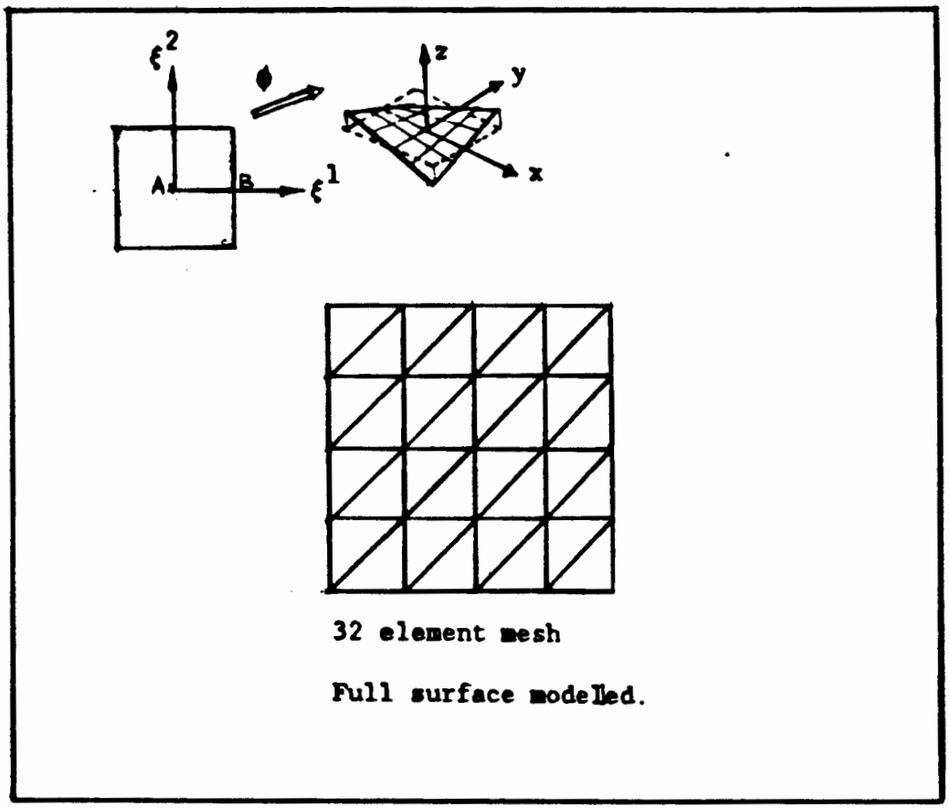

Figure 7.13 : HYP Mesh.

7.4.1 Static Analysis

(a) Integration Rule Investigation

The central deflection is compared with a finite difference solution obtained by Conner and Brebbia (1976).

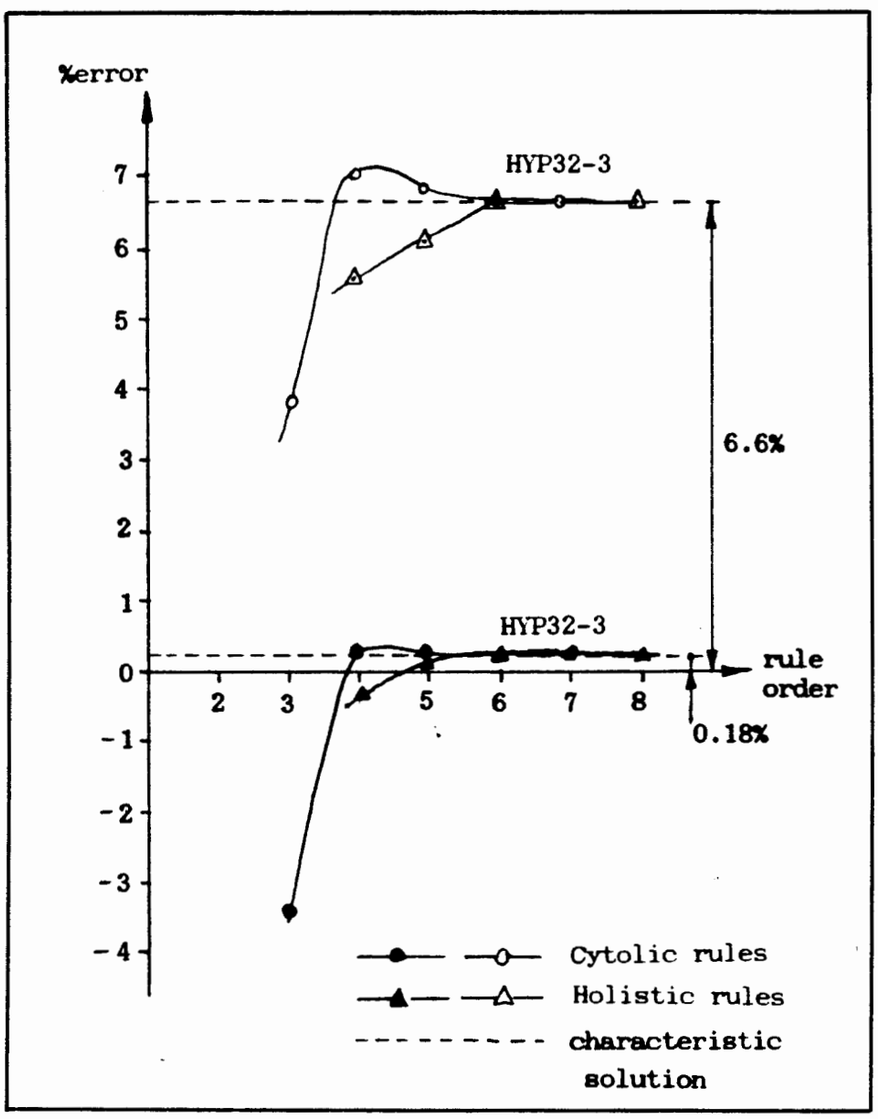

Figure 7.14 : HYP integration rule investigations

(b) Deflection Results

The deflection along line AB obtained from various analyses is shown in figure 7.15 Stress resultant results are omitted for this example since they show only information already illustrated by the preceding examples.

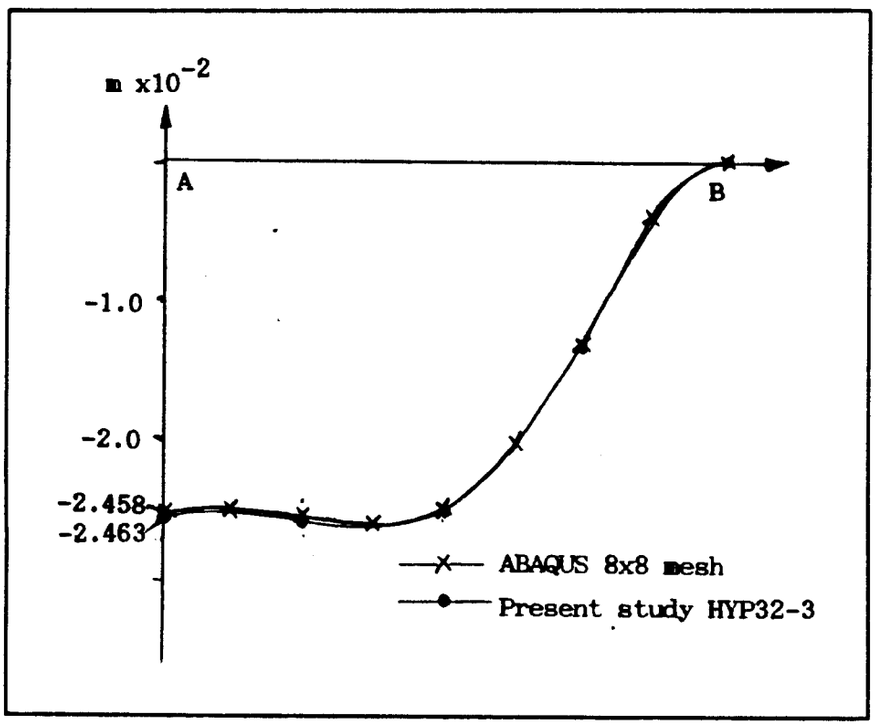

Figure 7.15 : HYP static analysis results

MODE	CONTOUR PLOT	3D PLOT
1.		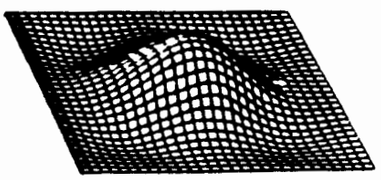
2.		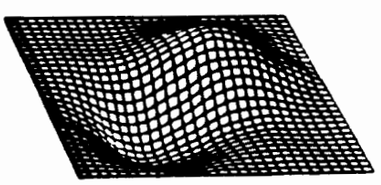
3.	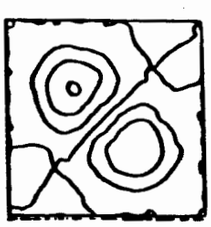	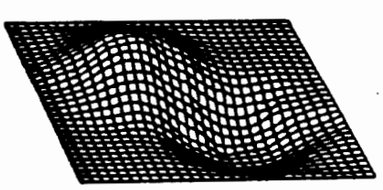
4.	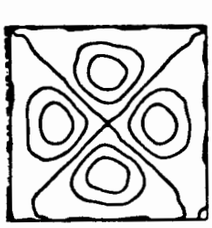	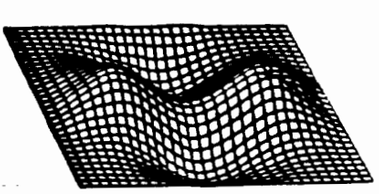
5.	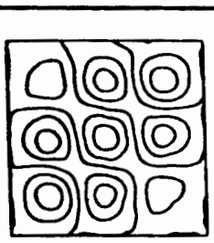	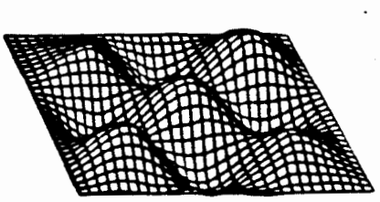

Figure 7.15 : HYP Eigenfunctions or Mode shapes.

7.4.3 Remarks

The effects observed for the barrel vault problem are reproduced with this example of more complex shell geometry. The results obtained for the eigenvalue analysis are especially note worthy since the number of degrees of freedom used is low. The values obtained for the natural frequencies using ABAQUS converge with mesh refinement, and the results obtained with the 12x12 mesh are taken to be most accurate.

CHAPTER 8

CONCLUSION

The analysis of convergence of finite element methods for shell problems has not been pursued to a great extent ; to date the major contributions have been those of Ciarlet (1976) and Bernadou (1980) (see also Bernadou and Ciarlet 1975). These authors have derived asymptotic error estimates for conforming finite element approximations for static problems for thin elastic shells of arbitrary geometry. Their work is based on the approach to shell problem formulation discussed in chapters 3 and 4. Extension of the formulation used by Ciarlet and Bernadou to include the eigenvalue problem proves a fairly simple exercise. In addition to this extension the aim of this study is to obtain some indication of how well this approach might be expected to work in practice. It has not prior to the present study been explicitly used as a basis for the development of a shell analysis program aimed at solving practical shell problems. This work therefore helps to fill the gap between theoretical convergence studies and practical aspects of the use of the finite element method for shell problems.

Good results have been obtained for both static and eigenvalue problems using reasonably coarse finite element meshes. The results of the various investigations carried out are discussed

with respect to the analytical studies of Ciarlet and Bernadou. Some limitations to the method are identified.

Integration rule investigations confirm Bernadou's findings in the sense that his prediction that rules exact for polynomials of order 6 and 7 (using 12 to 16 integration points) should be used is reflected in the results of the present study. In general the solutions obtained with lower order rules vary by only a small amount from those obtained using the "6 and 7" rules. The cost of computations can be substantially reduced by employing lower order rules since they require fewer integration points.

The order of interpolation of in-plane displacement component functions has been shown to effect to a large extent the accuracy of finite element approximations used to solve both static and eigenvalue problems for shells. This observation was also made by Clough and Wilson (1971) using a different shell formulation. A need for 3rd order polynomials for the interpolation of the in-plane displacement components is identified (i.e. k = 3 below). This requirement is not apparent from the asymptotic error estimate of Ciarlet (1976) where

$$\|\underset{\sim}{u}_h - \underset{\sim}{u}\| \leq Ch^{\min(k,\ell-1,m-2)}$$

where

k is the order of in-plane displacement interpolation

ℓ is the order of the transverse displacements interpolation

m is the order of interpolation used to obtain the approximate shell geometry

h is the characteristic measure of the finite element mesh, e.g. the diameter of the largest element.

Using this estimate as a basis for predicting the required in plane interpolation order, for example, with ℓ=m=4 (i.e. using the Bell triangle for both transverse displacements and approximate geometry) a value of k=2 would seem reasonable. The need for some additional hypothesis pertaining to the relationship between the values of k and l is thus indicated ; the possibility of this is in fact noted by Ciarlet.

The method of approximating the shell mid-surface geometry via the approximate mapping ϕ_h has proved successful for the examples tested. Although the shell geometries studied cover a range of cases none represents a very severe geometry, there is thus scope for further study of the approximation of shell geometry. The requirement for C^3 continuity of the geometric interpolation functions only on individual elements appears quite satisfactory. It is therefore best to use interpolation schemes which do not make use of derivative degrees of freedom. This makes it feasible to use a master element since no transformation of the mapping is necessary. Several limitations to the range of practical problems which can be tackled using this type of geometric representation have become apparent. These result from the assumption of regular surfaces (see chapter 3):

(a) The method breaks down where the mapping $\underset{\sim}{\phi}$ is singular, for example at the poles of a sphere the tangent basis vectors

have zero length and thus are undefined in direction;

(b) Kinks or folds in the shell surface cannot easily be accommodated since the tangent basis vectors and hence the covariant components of displacement which form the unknowns of the problem are not uniquely defined along the kink. It may be possible to overcome this by defining small elements over the kink. The geometry over the kink would then be represented by a regular surface with high curvature. This approach might well lead to numerical problems and is also questionable from a theoretical point of view since it is assumed that the ratio of radius of curvature to shell thickness is large.

Displacement solutions for static analyses show good agreement with independently obtained results ; however the evaluation of stress resultants does not prove a straightforward task. Integration points for cytolic rules which lie on the edges of elements may not be good sites for the evaluation of stress resultants, especially membrane forces. The resultants are dependent on the gradients of in-plane displacement component functions which are not well approximated near the edges of the C^0 elements used. Some further study is required in order to ascertain the best positions to sample the stress resultants.

Eigenvalue analyses have yielded some very accurate results ; relatively coarse meshes seem capable of predicting values for several natural frequencies. The method shows its greatest potential for these problems since, for the degenerate type

elements with which it might compete, reduced integration is not used for the calculation mass matrices. This together with the need for greater numbers of these elements brings the number of calculations required by the two methods to a comparable figure. Some extensive study of the free vibration of shells is required to test the limitations of both the present formulation and others before a valid conclusion can be drawn on this point.

This study is not aimed at developing a cheap, efficient, practical, general purpose shell element. It is generally accepted that conforming finite element approximations for shell problems do not provide a cost effective way of solving practical shell problems. The expense of the method is often associated with the high number of degrees of freedom required, for example the SHEBA element (Argyris and Lochner 1972) which uses 64 degrees of freedom. Using the approach followed in this study a successful element with 38 degrees of freedom can be formulated. This number of degrees of freedom compares favourably with that of some isoparametric, C^0 formulations; for example the quadratic Heterosis element (Hughes and Choen 1978), a 42 degree of freedom element formulated using the degeneration concept but which performs well in the thin shell range with reduced integration. In spite of the acceptable number of degrees of freedom the conforming elements remain inefficient since relatively large numbers of integration points are required and significantly many calculations are required to account for the shell geometry at each point. In addition to this inefficiency the limitations on the form of the shell geometry place severe restrictions on the

practical application of the approach followed in this study.

The study has provided a basis for an analysis of the convergence of eigenvalue problems for shells. To pursue the analysis of convergence of finite element approximations for shell problems the question of the relationship between in plane and transverse interpolation order should first be investigated.

The formulation and implementation of a full transient analysis for thin elastic shells should follow as a reasonably simple extension of this work. Similarly the addition of classical rate theory plasticity into the variational formulation should prove reasonably straight forward. Further developments using the approach followed in this study should however be considered carefully in the light of the divergence of this method from those which constitute the mainstream of shell finite element development and practice.

REFERENCES

ABAQUS (1982)

Theoretical Manual Hibbitt, Karlsson and Sorensen, Inc. (Providence, RI).

ADINA (1983)

System Verification Manual, Adina Engineering (Mass.).

Argyris, J H and Lochner, N (1971)

On the application of the SHEBA shell element, Comp Meths Appl Mech Engng 1 317-347.

Ashwel, D G and Gallagher, R H (editors) (1976)

Finite Elements for Thin Shells and Curved Members, John Wiley and Sons, (London)

Bathe, K J (1982)

Finite Element Procedures in Engineering Analysis, Prentice-Hall (Englewood Cliffs, NJ).

Bernadou, M (1980)

Convergence of conforming finite element methods for general shell problems, Int J Engng Sci 18 249-276.

Bernadou, M and Ciarlet, P G (1975)

Sur l'ellipticite du modele lineaire de coques de W T Koiter Comp Meths Appl Sci Engng (ed. R Glowinski and J L Lions) Lecture Notes in Economics and Mathematical Systems, Springer (Berlin), 134 89-136.

Blevins, R D (1979)

Formulas for Natural Frequency and Mode Shape, Van Nostrand Rheinhold (New York).

Carey, G F and Oden, T J

Finite elements : An Introduction, Prentice-Hall (Englewood Cliffs, NJ).

Ciarlet, P G (1976)

Conforming finite element methods for the shell problem Mathematics of Finite Elements and Applications (ed. J R Whiteman) Academic Press (London), II 105-123.

Ciarlet, P G (1980)

The Finite Element Method for Elliptic Problems North-Holland (Amsterdam).

Clough, R W and Tocher, J L (1965)

Finite element stiffness matrices for analysis of plates in bending Proc Conf Matrix Methods in Structural Mechanics Air Force Institute of Technology (Wright Patterson Air Force Base Ohio).

Clough, R W and Wilson, E L (1971)

Dynamic finite element analysis of thin shells Computers and Structures 1 33-56.

Cook, R D (1981)

Concepts and Applications of Finite Element Analysis, Wiley (New York).

Cowper G R, Kosko E, Lindberg G M and Olson M D (1969)

Static and Dynamic Applications of a High Precision Triangular Plate Bending Elemet, AIAA Journal, 7 1957-1965

Dovey, H H (1974)

Extension of three dimensional analysis to shell structures using the finite element idealisation, SESM Department of Civil Engineering Berkeley, Report No.74-2.

Dym, C L and Shames, I H (1973)

Solid Mechanics : A Variational Approach, McGraw-Hill (New York).

Eve, R A and Reddy, B D (1987)

Variational formulation and conforming finite element approximation of eigenvalue problems for thin elastic shells, Applied Mechanics Research Unit (University of Cape Town), Technical Report No.88

Flugge, W (1972)

Tensor Analysis and Continuum Mechanics , Springer (Berlin).

Hinton, E , Salonen, E M and Bicanic, N (1978)

A study of locking phenomena in isoparametric elements, Proc. 3rd MEFELAP conf., Brunel University, Uxbridge (ed. J R Whiteman) Academic Press (London).

Hinton, E and Owen, D R J (1984)

Finite element software for plates and shells, Pineridge Press (Swansea, UK).

Hughes, T J R and Choen, M (1978)

The 'heterosis' finite element for plate bending Computers and Structures 9 445-450.

Kanok-Nukulchai, W (1978)

A simple and efficient finite element for general shell analysis, Int J Num Meths Engng 14 179-200.

Kanok-Nakulchai, W, Taylor R L and Hughes, T J R (1981)
A large deformation formulation for shell analysis by the finite element method, Computers and Structures 12 19-27.

Koiter, W T (1970)
On the foundations of the nonlinear theory of thin elastic shells Parts I, II and III, Proc Konink Ned Akad Wetensch 73B 169-195.

Lyness, J N and Jespersen, D (1975)
Moderate degree symmetric quadrature rules for the triangle, J Inst Math Appl 15 19-32.

Mindlin, R D (1951)
Influence of rotary inertia and shear or flexural motions of isotropic elastic plates, J Appl Mech 37 1031-1036.

Reddy, B D (1986)
Functional Analysis and Boundary-Value Problems : An Introductory Treatment, Longman (London UK).

Stroud, A H (1971)
Approximate calculation of multiple integrals, Prentice-Hall (Englewood Cliffs, NJ).

Timoshenko, S P and Woinowsky-Krieger, S (1959)
Theory of Plates and Shells 2nd ed., McGraw-Hill (Kogakusha).

Wilson, E L, Taylor, R L, Doherty, W P and Ghaboussi (1973)
Incompatible displacement models, Num Comp Meths Struc Mech Academic Press (New York).

Zienkiewicz, O C (1977)
The Finite Element Method, McGraw-Hill (London UK).

A P P E N D I X A

NOTATION SYMBOLS AND ABBREVIATIONS

In general the notation used is defined in the text. Only those symbols used frequently throughout the text are listed here. Where the notation decribed here is not used the alternative "local" meaning of symbols is clearly indicated

a	determinant of the shell mid-surface metric tensor
$a_{\alpha\beta}$, $a^{\alpha\beta}$	components of the shell mid-surface metric tensor
$\underline{a}_\alpha$, $\underline{a}_3$ $\underline{a}^\alpha$, $\underline{a}^3$	shell mid-surface tangent basis vectors
$[A]$	matrix relating element nodal degrees of freedom and generalised parameters
$\{a_i\}$	a vector set of finite element degrees of freedom
$b_{\alpha\beta}$, b^α_β	component of the shell mid-surface curvature tensor
$B(.,.)$	a bilinear form
$[B]$	matrix relating element degrees of freedom and interpolated functions

$c_{\alpha\beta}$	components of the third fundamental form of the shell mid-surface
C(.,.)	mass term bilinear form
$[C_{IJ}]$	matrix used to define the mass term for the finite element approximations
ds dr	line elements
D(.,.)	stiffness term bilinear form
$[D_{IJ}]$	matrix used to define the stiffness term for the finite element approximations
$\underline{e}_i$	Cartesian coordinate system basis vectors
E^3, E^2	3 and 2 dimensional Euclidean spaces
E	Young's modulus
$\{F\}$ or $\{F_I\}$	global load vector
$\{f\}$	element load vector
$g_{\alpha\beta}$, $g^{\alpha\beta}$	components of a general surface metric tensor
$\underline{g}_\alpha$, $\underline{g}^\alpha$	general surface tangent basis vectors
h	shell thickness
H^0, H^1, H^m	Hilbert spaces
[H]	matrix used in defining Bell element shape functions
[I]	identity matrix

$\{s\}$	set of nodal values used to define the approximate shell mid-surface mapping on an element
t	time
$\underline{t}$	tangential vector
$[T]$	transformation matrix for Bell element
$\underline{u}$, $\underline{v}$	shell mid-surface displacement field
$\underline{u}_n$, $\underline{v}_n$	discretised shell mid-surface displacement field
$\underline{V}$	space of admissible shell mid-surface displacements
$\underline{V}_h$	finite element space of displacements
z	coordinate normal to shell mid-surface
$\gamma_{\alpha\beta}$	shell mid-surface strain tensor components
Γ	boundary of the domain of the problem
Γ^i_{jk}	Christoffel symbol
$\epsilon_{\alpha\beta}$	total strain tensor
$<\mu_i>$	monomial basis
ν	Poisson's ratio
ξ^α	shell mid-surface curvilinear coordinates
$\rho_{\alpha\beta}$	shell mid-surface change of curvature tensor components
ρ	material density
$\sigma_{\alpha\beta}$	total stress tensor
$\underline{\phi}$	shell mid-surface mapping

$\mathbb{E}_h$	finite element space of admissible shell geometries
$\psi_i^{(e)}$	finite element shape functions
Λ_i	finite element basis functions
ω	natural frequencies for the shell
Ω	domain of the shell problem in E^2
Ω_e	finite element sub domain

ABBREVIATIONS

BVP	boundary value problem
VBVP	variational boundary value problem
dofs	degrees of freedom
BVR	barrel vault roof example
FP	flat plate example
HYP	hyperbolic parabaloid example

A P P E N D I X B

EXPANSION OF THE BILINEAR FORMS

1. STRAIN ENERGY

$$D(u,v) = \int_{\Omega} \frac{Eh}{(1-\nu^2)} \Big[(1-\nu)\ \gamma^{\alpha}_{\beta}(u)\gamma^{\beta}_{\alpha}(v) + \nu\gamma^{\alpha}_{\alpha}(u)\gamma^{\beta}_{\beta}(v) + \frac{h^2}{12}\ \{(1-\nu)\rho^{\alpha}_{\beta}(u)\rho^{\beta}_{\alpha}(v) + \nu\rho^{\alpha}_{\alpha}(u)\rho^{\beta}_{\beta}(v)\} \Big] \sqrt{\bar{a}}\, d\xi^1 d\xi^2 \tag{4.5.4}$$

to be written in the form

$$D(u,v) = \int_{\Omega} \{U\}^T [D_{IJ}] \{V\}\ \sqrt{\bar{a}}\, d\xi^1 d\xi^2 \tag{5.5.1}$$

with

$$\{V\} = \{v_1, v_{1,1}, v_{1,2}, v_2, v_{2,1}, v_{2,2}, v_3, v_{3,1}, v_{3,2}, v_{3,11}, v_{3,12}, v_{3,22}\} \tag{5.5.2}$$

Expressions for doubly covariant components of mid-surface strain tensors have been presented in chapter 4.

$$\gamma_{\alpha\beta}(u) = \frac{1}{2}\ (u_{\alpha,\beta} + u_{\beta,\alpha}) - u_{\chi}\Gamma^{\chi}_{\alpha\beta} - u_3 b_{\alpha\beta} \tag{4.4.8}$$

$$\rho_{\alpha\beta}(u) = u_3 b_{\alpha\beta} + u_{\gamma,\beta} b^{\lambda}_{\alpha} + u_{\gamma,\beta} b^{\lambda}_{\beta} - u_{3,\lambda}\Gamma^{\gamma}_{\alpha\beta} + u_3 c_{\alpha\beta} + C^{\lambda}_{\alpha\beta} u_{\lambda} \tag{4.4.9}$$

where

$$C^{\lambda}_{\alpha\beta} = \frac{1}{2}\left(b^{\lambda}_{\alpha,\beta} + b^{\lambda}_{\beta,\alpha} - 2\Gamma^{\xi}_{\mu\beta}b^{\lambda}_{\xi}\right) \quad .$$

Using the relationships

$$\gamma^{\alpha}_{\beta} = \gamma_{\lambda\beta}\, a^{\lambda\alpha} \text{ and } \gamma^{\alpha}_{\beta} = \gamma_{\lambda\beta}\, a^{\lambda\alpha} \quad , \qquad (4.4.10)$$

$$\gamma^{\alpha}_{\beta}(u)\gamma^{\beta}_{\alpha}(v) = \gamma_{\lambda\alpha}(u)\gamma_{\mu\alpha}\, a^{\lambda\alpha}a^{\mu\beta} = \{U_I\}[P_{IJ}]\{V_J\} \quad ,$$

$$\gamma^{\alpha}_{\alpha}(u)\gamma^{\beta}_{\beta}(v) = \gamma_{\mu\alpha}(u)\gamma_{\lambda\beta}(v)a^{\lambda\alpha\mu\beta} = \{U_I\}[Q_{IJ}]\{V_J\} \quad ,$$

$$\rho^{\alpha}_{\beta}(u)\rho^{\beta}_{\alpha}(u) = \rho_{\lambda\beta}(u)\rho_{\mu\alpha}(v)\, a^{\lambda\alpha}a^{\mu\beta} = \{U_I\}[Q_{IJ}]\{V_J\} \quad ,$$

and

$$\rho^{\alpha}_{\alpha}(u)\rho^{\beta}_{\beta}(v) = \rho_{\mu\alpha}(u)\rho_{\lambda\beta}(v)\, a^{\lambda\alpha}a^{\mu\beta} = \{U_I\}[S_{IJ}]\{V_J\} \quad .$$

The matrix $[D_{IJ}]$ can then be expressed as

$$[D_{IJ}] = \frac{Eh}{(1-\nu^2)}\left[\{(1-\nu)[P_{IJ}] + \nu[Q_{IJ}]\} + \frac{h^2}{12}\{(1-\nu)[R_{IJ}] + \nu[S_{IJ}]\}\right] \quad .$$

The expansion of $\gamma_{\lambda\beta}(u)\ \gamma_{\mu\alpha}(v)$ is common to both $[P_{IJ}]$ and $[Q_{IJ}]$, similarly for $\rho_{\mu\alpha}(u)\rho_{\lambda\beta}(v)$ in $[R_{IJ}]$ and $[S_{IJ}]$. This fact is used to systimatcally find the coefficients of the matrices. All the matrices are symmetric (12x12) matrices. They can therefore be expressed by specification of the 78 coefficients (figure B.1.).

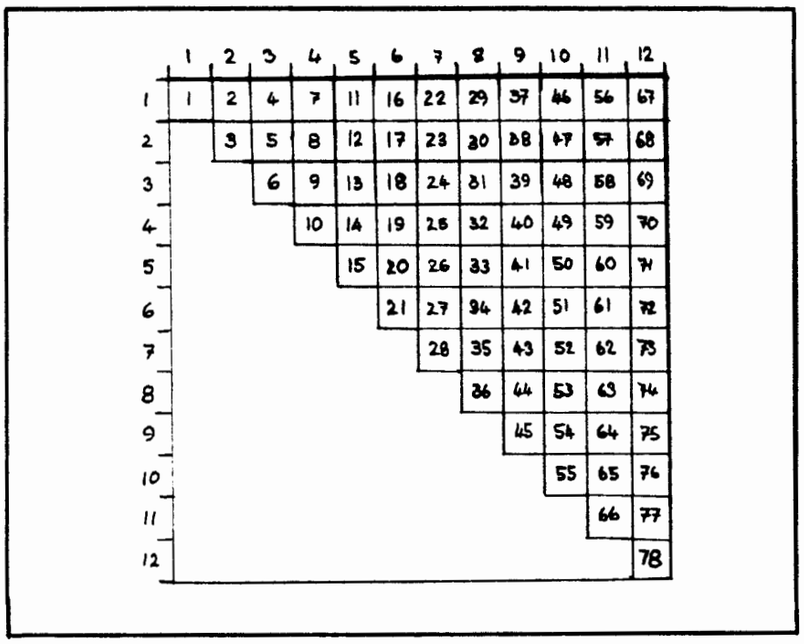

Figure B.1.

For the matrices $[P_{IJ}]$ and $[Q_{IJ}]$ only coefficients of terms in u_{α}, $u_{\alpha,\beta}$ and u_3 appear so that only 28 expressions are required. The full set of coefficient expressions are given in the following tables.

	P_{IJ}	Q_{IJ}
ROW 1		
1,1	$\Gamma^1_{\mu\alpha}\,\Gamma^1_{\lambda\beta}\,a^{\lambda\alpha}a^{\mu\beta}$	$\Gamma^1_{\mu\alpha}\,\Gamma^1_{\lambda\beta}\,a^{\lambda\beta}a^{\mu\alpha}$
1,2	$-\Gamma^1_{\mu\alpha}\,a^{1\alpha}a^{\mu 1}$	$-\Gamma^1_{\mu\alpha}\,a^{11}a^{\mu\alpha}$
1,3	$-\Gamma^1_{\mu\alpha}\,a^{1\alpha}a^{\mu 2}$	$-\Gamma^1_{\mu\alpha}\,a^{12}a^{\mu\alpha}$
1,4	$\Gamma^2_{\lambda\beta}\,\Gamma^1_{\mu\alpha}\,a^{\lambda\alpha}a^{\mu\beta}$	$\Gamma^2_{\lambda\beta}\,\Gamma^1_{\mu\alpha}\,a^{\lambda\beta}a^{\mu\alpha}$
1,5	$-\Gamma^1_{\mu\alpha}\,a^{1\alpha}a^{2\mu}$	$-\Gamma^1_{\mu\alpha}\,a^{12}a^{\mu\alpha}$
1,6	$-\Gamma^1_{\mu\alpha}\,a^{2\alpha}a^{2\mu}$	$-\Gamma^1_{\mu\alpha}\,a^{22}a^{\mu\alpha}$
1,7	$b_{\lambda\beta}\,\Gamma^1_{\mu\alpha}\,a^{\lambda\alpha}a^{\mu\beta}$	$b_{\lambda\beta}\,\Gamma^1_{\mu\alpha}\,a^{\lambda\beta}a^{\mu\alpha}$
ROW 2		
2,2	$a^{11}a^{11}$	$a^{11}a^{11}$
2,3	$a^{11}a^{12}$	$a^{11}a^{12}$
2,4	$-\Gamma^2_{\lambda\beta}\,a^{\lambda 1}a^{1\beta}$	$-\Gamma^2_{\lambda\beta}\,a^{\lambda\beta}a^{11}$
2,5	$a^{11}a^{12}$	$a^{11}a^{12}$
2,6	$a^{11}a^{12}$	$a^{11}a^{12}$
2,7	$-b_{\lambda\beta}\,a^{\lambda 1}a^{1\beta}$	$-b_{\lambda\beta}\,a^{11}a^{\lambda\beta}$
ROW 3		
3,3	$\frac{1}{2}\,a^{12}a^{12}+\frac{1}{2}\,a^{11}a^{12}$	$\frac{1}{2}\,a^{12}a^{12}$
3,4	$-\Gamma^2_{\lambda\beta}\,a^{\lambda 1}a^{2\beta}$	$-\Gamma^2_{\lambda\beta}\,a^{\lambda\beta}a^{12}$
3,5	$\frac{1}{2}\,a^{12}a^{12}+\frac{1}{2}\,a^{11}a^{12}$	$\frac{1}{2}\,a^{12}a^{12}$
3,6	$a^{22}a^{12}$	$a^{22}a^{12}$
3,7	$-b_{\lambda\beta}\,a^{\lambda 1}a^{2\beta}$	$-b_{\lambda\beta}\,a^{\lambda\beta}a^{12}$

	P_{IJ}	Q_{IJ}
ROW 4		
4,4	$\Gamma^2_{\lambda\beta}\,\Gamma^2_{\mu\alpha}\,a^{\lambda\alpha}a^{\mu\beta}$	$\Gamma^2_{\lambda\beta}\,\Gamma^2_{\mu\alpha}\,a^{\lambda\alpha}a^{\mu\beta}$
4,5	$-\,\Gamma^2_{\mu\alpha}\,a^{1\alpha}a^{2\mu}$	$-\,\Gamma^2_{\mu\alpha}\,a^{12}a^{\mu\alpha}$
4,6	$-\,\Gamma^2_{\mu\alpha}\,a^{2\alpha}a^{2\mu}$	$-\,\Gamma^2_{\mu\alpha}\,a^{22}a^{\mu\alpha}$
4,7	$b_{\lambda\beta}\,\Gamma^2_{\mu\alpha}\,a^{\lambda\alpha}a^{\mu\beta}$	$b_{\lambda\beta}\,\Gamma^2_{\mu\alpha}\,a^{\lambda\beta}a^{\mu\alpha}$
ROW 5		
5,5	$\frac{1}{2}\,a^{12}a^{12} + \frac{1}{2}\,a^{11}a^{22}$	$\frac{1}{2}\,a^{12}a^{12}$
5,6	$a^{22}a^{12}$	$a^{22}a^{12}$
5,7	$-\,b_{\lambda\beta}\,a^{\lambda 1}a^{2\beta}$	$-\,b_{\lambda\beta}\,a^{\lambda\beta}a^{12}$
ROW 6		
6,1	$a^{22}a^{22}$	$a^{22}a^{22}$
6,2	$b_{\lambda\beta}\,a^{\lambda 2}a^{2\beta}$	$b_{\lambda\beta}\,a^{\lambda\beta}a^{22}$
ROW 7		
7,1	$b_{\mu\alpha}\,b_{\lambda\beta}\,a^{\lambda\alpha}a^{\mu\beta}$	$b_{\mu\alpha}\,b_{\lambda\beta}\,a^{\lambda\beta}a^{\mu\alpha}$

	R_{IJ}	S_{IJ}
ROW 1		
1,1	$C^1_{\lambda\beta}\, C^1_{\mu\alpha}\, a^{\lambda\alpha}{}_a{}^{\mu\beta}$	$C^1_{\lambda\beta}\, C^1_{\mu\alpha}\, a^{\lambda\beta}{}_a{}^{\mu\alpha}$
1,2	$C^1_{\mu\alpha}(b^1_{\mu}\, a^{\lambda\beta}{}_a{}^{\mu 1} + b^1_{\beta}\, a^{1\alpha}{}_a{}^{\mu\beta})$	$2C^1_{\mu\alpha}\, b^1_{\chi}\, a^{\mu\alpha}{}_a{}^{1\chi}$
1,3	$C^1_{\mu\alpha}(b^1_{\lambda}\, a^{\lambda\alpha}{}_a{}^{\mu 2} + b^1_{\beta}\, a^{2\alpha}{}_a{}^{\mu\beta})$	$2C^1_{\mu\alpha}\, b^1_{\chi}\, a^{\mu\alpha}{}_a{}^{2}$
1,4	$C^2_{\lambda\beta}\, C^1_{\mu\alpha}\, a^{\lambda\alpha}{}_a{}^{\mu\beta}$	$C^2_{\lambda\beta}\, C^1_{\mu\alpha}\, a^{\lambda\beta}{}_a{}^{\mu\alpha}$
1,5	$C^1_{\mu\alpha}(b^2_{\mu}\, a^{\lambda\alpha}{}_a{}^{\mu 1} + b^2_{\beta}\, a^{1\alpha}{}_a{}^{\mu\beta})$	$2C^1_{\mu\alpha}\, b^2_{\chi}\, a^{\mu\alpha}{}_a{}^{1\chi}$
1,6	$C^1_{\mu\alpha}(b^2_{\mu}\, a^{\lambda\alpha}{}_a{}^{\mu 2} + b^2_{\beta}\, a^{2\alpha}{}_a{}^{\mu\beta})$	$2C^1_{\mu\alpha}\, b^2_{\chi}\, a^{\mu\alpha}{}_a{}^{2\chi}$
1,7	$C^1_{\lambda\beta}\, c_{\mu\alpha}\, a^{\lambda\alpha}{}_a{}^{\mu\beta}$	$C^1_{\lambda\beta}\, c_{\mu\alpha}\, a^{\lambda\beta}{}_a{}^{\mu\alpha}$
1,8	$-\Gamma^1_{\lambda\beta}\, C^1_{\mu\alpha}\, a^{\lambda\alpha}{}_a{}^{\mu\beta}$	$-\Gamma^1_{\lambda\beta}\, C^1_{\mu\alpha}\, a^{\lambda\beta}{}_a{}^{\mu\alpha}$
1,9	$-\Gamma^2_{\lambda\beta}\, C^1_{\mu\alpha}\, a^{\lambda\alpha}{}_a{}^{\mu\beta}$	$-\Gamma^2_{\lambda\beta}\, C^1_{\mu\alpha}\, a^{\lambda\beta}{}_a{}^{\mu\alpha}$
1,10	$C^1_{\alpha\mu}\, a^{1\alpha}{}_a{}^{1\mu}$	$C^1_{\alpha\mu}\, a^{11}{}_a{}^{\mu\alpha}$
1,11	$2C^1_{\mu\alpha}\, a^{1\alpha}{}_a{}^{2\mu}$	$2C^1_{\alpha\mu}\, a^{12}{}_a{}^{\mu\alpha}$
1,12	$C^1_{\alpha\mu}\, a^{2\alpha}{}_a{}^{2\mu}$	$C^1_{\alpha\mu}\, a^{22}{}_a{}^{\mu\alpha}$
ROW 2		
2,2	$2b^1_{\chi}\, b^1_{\xi}(a^{11}{}_a{}^{\chi\xi} + a^{1\chi}{}_a{}^{1\xi})$	$4b^1_{\chi}\, b^1_{\xi}\, a^{1\chi}{}_a{}^{1\xi}$
2,3	$2b^1_{\chi}\, b^1_{\xi}(a^{11}{}_a{}^{2\xi} + a^{12}{}_a{}^{\chi\xi})$	$4b^1_{\chi}\, b^1_{\xi}\, a^{1\chi}{}_a{}^{2\xi}$
2,4	$C^2_{\mu\beta}(b^1_{\alpha}\, a^{\lambda\alpha}{}_a{}^{1\beta} + b^1_{\mu}\, a^{\lambda 1}{}_a{}^{\mu\beta})$	$2C^1_{\lambda\beta}\, b^1_{\chi}\, a^{1\chi}{}_a{}^{\lambda\beta}$
2,5	$2b^1_{\chi}\, b^2_{\xi}(a^{11}{}_a{}^{\chi\xi} + a^{1\chi}{}_a{}^{1\xi})$	$4b^1_{\chi}\, b^2_{\xi}\, a^{1\chi}{}_a{}^{1\xi}$
2,6	$2b^1_{\chi}\, b^1_{\xi}(a^{12}{}_a{}^{\chi\xi} + a^{1\chi}{}_a{}^{2\xi})$	$4b^1_{\chi}\, b^2_{\xi}(a^{1\chi}{}_a{}^{2\xi} + a^{2\chi}{}_a{}^{1\xi})$
2,7	$c_{\lambda\beta}(b^1_{\alpha}\, a^{\lambda\alpha}{}_a{}^{1\beta} + b^1_{\mu}\, a^{\lambda 1}{}_a{}^{\mu\beta})$	$2c_{\lambda\beta}\, b^1_{\chi}\, a^{1\chi}{}_a{}^{\lambda\beta}$
2,8	$-\Gamma^1_{\lambda\beta}(b^1_{\mu}\, a^{\lambda 1}{}_a{}^{\mu\beta} + b^1_{\alpha}\, a^{\lambda\alpha}{}_a{}^{1\beta})$	$-2\Gamma^1_{\lambda\beta}\, b^1_{\chi}\, a^{\lambda\beta}{}_a{}^{1\chi}$
2,9	$-\Gamma^2_{\lambda\beta}(b^1_{\mu}\, a^{\lambda 1}{}_a{}^{\mu\beta} + b^1_{\alpha}\, a^{\lambda\alpha}{}_a{}^{1\beta})$	$-2\Gamma^2_{\lambda\beta}\, b^1_{\chi}\, a^{\lambda\beta}{}_a{}^{1\chi}$
2,10	$2b^1_{\xi}\, a^{11}{}_a{}^{1\xi}$	$2b^1_{\xi}\, a^{11}{}_a{}^{1\xi}$
2,11	$2(b^1_{\xi}\, a^{11}{}_a{}^{2\xi} + b^1_{\xi}\, a^{12}{}_a{}^{1\xi})$	$4b^1_{\xi}\, b^2_{\xi}\, a^{12}{}_a{}^{1\xi}$
2,12	$2b^1_{\xi}\, a^{21}{}_a{}^{2\xi}$	$2b^1_{\xi}\, a^{22}{}_a{}^{1\xi}$

	R_{IJ}	S_{IJ}
ROW 3		
3,3	$2b^1_\chi\, b^1_\xi(a^{22}{}_a{}^{\chi\xi} + a^{2\chi}{}_a{}^{2\xi})$	$4b^1_\chi\, b^1_\xi\, a^{2\chi}{}_a{}^{2\xi}$
3,4	$C^2_{\lambda\beta}(b^1_\alpha\, a^{\lambda\alpha}{}_a{}^{2\beta} + b^1_\mu\, a^{\lambda 2}{}_a{}^{\mu\beta})$	$2C_{\lambda\beta}\, b^1_\chi\, a^{2\chi}{}_a{}^{\lambda\beta}$
3,5	$2b^1_\chi\, b^2_\xi(a^{21}{}_a{}^{\chi\xi} + a^{2\chi}{}_a{}^{1\xi})$	$2b^1_\chi\, b^2_\xi(a^{1\chi}{}_a{}^{2\xi} + a^{2\chi}{}_a{}^{1\xi})$
3,6	$2b^1_\chi\, b^2_\xi(a^{22}{}_a{}^{\chi\xi} + a^{2\chi}{}_a{}^{2\xi})$	$4b^1_\chi\, b^2_\xi\, a^{2\chi}{}_a{}^{2\xi}$
3,7	$c_{\lambda\beta}(b^1_\alpha\, a^{\lambda\alpha}{}_a{}^{2\beta} + b^1_\mu\, a^{\lambda 2}{}_a{}^{\mu\beta})$	$2c_{\lambda\beta}\, b^1_\chi\, a^{2\chi}{}_a{}^{\lambda\beta}$
3,8	$-\Gamma^1_{\lambda\beta}(b^1_\mu\, a^{\lambda 1}{}_a{}^{\mu\beta} + b^1_\alpha\, a^{\lambda\alpha}{}_a{}^{1\beta})$	$-2\Gamma^1_{\lambda\beta}\, b^1_\chi\, a^{\lambda\beta}{}_a{}^{1\chi}$
3,9	$-\Gamma^2_{\lambda\beta}(b^1_\mu\, a^{\lambda 1}{}_a{}^{\mu\beta} + b^1_\alpha\, a^{\lambda\alpha}{}_a{}^{1\beta})$	$-2\Gamma^2_{\lambda\beta}\, b^1_\chi\, a^{\lambda\beta}{}_a{}^{1\chi}$
3,10	$2b^1_\xi\, a^{12}{}_a{}^{1\xi}$	$2b^1_\xi\, a^{11}{}_a{}^{2\xi}$
3,11	$2(b^1_\xi\, a^{1\xi}{}_a{}^{22} + b^1_\xi\, a^{12}{}_a{}^{2\xi})$	$4b^1_\xi\, a^{12}{}_a{}^{2\xi}$
3,12	$2b^1_\xi\, a^{22}{}_a{}^{2\xi}$	$2b^1_\xi\, a^{22}{}_a{}^{2\xi}$
ROW 4		
4,4	$C^2_{\lambda\beta}\, C^2_{\mu\alpha}\, a^{\lambda\alpha}{}_a{}^{\mu\beta}$	$C^2_{\lambda\beta}\, C^2_{\mu\alpha}\, a^{\lambda\beta}{}_a{}^{\mu\alpha}$
4,5	$C^2_{\mu\alpha}(b^1_\lambda\, a^{\lambda\alpha}{}_a{}^{\mu 1} + b^2_\beta\, a^{1\alpha}{}_a{}^{\mu\beta})$	$2C^2_{\mu\alpha}\, b^2_\chi\, a^{1\chi}{}_a{}^{\mu\alpha}$
4,6	$C^2_{\lambda\beta}(b^1_\alpha\, a^{\lambda\alpha}{}_a{}^{\mu 1} + b^2_\beta\, a^{2\alpha}{}_a{}^{\mu\beta})$	$2C^2_{\mu\alpha}\, b^2_\chi\, a^{2\chi}{}_a{}^{\mu\alpha}$
4,7	$C^2_{\lambda\beta}\, c_{\mu\alpha}\, a^{\lambda\alpha}{}_a{}^{\mu\beta}$	$C^2_{\lambda\beta}\, c_{\mu\alpha}\, a^{\lambda\beta}{}_a{}^{\mu\alpha}$
4,8	$-\Gamma^1_{\lambda\beta}\, C^2_{\mu\alpha}\, a^{\lambda\alpha}{}_a{}^{\mu\beta}$	$-\Gamma^1_{\lambda\beta}\, C^2_{\mu\alpha}\, a^{\lambda\beta}{}_a{}^{\mu\alpha}$
4,9	$-\Gamma^2_{\lambda\beta}\, C^2_{\mu\alpha}\, a^{\lambda\alpha}{}_a{}^{\mu\beta}$	$-\Gamma^2_{\lambda\beta}\, C^2_{\mu\alpha}\, a^{\lambda\beta}{}_a{}^{\mu\alpha}$
4,10	$C^2_{\mu\alpha}\, a^{1\alpha}{}_a{}^{1\mu}$	$C^2_{\mu\alpha}\, a^{11}{}_a{}^{\mu\alpha}$
4,11	$2C^2_{\mu\alpha}\, a^{1\alpha}{}_a{}^{1\mu}$	$2C^2_{\mu\alpha}\, a^{12}{}_a{}^{\mu\alpha}$
4,12	$C^2_{\mu\alpha}\, a^{2\alpha}{}_a{}^{2\mu}$	$C^2_{\mu\alpha}\, a^{22}{}_a{}^{\mu\alpha}$
ROW 5		
5,5	$2b^2_\chi\, b^2_\xi(a^{11}{}_a{}^{\chi\xi} + a^{1\chi}{}_a{}^{1\xi})$	$4b^2_\chi\, b^2_\xi\, a^{1\chi}{}_a{}^{1\xi}$
5,6	$2b^2_\chi\, b^2_\xi(a^{12}{}_a{}^{\chi\xi} + a^{1\chi}{}_a{}^{2\xi})$	$2b^2_\chi\, b^2_\xi(a^{2\chi}{}_a{}^{1\xi} + a^{2\xi}{}_a{}^{1\chi})$

	R_{IJ}	S_{IJ}
5,7	$c_{\lambda\beta}(b^2_\alpha\, a^{\lambda\alpha}a^{1\beta} + b^1_\mu\, a^{\lambda 1}a^{\mu\beta})$	$2c_{\lambda\beta}\, b^2_\chi\, a^{1\chi}a^{\lambda\beta}$
5,8	$-\Gamma^1_{\lambda\beta}(b^2_\mu\, a^{\lambda 1}a^{\mu\beta} + b^2_\alpha\, a^{\lambda\alpha}a^{1\beta})$	$-2\Gamma^1_{\lambda\beta}\, b^2_\chi\, a^{\lambda\beta}a^{1\chi}$
5,9	$-\Gamma^2_{\lambda\beta}(b^2_\mu\, a^{\lambda 1}a^{\mu\beta} + b^2_\alpha\, a^{\lambda\alpha}a^{1\beta})$	$-2\Gamma^2_{\lambda\beta}\, b^2_\chi\, a^{\lambda\beta}a^{1\chi}$
5,10	$2b^2_2\, a^{11}a^{12} + 2b^2_1\, a^{12}a^{12}$	$2b^2_\xi\, a^{11}a^{1\xi}$
5,11	$2(b^2_\xi\, a^{11}a^{2\xi} + b^2_\xi\, a^{12}a^{1\xi})$	$4b^2_\xi\, b^2_\xi\, a^{12}a^{1\xi}$
5,12	$2b^1_2\, a^{21}a^{22} + 2b^2_1\, a^{22}a^{11}$	$2b^2_\xi\, a^{22}a^{1\xi}$

ROW 6

6,6	$2b^2_\chi\, b^2_\xi(a^{22}a^{\chi\xi} + a^{2\chi}a^{2\xi})$	$4b^2_\chi\, b^2_\xi\, a^{2\chi}a^{2\xi}$
6,7	$c_{\lambda\beta}(b^2_\alpha\, a^{\lambda\alpha}a^{2\beta} + b^2_\mu\, a^{\lambda 2}a^{\mu\beta})$	$2c_{\lambda\beta}\, b^2_\chi\, a^{2\chi}a^{\lambda\beta}$
6,8	$-\Gamma^1_{\lambda\beta}(b^2_\alpha\, a^{\lambda\alpha}a^{2\beta} + b^2_\mu\, a^{\lambda 2}a^{\mu\beta})$	$-2\Gamma^1_{\lambda\beta}\, b^2_\chi\, a^{\lambda\beta}a^{2\chi}$
6,9	$-\Gamma^2_{\lambda\beta}(b^2_\alpha\, a^{\lambda\alpha}a^{2\beta} + b^2_\mu\, a^{\lambda 2}a^{\mu\beta})$	$-2\Gamma^2_{\lambda\beta}\, b^2_\chi\, a^{\lambda\beta}a^{2\chi}$
6,10	$2b^2_\xi\, a^{12}a^{1\xi}$	$2b^2_\xi\, a^{11}a^{2\xi}$
6,11	$2(b^2_\xi\, a^{22}a^{1\xi} + b^2_\xi\, a^{12}a^{2\xi})$	$4b^2_\xi\, b^2_\xi\, a^{12}a^{2\xi}$
6,12	$2b^2_\xi\, a^{22}a^{2\xi}$	$2b^2_\xi\, a^{22}a^{2\xi}$

ROW 7

7,7	$c_{\lambda\beta}\, c_{\mu\alpha}\, a^{\lambda\alpha}a^{\mu\beta}$	$c_{\lambda\beta}\, c_{\mu\alpha}\, a^{\lambda\beta}a^{\mu\alpha}$
7,8	$\Gamma^1_{\lambda\beta}\, c_{\mu\alpha}\, a^{\lambda\alpha}a^{\mu\beta}$	$\Gamma^1_{\lambda\beta}\, \beta_{\mu\alpha}\, a^{\lambda\beta}a^{\mu\alpha}$
7,9	$\Gamma^2_{\lambda\beta}\, c_{\mu\alpha}\, a^{\lambda\alpha}a^{\mu\beta}$	$\Gamma^2_{\lambda\beta}\, c_{\mu\alpha}\, a^{\lambda\beta}a^{\mu\alpha}$
7,10	$c_{\mu\alpha}\, a^{1\alpha}a^{1\mu}$	$c_{\mu\alpha}\, a^{11}a^{1\mu}$
7,11	$-2c_{\mu\alpha}\, a^{1\alpha}a^{2\mu}$	$-2c_{\mu\alpha}\, a^{12}a^{\mu\alpha}$
7,12	$-c_{\mu\alpha}\, a^{2\alpha}a^{2\mu}$	$-c_{\mu\alpha}\, a^{22}a^{\mu\alpha}$

	R_{IJ}	S_{IJ}
ROW 8		
8,8	$\Gamma^1_{\lambda\beta}\,\Gamma^1_{\mu\alpha}\,a^{\lambda\alpha}a^{\mu\beta}$	$\Gamma^1_{\lambda\beta}\,\Gamma^1_{\mu\alpha}\,a^{\lambda\beta}a^{\mu\alpha}$
8,9	$\Gamma^1_{\lambda\beta}\,\Gamma^2_{\mu\alpha}\,a^{\lambda\alpha}a^{\mu\beta}$	$\Gamma^1_{\lambda\beta}\,\Gamma^2_{\mu\alpha}\,a^{\lambda\beta}a^{\mu\alpha}$
8,10	$-\Gamma^1_{\mu\alpha}\,a^{1\alpha}a^{1\mu}$	$-\Gamma^1_{\mu\alpha}\,a^{\mu\alpha}a^{11}$
8,11	$-2\Gamma^1_{\mu\alpha}\,a^{1\alpha}a^{2\mu}$	$-2\Gamma_{\mu\alpha}\,a^{\mu\alpha}a^{12}$
8,12	$-\Gamma^1_{\mu\alpha}\,a^{2\alpha}a^{2\mu}$	$-\Gamma^1_{\lambda\beta}\,a^{\mu\alpha}a^{22}$
ROW 9		
9,9	$\Gamma^2_{\lambda\beta}\,\Gamma^2_{\mu\alpha}\,a^{\lambda\alpha}a^{\mu\beta}$	$\Gamma^2_{\lambda\beta}\,\Gamma^2_{\mu\alpha}\,a^{\lambda\beta}a^{\mu\alpha}$
9,10	$-\Gamma^2_{\mu\alpha}\,a^{1\alpha}a^{1\mu}$	$-\Gamma^2_{\mu\alpha}\,a^{\mu\alpha}a^{11}$
9,11	$-2\Gamma^2_{\mu\alpha}\,a^{1\alpha}a^{2\mu}$	$-2\Gamma^2_{\mu\alpha}\,a^{\mu\alpha}a^{12}$
9,12	$-\Gamma^2_{\mu\alpha}\,a^{2\alpha}a^{2\mu}$	$-\Gamma^2_{\mu\alpha}\,a^{\mu\alpha}a^{22}$
ROW 10		
10,10	$a^{11}a^{11}$	$a^{11}a^{11}$
10,11	$2a^{11}a^{12}$	$2a^{11}a^{12}$
10,12	$a^{12}a^{12}$	$a^{11}a^{22}$
ROW 11		
11,11	$2(a^{12}a^{12} + a^{11}a^{22})$	$4a^{12}a^{12}$
11,12	$2a^{12}a^{22}$	$2a^{22}a^{12}$
ROW 12		
12,12	$a^{22}a^{12}$	$a^{22}a^{22}$

2. KINETIC ENERGY "Mass Term"

The bilinear form

$$C(\dot{\underline{u}},\dot{\underline{v}}) = -\omega^2\rho \int_{\hat{\Omega}} \underline{u}.\underline{v}\, d\hat{\Omega}$$

$$= -\omega^2\rho \int_{\Omega} \Big[h u_\alpha v_\beta a^{\alpha\beta} + \frac{h^3}{12}(u_{3,\delta} v_{3,\lambda} + u_\gamma v_{3,\lambda} b^\gamma_\delta + u_{3,\delta} u_\mu b^\gamma_\lambda + u_\gamma v_\mu b^\gamma_\delta b^\mu_\lambda) a^{\delta\lambda} + h u_3 v_3 \Big] \sqrt{\bar{a}}\, d\xi^1 d\xi^2$$

is to be written in the form

$$C(\dot{\underline{u}},\dot{\underline{v}}) = -\lambda \underbrace{\int_{\Omega} \{U_J\}^T [C_{IJ}] \{V_J\} \sqrt{\bar{a}}\, d\xi^1\, d\xi^2}_{\text{"mass term"}}$$

Matrix $[C_{IJ}]$ is symmetric with non-zero coefficients in the positions shown below :

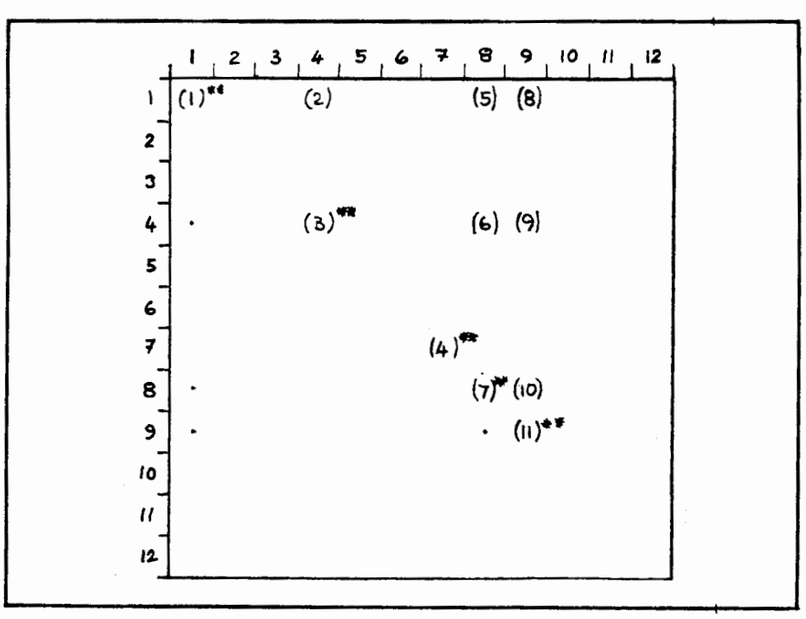

Expressions for these coefficients are given by

(1) $- h\, a^{11} + \frac{h^3}{\bar{1}\bar{2}}\, b^1_\delta b^1_\lambda\, a^{\delta\lambda}$ **

(2) $- h\, a^{12} + \frac{h^3}{\bar{1}\bar{2}}\, b^1_\delta b^2_\lambda\, a^{\delta\lambda}$

(3) $- h\, a^{22} + \frac{h^3}{\bar{1}\bar{2}}\, b^2_\delta b^2_\lambda\, a^{\delta\lambda}$ **

(4) $- h$ **

(5) $- \frac{h^3}{\bar{1}\bar{2}}\, b^1_\lambda\, a^{1\lambda}$

(6) $- \frac{h^3}{\bar{1}\bar{2}}\, b^2_\lambda\, a^{1\lambda}$

(7) $- \frac{h^3}{\bar{1}\bar{2}}\, a^{11}$ **

(8) $- \frac{h^3}{\bar{1}\bar{2}}\, b^1_\lambda\, a^{2\lambda}$

(9) $- \frac{h^3}{\bar{1}\bar{2}}\, b^2_\lambda\, a^{2\lambda}$

(10) $- \frac{h^3}{\bar{1}\bar{2}}\, a^{12}$

(11) $- \frac{h^3}{\bar{1}\bar{2}}\, a^{22}$ **

where ** indicates coefficient which is always non-zero.